UNIVERSIDADE FEDERAL DO AMAZONAS

INSTITUTO DE CIÊNCIAS EXATAS

PROGRAMA DE PÓS-GRADUAÇÃO EM GEOCIÊNCIAS

MARCELO EUSTAQUIO VERSIANI ELIAS

O REGISTRO DE PETROTRAMAS DO GRANITO MODERNA E DOS GRANITOS ADJACENTES, SÃO LUIZ DO ANAUÁ, RORAIMA.

MANAUS

2018

UNIVERSIDADE FEDERAL DO AMAZONAS – UFAM

INSTITUTO DE CIÊNCIAS EXATAS – ICE

PROGRAMA DE PÓS-GRADUAÇÃO EM GEOCIÊNCIAS

MARCELO EUSTAQUIO VERSIANI ELIAS

O REGISTRO DE PETROTRAMAS DO GRANITO MODERNA E DOS GRANITOS ADJACENTES, SÃO LUIZ DO ANAUÁ, RORAIMA.

Dissertação apresentada ao Programa de Pós-Graduação em Geociências da Universidade Federal do Amazonas (UFAM), como requisito para obtenção do título de Mestre em Geociências.

Orientador: Prof. Dr. Carlos Alejandro Salazar

MANAUS

Novembro de 2018

Ficha Catalográfica

Ficha catalográfica elaborada automaticamente de acordo com os dados fornecidos pelo(a) autor(a).

MARCELO EUSTAQUIO VERSIANI ELIAS

O REGISTRO DE PETROTRAMAS DO GRANITO MODERNA E DOS GRANITOS ADJACENTES, SÃO LUIZ DO ANAUÁ, RORAIMA.

Dissertação apresentada ao Programa de Pós-Graduação em Geociências da Universidade Federal do Amazonas (UFAM), como requisito para obtenção do título de Mestre em Geociências.

Aprovado em 23 de novembro de 2018.

BANCA EXAMINADORA

Prof. Dr. Carlos Alejandro Salazar, Presidente.
Universidade Federal do Amazonas

Prof.ª Dr.ª Rielva Solimairy Campelo do Nascimento, Membro.
Universidade Federal do Amazonas
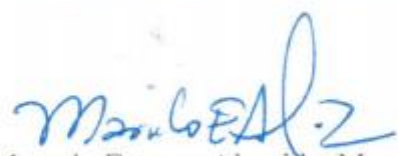
Dr. Marcelo Esteves Almeida, Membro.
CPRM/RJ

A todas as pessoas boas.

RESUMO

Diversos corpos graníticos Paleoproterozoicos do tipo-A intrudem o escudo das Guianas no Cráton Amazônico, dentre eles, o Granito Moderna (1.81 Ga), localizado entre a sede do município de São Luiz do Anauá e a Vila Moderna, no sudeste do estado de Roraima. Análises de anisotropia de susceptibilidade magnética (ASM, IRM e termomagnéticas), combinadas com dados estruturais de campo e dados petrográficos com enfoque microestrutural, foram realizadas a fim de se identificar o campo de esforços atuante, durante a colocação do Granito Moderna, correlaciona-lo à tectônica regional e à colocação de plutons graníticos do tipo-A Orosirianos na região. O Granito Moderna varia de monzogranito a sienogranito e está alojado em estrutura de direção NE-SW, na zona de contato entre os granitoides Martins Pereira (1,96-1,97 Ga) e Caroebe (1,89-1,90 Ga). O processo de cristalização plutônica compreende fluxo magmático com deformação plástica associada a alteração hidrotermal. Estruturas primárias semelhantes às observadas no Granito Moderna são presentes no Granito Caroebe, enquanto que o Granito Martins Pereira encontra-se predominantemente deformado em estado sólido. A deformação primária registrada nos granitos Moderna e Caroebe, apresenta direção principal ENE-WSW, com mergulho subvertical. As pontuais variações devem-se a zonas de cisalhamento NW-SE. As rochas analisadas apresentam orientação de foliações magmática e magnética concordantes, as quais refletem o campo de esforços, com encurtamento NW-SE, atuante no instante do alojamento crustal.

Palavras-chave: Cráton Amazônico, Escudo das Guianas, Domínio Uatumã-Anauá, Granito Moderna, Petrotramas Graníticas, Alojamento Plutônico, Anisotropia de Susceptibilidade Magnética ASM.

ABSTRACT

Several Paleoproterozoic A-type granite bodies intrude the Guiana shield in the Amazonian Craton, among them, Moderna granite (1.81 Ga), located between São Luiz do Anauá city and Moderna Village, in the southeast of Roraima state. Magnetic anisotropy analyzes (AMS, IRM and thermomagnetic) combined with field and microstructural focus petrographic data, were used to identify the field of stresses during the Moderna granite emplacement and correlate it with regional tectonics. The monzogranite with variations for syenogranite Moderna, presents NW-SE elongation in the contact zone between the calc-alkaline Martins Pereira (1.96 Ga) and Caroebe (1.89 Ga) granites, in transitional contact with these units, marked by hydrothermal alteration features, which do not affect the orientation of the rock's magmatic fabric and is responsible for its characteristic red color, associated with plastic deformation. The magnetic fabric, marked by magnetite, and magmatic fabric orientations of the three analyzed rock units have genetic equivalence and main direction around the E-W to NE-SW axis, in agreement with the regional structural framework that controls the Orosirian plutons emplacement in the central portion of the Guiana shield. Although there is a great difference in age, reported in the literature, between the crystallization of the granite units analyzed, these rocks developed minerals fabrics with similar orientation and strain mechanisms, indicating that the granite emplacements occurred syn-kinematicly under a dextral transpressive tectonic regime with plastic strain. Localized shear zones, sub-parallel to magmatic foliation orientation, demonstrate the persistence of the effort field at the end of the plutonic housing, while discrete posterior shear zones, NW-SE direction, deform restricted portions of the rock units in solid state.

Keywords: Amazonian Craton, Guiana Shield, Uatumã-Anauá Domain, Moderna Granite, Granite Petrofabrics, Plutonic emplacement, Anisotropy of Magnetic Susceptibility ASM.

LISTA DE FIGURAS

LISTA DE FIGURAS NO ARTIGO DO CAPÍTULO 4

LISTA DE TABELAS

LISTA DE TABELAS NO ARTIGO DO CAPÍTULO 4

SUMÁRIO

1 INTRODUÇÃO

1.1 Natureza e relevância do trabalho

O granito Moderna (Santos et al, 1997) é um dos diversos corpos graníticos do tipo-A que o Cráton Amazônico abriga, sendo alguns destes, fonte de recursos minerais essenciais ao desenvolvimento humano, como o depósito de Pitinga, relacionado ao granito Paleoproterozóico tipo-A Madeira (Valério, 2006; Bastos Neto et al., 2009; Bettencourt et al., 2015) localizado no norte do estado do Amazonas. Embora dados petrológicos, geoquímicos e estruturais que envolvam o granito tipo-A Moderna sejam escassos, existe um dado geocronológico (Santos et al, 1997) que aponta uma idade Orosiriana muito semelhante ao granito Madeira, alojado na mesma latitude, 200 km a sul do granito Moderna, que detém um vasto acervo de estudos geológicos, inclusive, recentemente, no âmbito da geologia estrutural de detalhe (Siachoque et al.,2017). Estudos dessa natureza, têm contribuído para o melhor entendimento sobre os modelos de colocação de plútons graníticos.

A área de estudo (Figura 1) localiza-se nas proximidades da Vila Moderna, pertencente ao município de São Luiz do Anauá, a sul do Rio Anauá, na altura do quilômetro 50 da rodovia BR 210. A partir de Manaus, o principal trajeto é feito pela rodovia BR 174, até a rotatória nas imediações da Vila Novo Paraíso que, após aproximadamente 500 km percorridos, dá acesso à BR 210. Seguindo à direita para a rodovia também pavimentada, BR 210, por cerca de 50 Km, chega-se à Vila Moderna. A paisagem é dominada por extensas planícies, com morros em meia laranja (Figura 2) e serras pontuais, alinhadas e/ou dispersas com elevações aproximadas de 300 metros, onde a vegetação, predominantemente de porte médio, torna-se mais densa. As diversas áreas de pasto inseridas em meio à floresta, favorecem as exposições rochosas, e as "vicinais" (estradas ortogonais à rodovia principal) 13, 17 e 19, sentido norte, e 14, 16 e 18, sentido sul, entre o Município de São Luiz do Anauá e a Vila Moderna, facilitam o acesso ás porções mais interioranas da área de estudo, que abrange aproximadamente 90 Km2.

Sob a denominação de unidade Granito Moderna (Santos et al., 1997), foram agrupados vários plútons (ALMEIDA et al., 2008), os quais encontram-se alongados segundo um trend NW-SE, onde a orientação das principais estruturas regionais é NE-SW a E-W. (ALMEIDA et al., 2008). A maioria dos Trabalhos geológicos desenvolvidos na região tem foco em mapeamento litológico, geoquímico e geocronológico (ALMEIDA et al., 2006; SANTOS et al., 1997). Entretanto, estudos detalhados de geologia estrutural ainda são escassos, embora sejam indispensáveis para a compreensão do contexto geodinâmico em que esses corpos

graníticos se originaram e se alojaram na crosta terrestre.
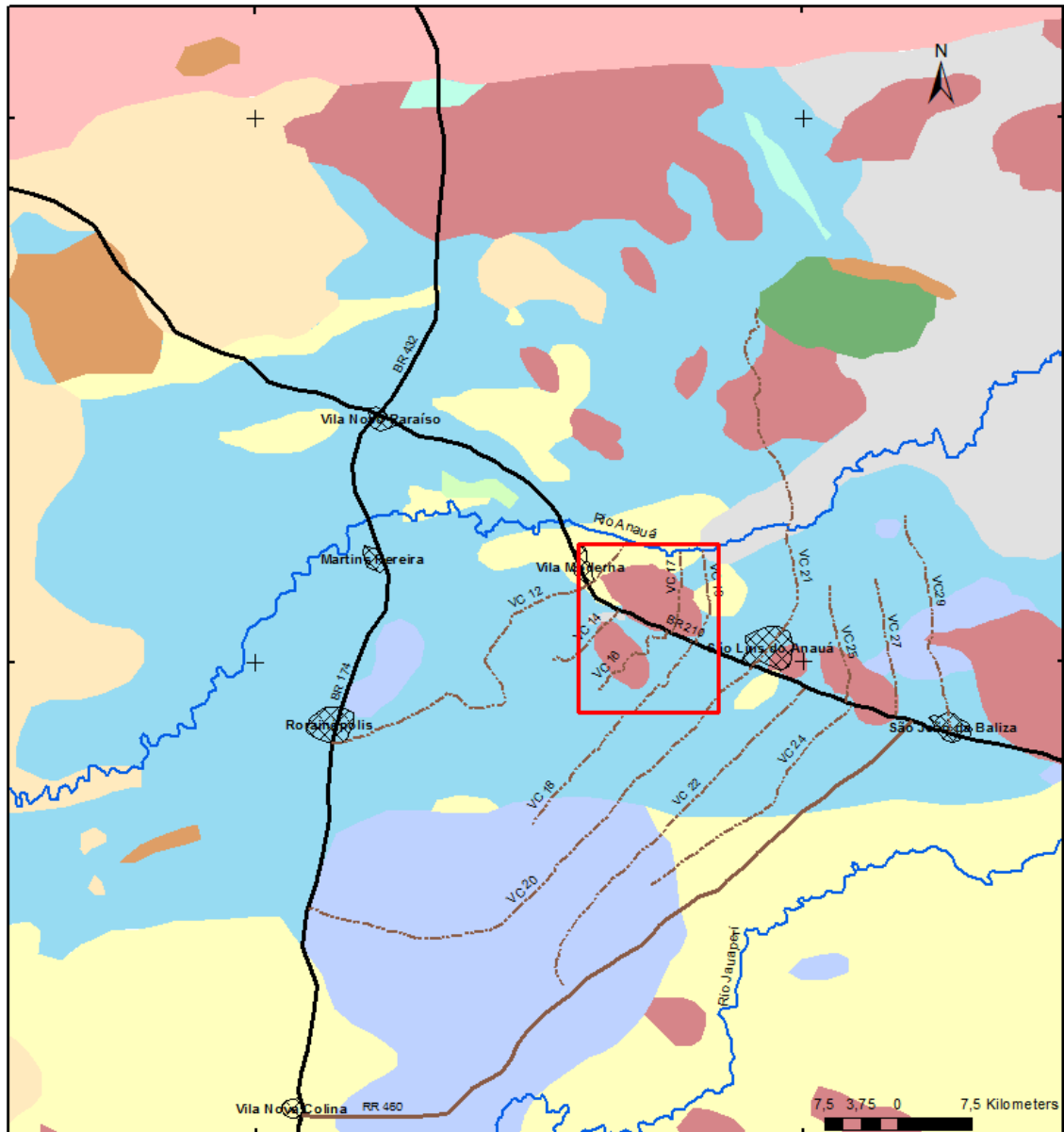
Figura 1 - Mapa geológico simplificado, adaptado de Almeida 2006, de parte da região sudeste de Roraima no escudo das Guianas (A) com a localização da Área de estudo destacada em vermelho (B).

Figura 2. Vista para sul a partir do alto da Serra da Antena.

As classificações de rochas graníticas, normalmente relacionam a fonte dos magmas graníticos com a composição química da rocha (ARTH, 1979; PEARCE, 1984; EBY, 1992). Algumas dessas classificações, associam a formação de granitos metaluminosos com a fusão parcial de rochas ígneas e de granitos peraluminosos com fontes metassedimentares (Chappell & White, 1974). Granitos com alto conteúdo em N_2O+K_2O, alta razão Ga/Al e enriquecidos em Nb, Ta, Zr e Hf, foram denominados de granitos tipo A (Loiselle & Wones, 1979., Collins et al., 1982; Whalen et al., 1987), os quais foram geneticamente relacionados a ambientes de tectônica distensiva (Martin et al., 1994; Dall'Agnol et al., 2005; Bonin et al 2007; Zhao et al., 2008; Karsli et al., 2012; Frost & Frost, 2011). Essa correlação tem predominado nas interpretações tectônicas sobre granitos tipo-A do Cráton Amazônico (Santos et al., 1997; Dall'Agnol et al., 1999; CPRM, 2003). Entretanto, são reportadas ocorrências de granitos Tipo-A gerados em ambiente de orogenia distal (Ahall et al, 2000) no escudo Báltico, amalgamado ao escudo das Guianas no supercontinente Columbia, durante o Orosiriano (Johansson, 2009; Evans, 2013).

Além de ser um importante formador de crosta, magmatismo granítico é considerado

um indicador de alterações térmicas crustais (Bonin et al., 2007). Plútons se comportam como potenciais marcadores da tectônica atuante no instante do seu alojamento. Quando um plúton se aloja na crosta (Hutton 1988, Paterson et al.1989, Miller & Paterson 1994, Fowler et al 1995), a paragênese mineral adquire arranjo textural e estrutural, de forma a indicar o regime tectônico no qual este se posicionou.

De modo geral, os minerais tendem a formar tramas compatíveis com a orientação dos esforços dominantes que os afetam. Petrotramas tendem a se registrar durante a fase de cristalização de um plúton (Kerr & Lister 1991; Bouchez et al., 1997, Petford et al., 2000), ou no estado solido por deformação (Tullis & yund, 1977., Patterson et al 1989, Vernon et al 2000, Rosemberg et al., 2005). Análises de petrotramas graníticas e sua caracterização, possibilitam a reconstituição do campo de esforços atuantes sobre o plúton, no instante de sua colocação. Dessa forma, a comparação entre as condições físicas de acomodação granítica (Brown & Solar 1998; Rosenberg 2005., Zac et al., 2012), refletidas na petrotrama, e as condições físicas responsáveis pela deformação regional, registrada nas rochas adjacentes, permite inferências a respeito da evolução tectônica de determinada região (Fossen et al., 1994; Fossen & Tikoff, 1998).

Estudos estruturais em granitos se focam na compreensão de mecanismos relacionados com a ativação de estruturas que controlam o espaço de acomodação (Hutton, 1988, Patterson 1989), e a relação entre tais estruturas com a evolução regional do campo de esforços durante o magmatismo (McCarty et al 2015, Zibra et al 2017). Os resultados de tais estudos levaram a postular a existência de anisotropias na crosta, desenvolvidas sob diferentes regimes tectônicos (transcorrente, transpressivo ou transtrativo), que controlam o alojamento de plútons (Neves et al 1996., Gleizes et al., 1997; Bouchez et al., 1997; Brown 2001; Žák, et al., 2012; Zibra et al., 2017).

Ao se cristalizarem, granitos normalmente não registram petrotramas claramente distinguíveis em escala de afloramento, para que possam ser relacionadas com a deformação associada a seus processos de colocação na crosta. Entretanto, tais tramas podem ser reconhecidas mediante estudos de anisotropia de susceptibilidade magnética (ASM; Bouchez, 1997; Tarling & Hrouda, 1993; Archanjo et al., 1995; Žák et al., 2009). As tramas de ASM, normalmente pouco desenvolvidas em granitos do tipo-A, são comumente obliteradas por eventos de alteração hidrotermal tardi a pós-magmática (Archanjo et al., 2009; Nédélec et al., 1994, 2015; Price et al., 1998), que pode, inclusive, produzir magnetita fina e hematita em magnetita-granitos (Nédélec et al., 2015).

O presente trabalho tem foco no entendimento e caracterização do regime estrutural

local, e a consequente relação deste, com o regime estrutural regional descrito na literatura, relacionado ao alojamento do granito tipo A Moderna (1.81 Ga). Para tanto, foram analisadas amostras referentes ao Granito Moderna e aos granitos adjacentes (Martins Pereira) e/ou hospedeiros (Caroebe). Os mecanismos de alojamento e o regime de deformação do estado magmático ao sólido, foram caracterizados com base nos dados de ASM; dados petrográficos microestruturais, e dados estruturais de campo, afim de identificar a distribuição e a cinemática da deformação interna do plúton.

1.2 Objetivos

O objetivo geral desta pesquisa, consiste em determinar os mecanismos de alojamento do Granito Moderna e correlacionar o magmatismo Moderna local ao contexto tectônico regional. Para cumprir tal objetivo pretende-se:

a)   Determinar a organização das tramas mineral e magnética do Granito Moderna;

b)   Interpretar a deformação interna, a partir dos mecanismos de deformação em escala microscópica;

c)   Discutir prováveis relações entre estruturas regionais e tramas magnéticas;

d)   Modelar o campo de esforços atuante durante o alojamento granítico.

2   MATERIAIS E MÉTODOS

A realização da pesquisa é embasada por técnicas analíticas específicas, que possibilitam a obtenção da organização interna da trama mineralógica do granito Moderna e das rochas encaixantes adjacentes. Tais métodos permitem definir a origem da deformação, a organização espacial e a hierarquia temporal das petrotramas presentes nas rochas. As etapas envolvidas na sistematização do trabalho são descritas a seguir:

Integração de informações geológicas e análise de sensoriamento remoto. Os procedimentos metodológicos a serem aplicados incluem, na primeira etapa, a revisão e consulta de fontes bibliográficas e cartográficas relacionadas à geologia da área de interesse, com foco em dados estruturais, geotectônicos, geocronológicos, geoquímicos, mineralógicos e petrogenéticos, além de informações a respeito da própria metodologia analítica específica, a ser empregada na pesquisa. Esse acervo de dados, que incluí consulta de trabalhos de mapeamento regional, artigos científicos, monografias, resumos publicados em eventos, livros, teses e dissertações, encontra-se disponível em centros de documentação e na rede internacional de computadores. A área de afloramento do granito Moderna, foi analisada por meio de imagens

de satélite do tipo Landsat SAR-SIPAM e geocover, onde foram identificadas variações nos padrões de relevo; tipos e densidade de vegetação e drenagem, feições estruturais como lineamentos, além de favorecer na estimativa dos limites dos corpos ígneos e na seleção de sítios adequados para percursos e coleta de dados. A integração e compilação digital foram realizadas em sistema de informação georreferenciada por meio do software ArcGIS 10.1

Trabalho de campo. O mapeamento geológico-estrutural da área de estudo, consistiu em levantamentos geológicos ao longo de estradas, ramais, fazendas e trilhas abertas na selva, realizados em duas campanhas de 7 dias: a primeira em abril e a segunda em outubro de 2017. Foram descritos 68 afloramentos, nos quais se observou os aspectos texturais, mineralógicos e estruturais, aferindo, quando identificadas, as atitudes das estruturas planares e lineares; bem como caracterizadas as feições geométricas e cinemáticas observadas nas rochas. Os dados de orientação de estruturas aferidos em campo, foram tratados em estereograma, hemisfério inferior, de Schimidt. A atitude das estruturas planares se apresenta em notação strike/dip e das lineares, em notação dip/strike.

Preparação de amostras. O procedimento foi iniciado em campo, com a orientação de blocos e cilindros de rocha. No Laboratório de Laminação da Universidade Federal do Amazonas (UFAM), os blocos foram cortados, primeiramente de forma paralela ao plano da foliação principal, a fim de se identificar a lineação mineral ou de estiramento. Após essa primeira etapa, o bloco foi novamente cerrado, agora de forma paralela à lineação e perpendicular à foliação. Com os devidos planos de orientação identificados, a lâmina da rocha pôde ser confeccionada, segundo o plano que permite a correta interpretação cinemática das estruturas. O bloco rochoso foi preservado, quando possível, em formato de paralelepípedo para que fossem tomadas fotografias digitais de alta resolução para análises de orientação preferencial de forma dos minerais, e para obtenção de indicadores cinemáticos. Foram elaboradas 24 lâminas e 19 paralelepípedos de rocha, todos orientados. Apenas o tablete de rocha foi produzido no laboratório de laminação da UFAM. As etapas seguintes de confecção da lâmina, foram realisadas no laboratório de laminação do Serviço Geológico do Brasil regional de Manaus (CPRM). Quando entregues, as lâminas ainda foram adequadas mediante polimento fino realizado na UFAM, para as análises petrográficas, microestruturais e obtenção de imagens.

Os cilindros de rochas coletados para análises de ASM foram cerrados em espécimes de 2,2 cm de diâmetro e 2,2 cm de comprimento, gerando 796 espécimes orientados. Esse procedimento foi realizado no Laboratório de Laminação da UFAM por meio de cerra especializada. Todos os espécimes foram devidamente identificados, orientados e embalados

em filme de policloreto de vinila para a realização das análises magnéticas.

Análises laboratoriais envolveram o uso de técnicas e equipamentos específicos, cujos procedimentos são descritos a seguir:

Análises Petrográficas consistem na observação de lâminas petrográficas delgadas, polidas em microscópio petrográfico de luz transmitida e refletida, marca Olympus, modelo BX51, do Laboratório de Microscopia Petrográfica da Universidade Federal do Amazonas. Foi realizada, nas lâminas, a identificação dos minerais da rocha por meio das características óticas, bem como a analise textural dos componentes da rocha, e de mecanismos de deformação, enfatizadas nas relações de limites e estrutura interna de cristais. Envolve, ainda, a análise cinemática segundo o plano de orientação XZ. A classificação modal para rochas graníticas se fez a partir da qualificação e quantificação das fases minerais, obtidas por estimativa visual. A nomenclatura das rochas foi realizada seguindo os postulados de Streckeisen (1976). Finalmente foi realizada captura de fotografais de feições microscópicas, para ilustrar o texto.

Anisotropia de Susceptibilidade Magnética (ASM). Esse método permite caracterizar, em três dimensões, a trama magnética das rochas pouco afetadas por processos deformacionais posteriores à cristalização completa do magma que a originou (Paterson et al.,1989). Na ASM, além da capacidade de magnetização da amostra ser quantificada, as direções em que essa magnetização é favorecida ou dificultada também são registradas. As análises de ASM e medidas da resposta magnética da rocha em campo magnético e temperatura variáveis, para determinar o marcador magnético da rocha, foram realizadas no Laboratório de Paleomagnetismo e Magnetismo de Rochas do Instituto de Astronomia, Geofísica e Ciências Atmosféricas da Universidade de São Paulo.

As medidas de ASM foram executadas por meio de um susceptibilímetro Kappabridge, modelo MFK1-FA, da fabricante AGICO Ltda, e um susceptibilímetro Kappabridge modelo KLY-4S, também fabricado pela AGICO Ltda. O software Anisoft 4.2, AGICO Ltda combina as medições da susceptibilidade magnética nos três planos espaciais, perpendiculares, e fornece um valor da medida volumétrica da susceptibilidade magnética como dado de referência para a geração de um tensor representativo da susceptibilidade de cada espécime analisado. Os resultados obtidos são tratados e analisados no mesmo software, que fornece também os parâmetros escalares [grau de anisotropia Pj ≥ 1 e forma T variando de -1 (forma linear) até 1 (forma planar)]; e os parâmetros direcionais [foliação magnética (plano perpendicular a K3) e lineação magnética (indicada por K1)]. A representação da trama magnética é feita por meio de elipsoides referentes aos espécimes de cada afloramento amostrado e analisado. A integração dos dados obtidos individualmente reflete a trama magnética das rochas em escalas pontuais,

de afloramento, local ou regional, de acordo com a abrangência da amostragem e do interesse da pesquisa. Os parâmetros direcionais são levados a compor os mapas de foliação e lineação magnética, as quais correspondem à trama magnética das rochas analisadas. O tratamento dos dados de ASM e a avaliação da qualidade dos mesmos envolvem procedimentos estatísticos que permitem comparar as petrotramas mineral e magnética. A integração dos dados e o mapeamento de parâmetros escalares e direcionais dos elipsoides representativos das petrotramas, auxiliaram na elaboração de interpretações e hipóteses sobre as condições de colocação do granito Moderna.

Analises Termomagnéticas: a Temperatura de Curie/Néel (TC/TN, especificas para cada tipo de mineral) pode ser determinada em experimentos termomagnéticos (variação da susceptibilidade K com a temperatura T). A amostra é constituída por cerca de 0,25 cm3 de rocha moída que é colocada no porta-amostras do equipamento CS-3 acoplado ao susceptibilímetro Kappabridge modelo KLY-4S, fabricado pela AGICO Ltda, onde é progressivamente aquecida desde a temperatura ambiente $\approx$18oC até $\approx$750°C (ciclo de aquecimento). Subsequentemente é realizado o ciclo inverso até a temperatura ambiente (ciclo de resfriamento). A cada intervalo de 3°C a susceptibilidade magnética é medida e registrada. As curvas termomagnéticas que representam a variação da susceptibilidade magnética (K) e da temperatura (T) foram obtidas e analisadas a partir do software Cureval V.8 da AGICO Ltda, e descrevem o comportamento termomagnético de minerais.

Magnetização Remanente Isotérmica (IRM): o método consiste em selecionar um espécime representativo de um conjunto de valores de susceptibilidade volumétrica, para caracterizar seu comportamento magnético mediante indução de campos magnéticos variáveis (a temperatura ambiente $\approx$ 18°C constante) até a provável saturação magnética dos diferentes constituintes magnéticos do espécime analisado. Inicialmente se faz uma medida da magnetização remanente natural (MRN) do espécime. Em seguida são aplicados na amostra campos magnéticos sucessivamente maiores por meio do magnetizador tipo pulse (magnetizador Pulse Magnetizer MMPM-10). Cada campo magnético é aplicado ao longo do eixo do espécime (direção z) e a magnetização remanente é medida em cada etapa por um magnetômetro de rotação (JR-6A da fabricante AGICO Ldta). A medida da magnetização remanente, depois de aplicado o campo magnético, é feita mediante rotação do espécime em três posições diferentes. Um campo magnético indutor, gradativamente mais alto (até 2 Teslas), é aplicado ao espécime de rocha até que sua magnetização atinja a saturação representativa de seus constituintes magnéticos.

3   GEOLOGIA REGIONAL

A evolução geológica do Cráton Amazônico é interpretada de formas distintas de acordo, principalmente, com a linha de pesquisa e atuação dos diversos autores que o estudaram ao longo dos anos.

Amaral (1974, 1984), a partir da integração de dados geológicos e geocronológicos oriundos de mapeamento geológico regional, fez a primeira compartimentação do Cráton Amazônico em complexos metamórficos de alto grau e terrenos greenstonebelts gerados nos intervalos 3,4-3,0 Ga (evento Guriense) e entre 2, 75-2,5 Ga (evento Guianense); e metamorfismo de alto grau e migmatização teriam sido gerados no intervalo 2,2-1,8 Ga pelo evento regional Transamazônico. Magmatismo e sedimentação são entendidos como produtos de ativações da plataforma em intervalos do Meso e Neoproterozóico.

Atualmente, os modelos mais adotados são os de Cordani et al., 1979; Tassinari & Macambira, 1999, 2004; Tassinari et al., 2000; Santos et al., 2000, 2006, que compartimentam o cráton em províncias com base, principalmente, em dados geocronológicos. Esses modelos têm em comum a concepção de que o cráton foi estruturado pela amalgamação de blocos crustais em torno de um núcleo arqueano. Entretanto, a interpretação da geodinâmica Pré-cambriana e os limites entre as províncias os diferenciam (Figura 3 A e B).
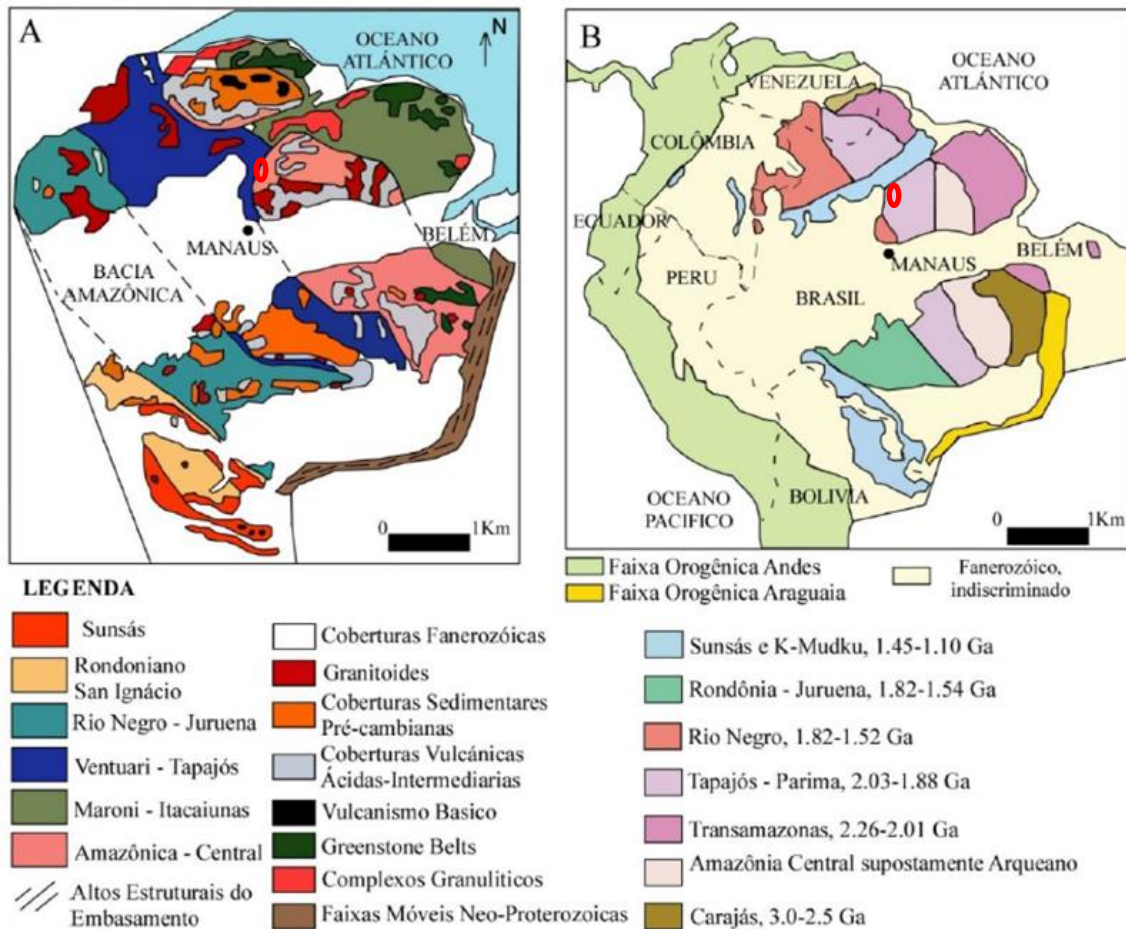
Figura 3: Províncias Geocronológicas do cráton Amazônico. A) Segundo Tassinari e Macambira (1999) e B) Segundo Santos *et al.,* (2006) (Destaca-se a área de estudo do presente trabalho em vermelho).

O Escudo das Guianas, que corresponde à parte norte do Cráton Amazônico, é representado no estado de Roraima, por expressivas exposições graníticas, sejam elas geradas em ambientes compressivos ou extensivos e afetadas ou não por eventos deformacionais posteriores (ALMEIDA, 2006). A individualização dessas massas continentais graníticas e o avanço do conhecimento cartográfico e geológico dos últimos anos, tornou possível a compartimentação da província Tapajós-Parima (Santos et al., 2006), no estado de Roraima, em grandes domínios tectono-estratigráficos (REIS et al., 2003) (Figura 4 A e B) e, localmente, sua distinção em "subdomínios" (ALMEIDA, 2006).
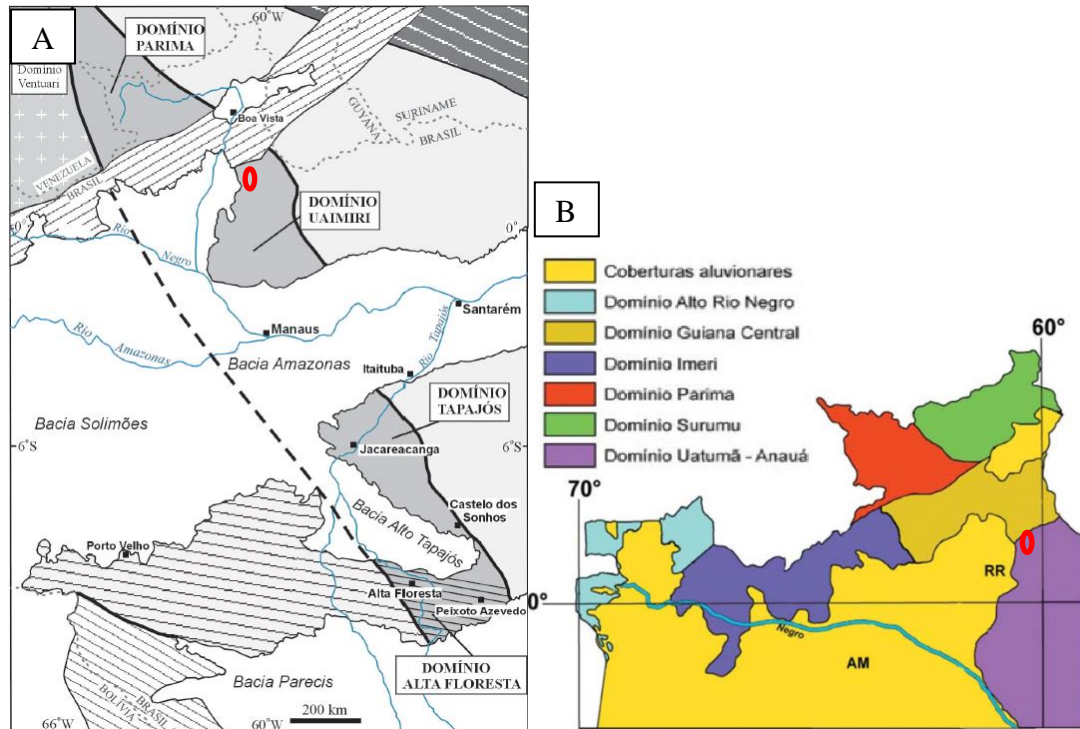
Figura 4: A) Domínios tectono-estratigráficos da província Tapajós-Parima. Retirado de Santos et al., 2004.; B) Domínios tectonoestratigráficos propostos por Reis & Fraga (2000) e Reis et al. (2003; 2006a) para o estado de Roraima. Retirado de reis et al., 2014 (Destaca-se a área de estudo do presente trabalho em vermelho).

Para as diferentes associações litológicas do estado de Roraima, são propostos quatro subdomínios litoestruturais-geocronológicos (CPRM 2006, modificado de REIS et al., 2003) contidos na província Tapajós-Parima (SANTOS et al., 2006). A Tabela 1 expõe uma resumida abordagem tectono-estratigráfica sobre os domínios propostos para o estado de Roraima segundo Reis & Fraga (2000); Reis et al. (2003) e CPRM (2006).

Tabela 1: Principais características estruturais, litológicas e geocronológicas dos domínios tectonoestratigráficos de Roraima. Retirada de Almeida 2006.

Domínio	Arcabouço Estrutural	Litologia	Idade (Ga)
Surumu	WNW-ESE e E-W	Vulcânicas e granitoides, rochas sedimentares, intrusões máfico-ultramáficas, rochas supracrustais e ortognaisses	1,98-1,78
Parima	NW-SE	Terreno granito-greenstone, complexos gnáissicos (embasamento), rochas (vulcano)sedimentares, vulcânicas e granitóides	1,96-1,93
Guiana Central	NE-SW	Cinturão de alto grau metamórfico. Ortognaisses, granitos, rochas supracrustais, intrusões AMG e stocks alcalinos	1,97-1,93
Uatumã-Anauá	NW-SE e NE-SW	Terreno granito-gnáissico. Granitóides e vulcânicas. Núcleos do embasamento.	2,03-1,81

Mapeamentos geológicos na escala regional identificaram no Domínio Uatumã-Anauá (Almeida, 2006), sudeste do Estado de Roraima, porção centro-sul do Escudo das Guianas, um

amplo domínio de granitoides calci-alcalinos a alcalinos, além de granitos peraluminosos de natureza crustal subordinados (ALMEIDA, 2006). Esses granitoides estão distribuídos em diferentes associações magmáticas com idades, estilos de deformação e afinidades químicas distintos. Almeida (2006), por meio de mapeamento geológico, realizou o reconhecimento e distinção de algumas dessas associações. As quais são apresentadas na Tabela 2.

Tabela 2: Sequência estratigráfica local

Granitos intrusivos		Granito Moderna	Tipo-A, 1.81 Ga
	Suite intrusiva Madeira	Granito Madeira	Tipo-A, 1.82 – 1.79 Ga
	Suíte Intrusiva Mapuera	Granito Mapuera	Tipo-A, 1.87 Ga
		Granito Abonari	
	Suite Intrusiva Água Branca	Granito Igarapé Azul	Tipo I, cálcioalcalino, 1.89 Ga
		Granito Caroebe — Fácies Alto Alegre	Tipo I, cálcioalcalino, 1.89 Ga
		Granito Caroebe — Fácies Jaburuzinho	Tipo I, cálcioalcalino, 1.90 Ga
	Terreno Granítico Martins Pereira-Anauá	Granito Serra Dourada	Tipo S, 1.96 Ga
		Granito Martins Pereira	Tipo I, calcioalcalino, 1.97 Ga
Embasamento metamórfico	Complexo Anauá		TTG e ortognaisses, 2.03 Ga
	Grupo Cauarane		Metavulcanossedimentares, 2.07 Ga

Os granitoides do setor sul (1,90-1,89 Ga), que incluem os granitos lgarapé Azul e Caroebe da suíte Água Branca (tipo I, cálcio-alcalino), são isotrópicos (ALMEIDA et al. 2006). Ao norte essas rochas intrudem granitos calci-alcalinos tipo I (Martins Pereira) e granitos tipo-S (Serra Dourada), inseridos na porção considerada deformada do DUA. Dois eventos intrusivos, graníticos do tipo A são registrados pelos granitoides Mapuera-Abonari (~1,87 Ga.) e Moderna (~1,81 Ga., SANTOS et al. 2006).

O escudo das Guianas (Almeida et al., 1981) compõe o Cráton Amazônico juntamente ao escudo Brasil Central, duas das maiores regiões de crosta Paleoproterozóica do Planeta (Voicu et al., 2001). Consistem basicamente de cinturões de rocha verde, granulitos, intrusões graníticas, rochas vulcânicas ultramáficas e coberturas sedimentares (Almeida et al., 2000, 2008; Fraga et al., 2009; Reis et al., 2003; Valério et al., 2009). A área de estudo (Fig. 1 A) localiza-se na porção central do Escudo das Guianas. De acordo com o modelo tectono-geocronológico de Santos et al. (2000), o granito Moderna está inserido na porção considerada deformada (deformação heterogênea penetrativa) do Domínio tectono-estratigráfico Uatuma-Anauá (Almeida et al., 2008) da Província Tapajós-Parimã (2,03-1,88 Ga), a qual é dominada

por granitóides calci-alcalinos a alcalinos com idades e petrogêneses ainda pouco esclarecidas.

Os granitos Tipo A do sudeste de Roraima e norte do Amazonas, ocorreram em dois principais eventos magmáticos (Costi et al. 2000, CPRM 2000, 2003): Abonari-Mapuéra (1.88-1.86 Ga) e Moderna-Madeira (1.82-1.79 Ga, Santos et al., 1997., Almeida, 2007). Entretanto, abordagem de cunho estrutural sobre o contexto tectônico de colocação, a sul, do plúton Madeira, postula novas ideias (Siachoque et al., 2017) para o alojamento desses granitos.

Apesar de granitos colocados sob controle tectônico tenderem a adotar formas alongadas conforme o trend estrutural regional e a desenvolver estruturação interna concordante com as estruturas das rochas encaixantes (Castro, 1986; Ingram & Hutton, 1994; Tikoff & Saint Blanquat, 1997), são correlacionados (Santos et al., 1997) ao granito Moderna dois corpos graníticos justapostos e alongados na direção NW-SE, oposta ao trend estrutural regional principal NE-SW. Essem granitos têm alojamento associado a zonas de cisalhamento NW-SE de cinemática dextral (Almeida et al., 2006) que controlam a colocação de granitos Orosirianos na região sudeste de Roraima e norte do Amazonas (Costi et al. 2000, CPRM 2000, 2003, Almeida, 2007; Siachoque et al., 2017). Pelo menos quatro corpos graníticos são correlacionados ao magmatismo Moderna (1.81 Ga).

O alvo do presente trabalho (Fig. 1 B) encontra-se na região de contato entre os granitos Martins-Pereira ([meta]monzogranitos de 1.97 Ga.;Almeida et al., 2002) e Caroebe (dioritos, monzodioritos, monzonitos, tonalitos, granodioritos, monzonitos e monzogranitos de 1.89 Ga.; Almeida, 2006), na zona rural do município de São Luís do Anauá, sudeste do estado de Roraima

4   RESULTADOS

Os resultados obtidos nesta pesquisa encontram-se materializados em forma de artigo submetido ao *Journal of South American Earth Sciences* e são apresentados a seguir:

PETRO-FABRIC PATTERN OF THE MODERNA GRANITE AND COUNTRY ROCKS, SOUTHEASTERN RORAIMA, AMAZON CRATON, BRAZIL

Marcelo Eustáquio Versiani Elias[1]; Carlos Alejandro Salazar[1]

[1]Department of Geosciences, Federal University of Amazonas, Av. General Rodrigo Otávio, n° 6.200, Campus Universitário Senador Arthur Virgílio Filho, Setor Norte, Coroado I, CEP: 69077-000, Manaus, Amazonas, Brazil;

Abstract Several Paleoproterozoic A-type granite bodies intrude the Guiana shield in the Amazonian craton, among them, Moderna granite (1.81 Ga), located between São Luiz do Anauá city and Moderna village, in the southeast of Roraima state. Magnetic anisotropy analyzes (AMS, IRM and thermomagnetic) combined with field

and microstructural focus petrographic data, were used to identify the field of stresses during the Moderna granite emplacement and correlate it with regional tectonics. The monzogranite with variations for syenogranite Moderna, presents NW-SE elongation in the contact zone between the calc-alkaline Martins Pereira (1.96 Ga) and Caroebe (1.89 Ga) granites, in transitional contact with these units, marked by hydrothermal alteration features, which do not affect the orientation of the rock's magmatic fabric and is responsible for its characteristic red color, associated with plastic deformation. The magnetic fabric, marked by magnetite, and magmatic fabric orientations of the three analyzed rock units have genetic equivalence and main direction around the E-W to NE-SW axis, in agreement with the regional structural framework that controls the Orosirian plutons emplacement in the central portion of the Guiana shield. Although there is a great difference in age, reported in the literature, between the crystallization of the granite units analyzed, these rocks developed minerals fabrics with similar orientation and strain mechanisms, indicating that the granite emplacements occurred syn-kinematicly under a dextral transpressive tectonic regime with plastic strain. Localized shear zones, sub-parallel to magmatic foliation orientation, demonstrate the persistence of the effort field at the end of the plutonic housing, while discrete posterior shear zones, NW-SE direction, deform restricted portions of the rock units in solid state.

1. INTRODUCTION

The Amazonian Craton hosts several A-type granite bodies, some of them are source of essential to human development mineral resources, such as Pitinga deposits, related to Paleoproterozoic A-type Madeira granite (Costi et al. 2000; Bastos Neto et al., 2009; Bettencourt et al., 2015) located in the northern of Amazonas state. Although petrologic, geochemical and structural data involving the A-type Moderna granite are scarce, there is a geochronological data (Santos et al., 1997) that points to an Orosirian age very similar to Madeira granite, which has a large collection of geological studies (Carvalho Filho et al., 1984; Costi, 2000; Costi et al., 2002, 2009; Ferron et al., 2010, 2006; Lenharo et al., 2003; Pierosan et al.,2011a, b; Valério et al., 2009) including, recently, structural detail geology (Siachoque et al., 2017), located at the same latitude, 200 km south of Moderna granite. Studies of this nature, have contributed to a better understanding of granite plutons emplacement models.

A-type granites (Chappell & White, 1974; Loiselle & Wones, 1979) are genetically related to distensive tectonic environments (Martin et al., 1994; Dall'Agnol et al., 2005, Bonin et al 2007, Zhao et al., 2008, Karsli et al., 2012; Frost & Frost, 2011). This correlation has predominated in the tectonic interpretations of Amazonian craton A-type granites (Santos et al., 1997; Dall'Agnol et al., 1999; CPRM, 2003). however, occurrences of A-type granites generated in an environment of distal orogeny (Ahall et al., 2000) on the Baltic shield, amalgamated with the Guianas shield in the supercontinent Columbia during the Orosirian (Johansson, 2009; Evans, 2013).

In addition, granitic magmatism is an important crust former and is considered a crustal thermal changes indicator (Bonin et al., 2007). Plutons behave as potential tectonics acting markers at the time of their accommodation. When a pluton intrudes in the crust (Hutton 1988, Paterson et

al.1989, Miller & Paterson 1994, Fowler et al 1995), mineral distribuction acquires a textural arrangement in order to indicate the tectonic regime in which it was positioned. In general, the minerals tend to form fabrics compatible with the orientation of the dominant efforts that affect them. Petro- fabrics tend to register itself during the pluton crystallization phase (Kerr & Lister 1991; Bouchez et al., 1997, Petford et al., 2000) or in the solid state by deformation (Tullis & Yund, 1977, Patterson et al. 1989, Vernon et al., 2000, Rosemberg et al., 2005). Analyzes of granite petro-fabrics and their characterization make it possible to reconstitute the field of stresses acting on the pluton at the moment of its placement. Thus, the comparison between the physical conditions of granite accommodation (Brown & Solar 1998, Rosenberg 2005, Zac et al., 2012), reflected in the petro-fabric, and the physical conditions responsible for the regional deformation recorded in host and adjacent rocks, allows inferences about the region tectonic evolution (Fossen et al., 1994; Fossen & Tikoff, 1998).

Structural studies on granites focus on the understanding of mechanisms related to the activation of structures that control the accommodation space (Hutton et al., 1988, Patterson et al., 1989). The relationship between these structures and the regional evolution of the stress field during magmatism (McCarty et al., 2000; Zibra et al., 2017). The results of such studies have led to postulate the existence of crust anisotropies, developed under different tectonic regimes (transcurrent, transpressive or transtrative), which control pluton accommodation (Neves et al 1996, Gleizes et al., 1997; Bouchez et al.,1997; Zibra et al., 2017; Brown, 2001; Žák et al., 2012; Zibra et al., 2017).

When crystallize, granites usually do not register clearly outcropping scale distinguishable petrofabric, to be related to the deformation associated to their placement processes in the crust. However, such fabrics can be recognized by anisotropy of magnetic susceptibility (AMS; Bouchez, 1997; Tarling & Hrouda, 1993; Archanjo et al., 1995; Žák et al., 2009). Asymmetric and nonlinear ASM fabrics usually developed in A-type granites can be obliterated by late-to post-magmatic hydrothermal alteration events (Archanjo et al., 2009, Nédélec et al., 1994, 2015, Price et al. 1998), which may even produce fine magnetite and hematite in magnetite-granites (Nédélec et al., 2015)

The present research focuses on the understanding and characterization of the local structural regime, and its consequent relation with the regional structural regime, related to the A-type Moderna granite emplacement (1.81 Ga). For this, samples of Moderna and adjacent granites (Martins Pereira and Caroebe) were analyzed. The emplacement mechanisms and the deformation regime of magmatic to solid state were characterized based on AMS; microstructural petrographic, and field structural data, in order to identify the distribution and

kinematics of the pluton internal deformation.

2. GEOLOGICAL SETTING

The Amazonian Craton is formed by the shields of the Guianas and Central Brazil, in a continuous crust, composed by several fragments that form the Craton (Almeida et al., 1981). It consists mainly of greenstone belts, granulites, granite intrusions, ultramafic volcanic rocks and sedimentary covers (Almeida et al., 2000, 2008; Fraga et al., 2009; Reis et al., 2003; Valério et al., 2009). The study area is located in Guiana Shield central portion (Fig. 1 A) and Moderna Granite intrudes the northern portion of the Uatumã-Anauá Domain (Almeida et al., 2007), in the Tapajós-Parima Province (Santos et al., 2000). This subdomain is characterized by penetrative heterogeneous deformation and widespread calc-alkaline and alkaline granitoids. The Tapajós-Parima Province in SE Roraima and NE Amazonas shows two main A-type granitic events (Costi et al., 2000, CPRM 2000, 2003): Abonari-Mapuera (1.88-1.86 Ga) and Moderna-Madeira (1.82-1.79 G; Santos et al., 1997, Almeida et al., 2007). Furthermore, a structural approach to the tectonic context of the Madeira pluton postulate new ideas (Siachoque et al., 2017) for the accommodation of these granites. In this sense, other granitic bodies in the region must be analyside.
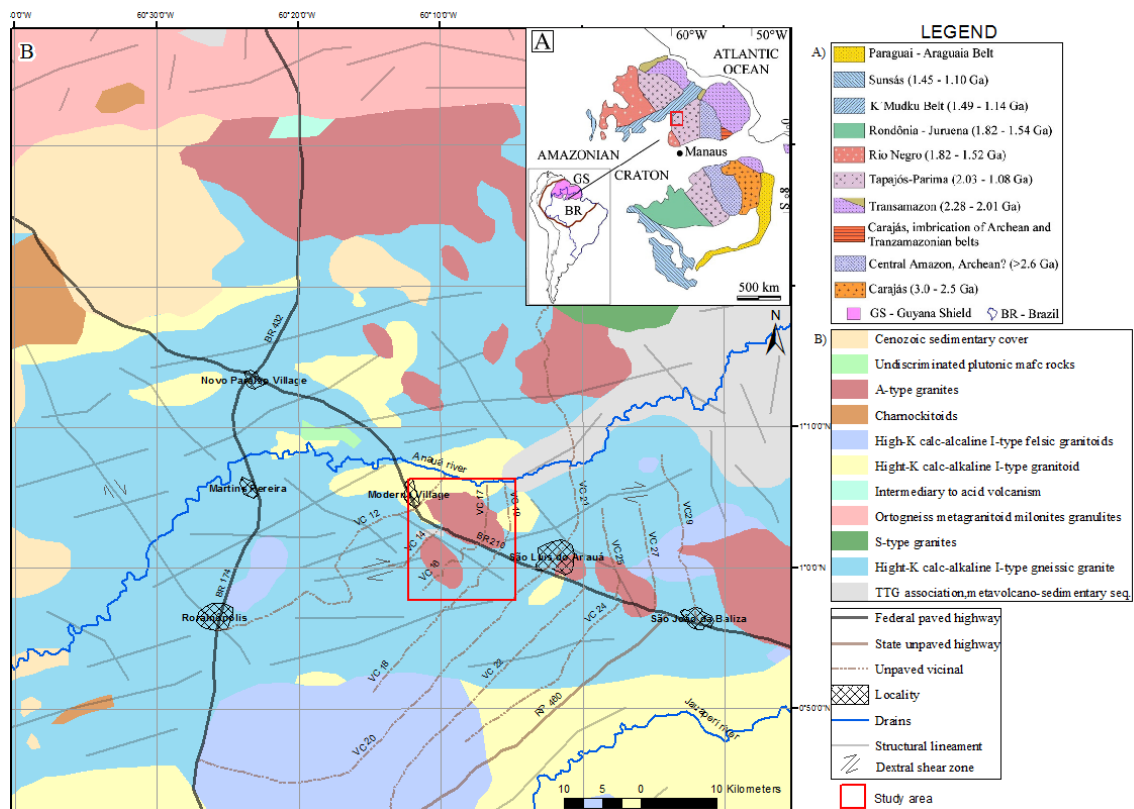
Fig. 1. Location of the study area. (A) Guianian Shield highlighted on the South America map with tectonic provinces of the Amazonian craton (Santos, 2003); (B) Simplified geological map of the Northern Uatumã-Anauá Domain (Almeida, 2006), highlighting the study area.

Granites with placement in tectonically active areas tend to present bodies with greater

structural control and the presence of internal structures compatible with the regional structuring (Castro, 1986; Ingram and Hutton, 1994; Tikoff and Saint Blanquat, 1997). Moderna granite (Santos et al., 1997) are two juxtaposed and elongated granite bodies in NW-SE direction, opposite the main regional structural trend, which emplaced controlled by NW-SE shear zones of dextral kinematics (Almeida et al. , 2006) that control the placement of Orosirian granites in Roraima southeast and northern Amazonas region (Costi et al., 2000, CPRM 2000, 2003, Almeida, 2007). At least four granite bodies are correlated to Moderna magmatism (1.81 Ga), the target of this work (Fig. 1B) intrudes granitic rocks in the contact region between Martins-Pereira (1.97 Ga [meta] monzogranites; Almeida et al., 2002) and Caroebe (1.89 Ga diorites, monzodiorites, monzonites, tonalites, granodiorites, monzonites and monzogranites; Almeida et al., 2007) in the rural area of São Luís do Anauá city, southeast of the Roraima state (Fig. 2A).

3 RESULTS

This item shows the field relationship and petrography of Moderna Granite and country rocks (Fig 2B). The main features of these rocks are described below.

MARTINS PEREIRA GRANITE

Field Geology

The Martins Pereira Granite occurs in the west and south of the mapped area. They are monzogranites with variations for granodiorites and tonalites, which occur with dark gray to light gray and porphyritic texture with centimetric phenocrysts (1 to 6 cm) of K-feldspar in medium to fine quartz-feldspathic matrix (Fig. 3 A). Felsic pockets of ellipsoidal or irregular geometry with a length of 20 to 80 cm in length and fine to medium equigranular texture are common. The rocks exhibit well-defined primary foliation with feldspar aligned crystals with tabular shape and locally exhibit milonite texture marked by stretched feldspar and aligned mafic minerals, particularly evident in the vicinity of contact with Caroebe and Moderna granites in the southern portion of the study area. In these portions, aligned tabular feldspars occur in abrupt contact with stretched feldspars, rocks that preserve primary deformation characteristics along with mesomylonitic deformation features, which define narrow and sinuous shear bands.

Pockets and lenses of light gray rock and medium to fine equigranular texture, exhibit orientation concordant to host rock primary foliation and internally they have isotropic appearance. They are restricted bodies and the boundaries are lobed to irregular and usually of diffuse transition, that materialize migmatization effects due to Caroebe-Igarapé Azul

magmatic event (1,90 Ga; Almeida et al. 2007 e Almeida and Macambira 2007).

There are also small dark gray enclaves of diorite composition and medium to fine equigranular texture, with elliptical shape and orientation concordant with the host rock foliation. These enclaves usually have internal structures marked by aligned biotite crystals, with formation of lenses oriented according to the mylonitic foliation.
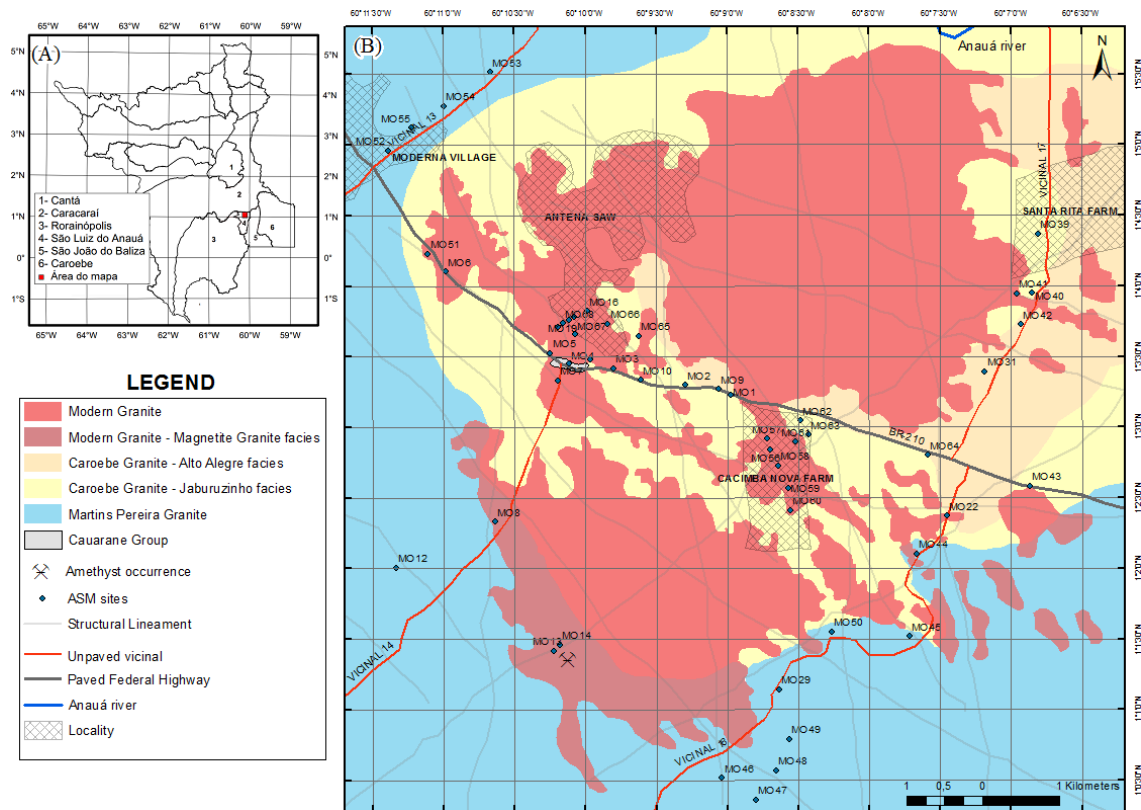
Fig 2. (A) Location of the study area in the state of Roraima; (B) Lithological map of the study area with the location of the ASM sampling points.

Light gray granite dykes (5 to 12 cm in width) of fine texture, outcrop in a restricted way, embedded concordant with the plane of primary foliation, contain mafic enclaves and locally form lenses oriented according to milonitic foliation (Fig 3 C).

Petrography

The rocks are composed by isolated K-Feldspar (34% -54%) phenocrysts that are presented in tabular form or stretched; in the matrix, they form clusters of subhedral crystals, ranging in size from ~ 1.0 cm to ~ 6.5 cm; commonly present internal oscillatory zoning, undulose extinction and flaming-perthite development (Fig. 3 D). Plagioclase (17%-26%) occurs as individual crystals of ~ 1.0 cm, or in aggregates, with subhedral to anhedral and polysynthetic twinning; presents a planar sliding that generates boundary migration; also shows size reduction with subgrain rotation (Fig. 3 E) Quartz (9% -25%) is distributed in crystalline aggregates, with anhedral forms, normally stretched, and 0.2 to 1.1 cm in length, arranged interstitially in the

boundaries between feldspars, with planar sliding, size reduction, and boundary migration. Biotite crystals form oriented aggregates with some individual crystals of hornblende and magnetite (Fig. 3 F). Biotite represent 7% to 13% in composition volume of the rocks and exhibit normally subhedral shapes; they are often aligned, defining the preferred shape orientation.
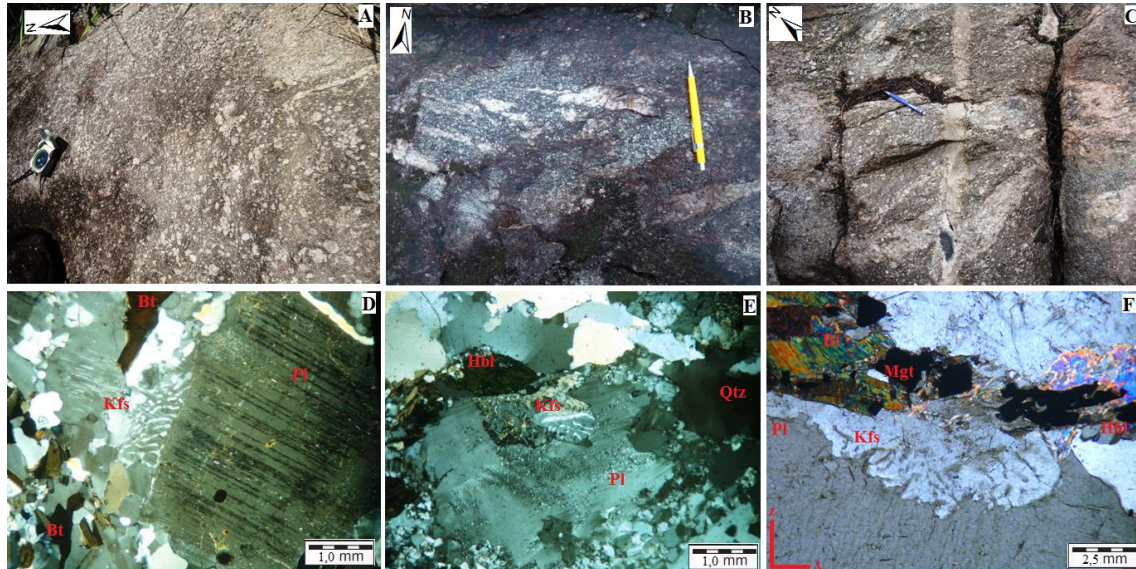
Fig. 3. Field and petrographic features of Martins Pereira Granite.. (A) Magmatic flow oriented K-feldspar phenocrysts, locally related to shear with plastic deformation and leukogranitic pockets in upper right corner (MO48); (B) stretched feldspars marking E-W shear zone (MO 29); (C) tonalite dyke with diorite enclave oriented according to shear zones mylonitic foliation with formation of felsic pockets oriented according to the magmatic flow foliation (MO29). Photomicrographs in crossed nichols: (D, E) biotite (Bt) oriented, associated to subhedral hornblende (Hbl) filling fracture; stretched plagioclase (Pl) with polysynthetic twining, perthite K-feldspar (Kfs) exhibit size reduction with subgrain rotation; Plagioclase (Pl) with size reduction by subgrain rotation, and anhedral quartz (Qtz) with undulose extinction. (F) aggregates of biotite (Bt), altered hornblende (Hbl) and oriented euhedral magnetite (Mgn) (MO46).

CAROEBE GRANITE

The Caroebe Granite occurs maily in the northeast of the mapped area. Corresponds to rocks grouped in two facies: i) Jaburuzinho and ii) Alto Alegre.

i) Jaburuzinho facies

Field Geology

The Jaburuzinho facies is represented by light gray monzogranite, which varies for granodiorite and tonalite. These rocks exhibit porphyritic texture in coarse to medium matrix and medium to coarse equigranular texture, constituted by tabular and anhedral phenocrysts of K-feldspar arranged according to preferential shape orientation, in a plagioclase, quartz and mafic minerals matrix. Subcircular to elliptic millimetric hornblende, biotite and opaque aggregates with diffuse boundaries, which usually show preferential shape orientation and are arranged aligned according to the magmatic flow (Fig. 4 A). Jaburuzinho facies is in intrusive and locally

tectonized contact with the Martins Pereira granite, usually associated to shear zones; and it is in transitional contact with Alto Alegre facies, where it occurs with difuse contact. Lenticular fine texture enclaves of dioritic composition present elliptic forms with greater axis between 5 cm and 20 cm, and fine and medium textured felsic granite enclaves present major axis of 10 cm to 40 cm. These felsic enclaves contain dropped feldspar crystals and are aligned according to the host rock felsic minerals orientation. The Jaburuzinho facies granites are intruded by fine to medium texture granite of Alto Alegre facies, in dikes form with diffuse boundaries whose orientation is similar to the magmatic foliation of the nesting rock (Fig. 4 B).

Petrography

The mineral composition (Fig. 4 C) includes tabular to anhedral plagioclase (20% -37%) crystals, with well-marked oscillatory zoning (Fig. 4 D), polysynthetic and Carlsbad twinning, sometimes altered to muscovite of up to 0,1 mm in size, mainly in the core of zoned crystals. Internal plastic deformation mechanisms in plagioclase crystals include planar slipping that generates boundary crystal migration and lobed contour (Fig. 4 E), locally with cusp boundary; there is still folded mechanical twinning and size reduction with subgrain rotation. Microperthitic (Fig. 4 F) K-feldspar (10% - 30%) occurs as isolated tabular phenocrysts and, when it is part of the matrix, in aggregates with anhedral to subhedral shape; contains plagioclase, magnetite and apatite inclusions, as well as exhossolutions of mirmekite in the limits with plagioclase phenocrysts in addition to stretching and undulating extinction without crystal size reduction. Quartz (7% -25%) presents itself as isolated anhedral crystals with undulose extinction or in aggregates with sutured contact associated to mafic minerals, presenting stretch with planar sliding and reduction of grain size with boundary migration. Subhedral to euhedral hornblende crystals (3% - 19%), in clusters or isolated in the matrix, occasionally present mechanical twinning (Fig. 4F) and partial alteration for biotite and chlorite on the edges; some crystals have fractures filled by quartz (Fig. 4 E, F) crystals (1% - 20%), in aggregates or isolated in the matrix, commonly present partial alteration for biotite and chlorite. Biotite Crystals (5% -15%) occur with lamellar shape in clusters, associated with hornblende, epidote and magnetite crystals, generally aligned along the major axis. The accessory minerals (4% -9%) comprises euhedral to subhedral epidote commonly associated with hornblende, biotite and magnetite aggregates; allanite as subhedral zoned crystals, associated to biotite; titanite with losangular or subhedral shape; and prismatic euhedral zircon. Muscovite and chlorite occur as secondary minerals.
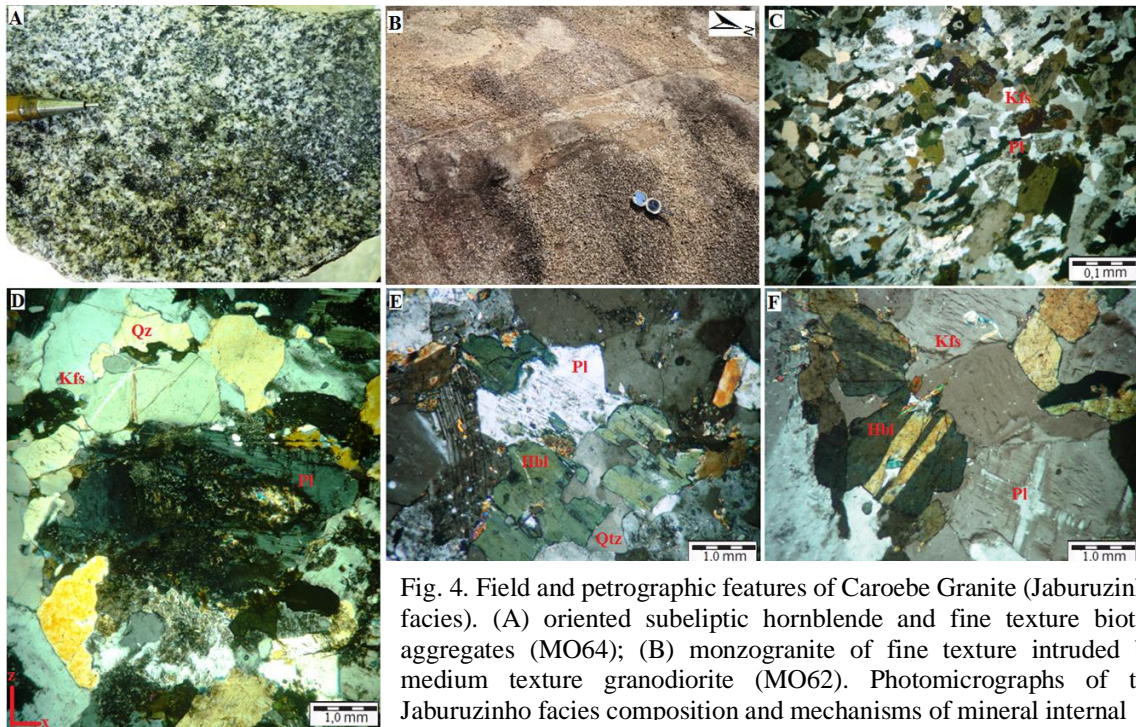
Fig. 4. Field and petrographic features of Caroebe Granite (Jaburuzinho facies). (A) oriented subeliptic hornblende and fine texture biotite aggregates (MO64); (B) monzogranite of fine texture intruded by medium texture granodiorite (MO62). Photomicrographs of the Jaburuzinho facies composition and mechanisms of mineral internal deformation: (C) usual rock texture defined by the preferred orientation of K-feldspar (Kfs) and zoned plagioclase (Pl) crystals (MO25); (D) stretched quartz (Qz) with bounded boundaries filling K-feldspar fracture (Kfs), plagioclase (Pl) zoned with grain boundary migration and internal slip (MO25); (E) Hornblende crystals (Hbl) with mechanical twinning, altered for biotite at the border and with irregular internal fracture, filled by quartz (Qz) that shows a cusp boundary following hornblende cleavage directions, and plagioclase (Pl) with folded polysynthetic twining planar sliding and crystal boundary migration (MO25); (F) microperthitic K-feldspar (Kfs) crystals, hornblende (Hbl) with mechanical twinning and internal plagioclase (Pl) filled fracture with planar sliding (MO25).

ii) Alto Alegre facies

Field Geology

Is constituted by biotite monzogranite that varies to granodiorite, exhibits equigranular fine to medium texture and medium to coarse porphyritic texture; it still comprises restricted syenogranite of medium equigranular massive texture (Fig. 5 A). Locally it has light gray K-feldspar oriented phenocrystals in plagioclase, quartz, biotite and amphibole matrix, that marks the magmatic foliation. It presents dioritic mafic enclaves of fine texture with elliptical shape, where the largest axis is orientated according to the alignment of K-feldspar crystals. It contains monzogranite xenoliths near to the limits with the Jaburuzinho facies (Fig. 5 B).

Petrography

The dominant rock (Fig. 5 C) is composed by tabular to anhedral plagioclase (20% - 35%) crystals with polysynthetic gemination, eventually stretched, with about 0.3 mm of major axis with subtle preferential shape orientation, which form aggregates; presents composite zonation well marked by the alteration to sericite, more present in the nucleus and internal planar sliding (Fig. 5 D) that acts as an anti-static dextral shear marking on the x-axis. K-feldspar (12% -35%)

anhedral to subhedral phenocrysts with biotite, plagioclase and oxides inclusions, presents mantle-core structure, flamming-perthite, stretch, planar slidding, crystal boundary migration, undulose extinction, size reduction with border corrosion and cusp limits; in matrix, it is normally oriented according to the arrangement of plagioclase crystals and mafic minerals. Two generation (Fig. 5 E) anhedral quartz crystals (15% -30%) occur in aggregates or included in K-feldspar phenocrysts of and plagioclase and K-feldspar; the first generation commonly exhibits undulose extinction in chessboard, planar slidding, stretching and preferential orientation of shape; the second one presents with fine texture interstitial in fractures. Biotite (6% -12%) occurs as isolated crystals with lamellar habit and preferential shape orientation, filling fractures or included in feldspar; It formd aggregates with amphibole crystals, exhibits inclusions of iron oxides and change in edges for muscovite (Fig. 5 F); locally, fine interstitial biotite forms a second generation of crystals. The Hornblende (4%-14%) has a constant presence as 0.2 mm in length subedial crystals and is usually associated to biotite in clusters of aligned crystals, where occurs anhedral and altered to chlorite. Among the accessory minerals, it is observed subhedral epidote, associated mainly to hornblende; anhedral titanite associated with iron oxides; euehdral allanite with alteration halo when included in biotite; apatite and zircon in isolated prismatic crystals. Muscovite and chlorite occurs as alteration product mainly of plagioclases, biotite and hornblende respectively.

MODERNA GRANITE

Field Geology

The so-called Moderna Granite appears for about 35 km^2, mainly in the form of boulders (Fig. 6 A). Its main features are observed in the Serra da Antena region, between São Luiz do Anauá city and Moderna Village (Fig. 2 B). It has a coarse, slightly porphyritic texture, characteristic reddish color (Fig. 6 B), which becomes progressively paler further it is from of Serra da Antena, giving rise to gray pinkish to yellowish colors. It presents magmatic foliation defined by the discrete preferential shape orientation of feldspar crystals and, locally, the preferential orientation of stretched quartz and of mafic minerals aligned define mylonitic foliation.

Incomplete assimilation features demonstrate a diffuse and progressive transition to the Caroebe Granite rocks. Xenoliths of varying sizes and low degrees of assimilation represent intrusive contact with Cauarane Group metamorphic rocks (Fig. 6 A). Granitic composition pegmatitic dykes, with thickness between 1 cm and 50 cm, intrude Moderna granite. Syenogranitic dykes of fine texture and widths ranging from 20 to 70 cm are also finded.
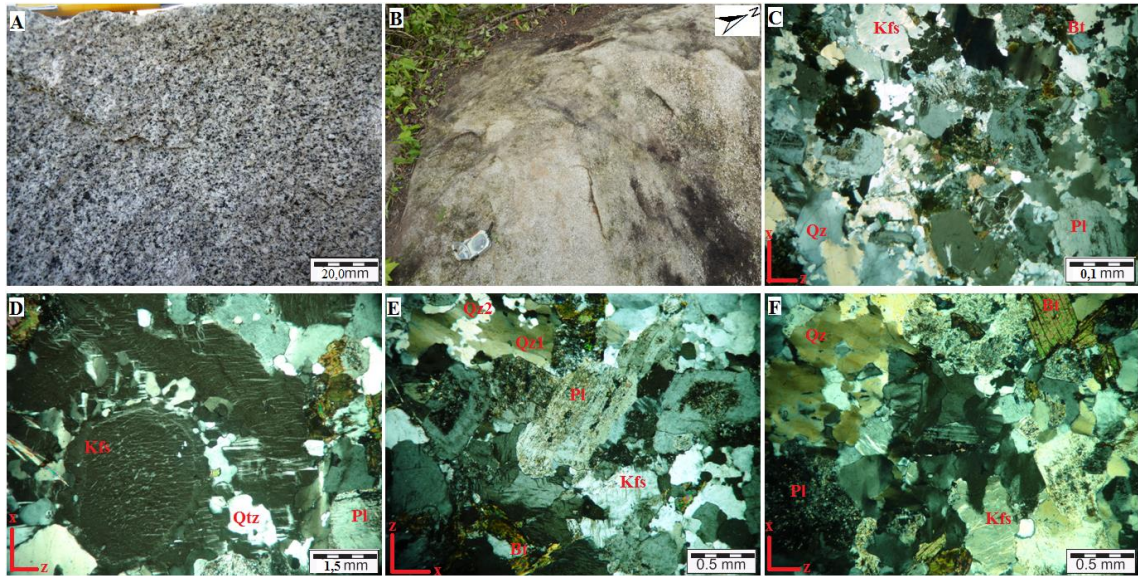
Fig. 5. Field and petrographic features of Caroebe Granite (Alto Alegre facies): A) medium-textured, sub-porphyritic to equigranular monzogranite (MO38); B) fine to medium-textured rock, where a mylonitic foliation is observed, in contact with medium-to-coarse matrix, with magmatic foliation (MO33). Photomicrographs of mineral composition and internal deformation: C) aggregate of K-feldspar (Kfs) subhedral, plagioclase (Pl) anhedral, biotite (Bt) crystals and quartz crystals (Qtz), subtly aligned (MO33). D) K-feldspar crystal (Kfs) with folded perthites and with plagioclase crown (Pl) and quartz (Qtz) anhedral, displays planar slidding, tartan twinning and border migration (MO38). E) quartz (Qtz1) stretched with planar slid and internal fracture filled by quartz (Qtz2) of posterior generation and plagioclase (Pl) with planar sliding (MO33). F) Deformed fibrous biotite (Bt) with corroded edges with fine iron oxides, quartz (Qtz) with planar sliding in two crystallographic directions and a cusp limit with microperthític K-feldspar (MO38).

Petrography

Moderna Granite shows monzogranite (dominant) to syenogranite types, in intrusive contact with Martins Pereira granites, presents annomolous magnetite concentration in the Magnetite-granite facies. Moderna Granite mineral composition consists of (Fig. 6C) tabular subhedral to anhedral perthitic K-feldspar (25% - 55%) crystals with a mean size of ~ 0.5 mm, that commonly have undulose extinction, oscillatory zoning and cloudy appearance; some of the crystal boundaries are lobed due to planar slidding; Inclusions of biotite, iron oxides and plagioclase with Carlsbad and Tartan-type twining are common.

Tabular subhedral plagioclase crystals (22% -36%) with a mean size of ~ 0.4 mm present polysynthetic twinning and 3:1 axial ratio. Preferential shape orientation according to k-feldspar crystals marks the rock magmatic foliation. Plagioclase crystals is commonly altered to sericite, mainly in the zoned crystals' core, where acicular to prismatic muscovite crystals develop. It presents mechanical twinning and mirmekite when in contact with K-feldspar crystals. And also occurs as perthitic K-feldspar oriented inclusions (Fig. 6 D) and as new grains by size reduction with subgrain rotation (Fig. 6 E). Quartz (22% -30%) occurs as anhedral crystals with a mean size of ~ 0.3 mm, usually exhibit undulose extinction, planar sliding (Fig.

6 F) and subtle preferential shape orientation; it also presents stretched or interstitial filling fractures or in aggregates. Hornblende crystals (5% -12%) are generally isolated, with a subhedral shape an average size of 0.3 mm and usually exhibit poiquilitic texture with plagioclase, iron oxides, epidote and allanite inclusions; crystals edges and cleavage planes are eventually altered for biotite and/or chlorite; it also occur in a diffuse anhedral shapes in mafic aggregates, altered for chlorite. Biotite (4% - 12%) occurs as dispersed crystals up to 3.0 mm in length, with elongated shape and fibrous appearance by well-defined cleavage; it also occurs as 0.4 mm lamellar crystals in mafic aggregates, that present alteration for chlorite and sericite on the borders. A second generation of biotite (Fig. 7 A, C, D) displays radial acicular habit in mafic aggregates, including or between feldspar grains and filling fractures, it represents a late phase of internal deformation (Fig. 7 C). The accessory minerals (4%-11%) are: epidote euhedral crystals up to 0.2 mm or fine anhedral forming mafic aggregates; allanite zoned euhedral crystals of up to 0.3 mm or as aggregate of fine prismatic crystals; losangular titanite (Fig. 7 B), zircon and apatite prismatic crystals. Opaque minerals with 0.3 mm in diameter, usually exhibit euhedral to subhedral shape, they occur in ellipsoidal form or as aggregates that fill fractures. Muscovite and chlorite occur as secundary minerals.
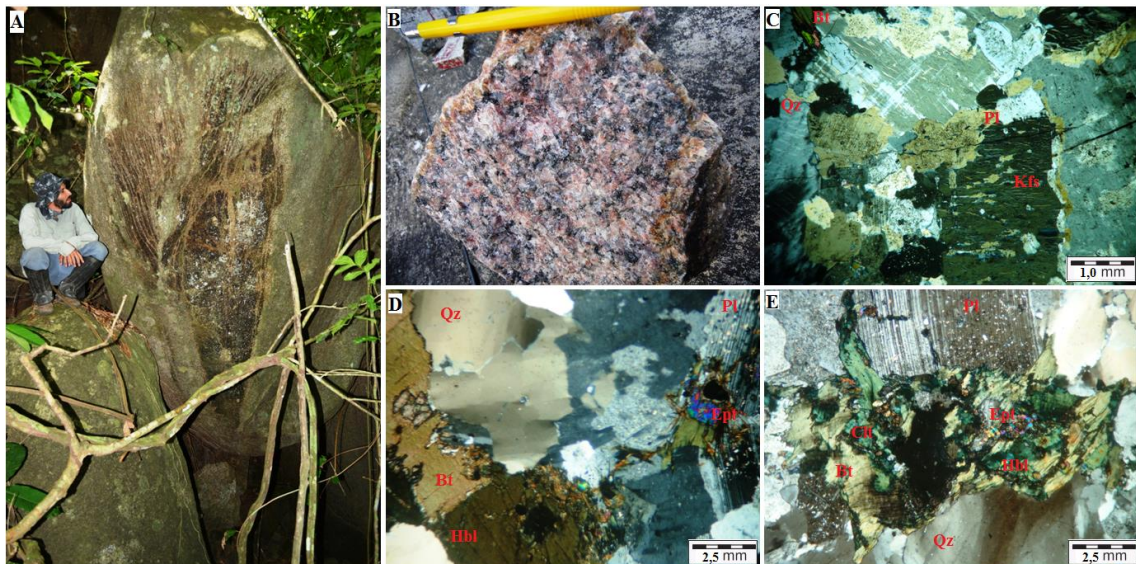
Fig. 6. Field and petrographic features of Moderna Granite: (A) xenolith of the Cauarane Group with about 3.0 m length in Moderna Granite boulder (MO20); (B) hand sample with coarse texture and Moderna Granite diagnostic reddish color (MO35). Photomicrographs of mineral composition C) Perthitic K-feldspar (Kfs) with mechanical twinning, plagioclase (Pl) inclusions and cusp boundaries with zoned plagioclase; quartz (Qtz) occupying fracture in K-feldspar and lamellar biotite (Bt) (MO6); (D) biotite (Bt) with inclusion of euhedral epidote (Ept), hornblende (Hbl) with magnetite inclusion and altered in border to biotite (MO6); (E) aggregate of biotite (Bt) and hornblende (Hbl) crystals altered for chlorite (Clt), epidote (Epd) and iron oxides, occupying angular and discontinuous fractures in plagioclase (Pl) with displaced mechanical twinning; quartz (Qtz) with planar sliding (MO34).

Hornblende and fibrous biotite crystals are partially replaced by chlorite (Fig 7A, B); Epidote

crystals are formed associated with acicular reddish fine secondary biotite (Fig. 7A, C, D), filling interstices between crystals and discontinuous fractures; Plagioclase crystals with internal ateration to clinozoisite (Fig. 7D). Are characteristics of alteration observed mainly in the Moderna isotropic granite of Serra da Antena or in portions of the rock submitted to mylonitic deformation. These characteristics are shown associated with high temperature deformation mechanisms, such as folded mechanical twinning and fluted oriented mirmekite (Fig. 7F) in plagioclase crystals in contact with crystals of microperthitic K-feldspar, planar sliding with boundary displacement, internal undulose extinction reflecting size reduction, quartz stretching with internal planar sliding generating chessboard extinction and incipient sigmoidal shape (Fig. 7G). Shear zones produce discrete mylonitc bands showing strain mechanisms such as size reduction with subgrain rotation, tartan twining development, fractures planar sliding in feldspar crystals (Fig. 7G), ondulations recorded on flaming perthite (Fig. 7 H) and locally, they form pressure shadows in plagioclase crystals with kink folded polysynthetic twinning (Fig. 7 I).
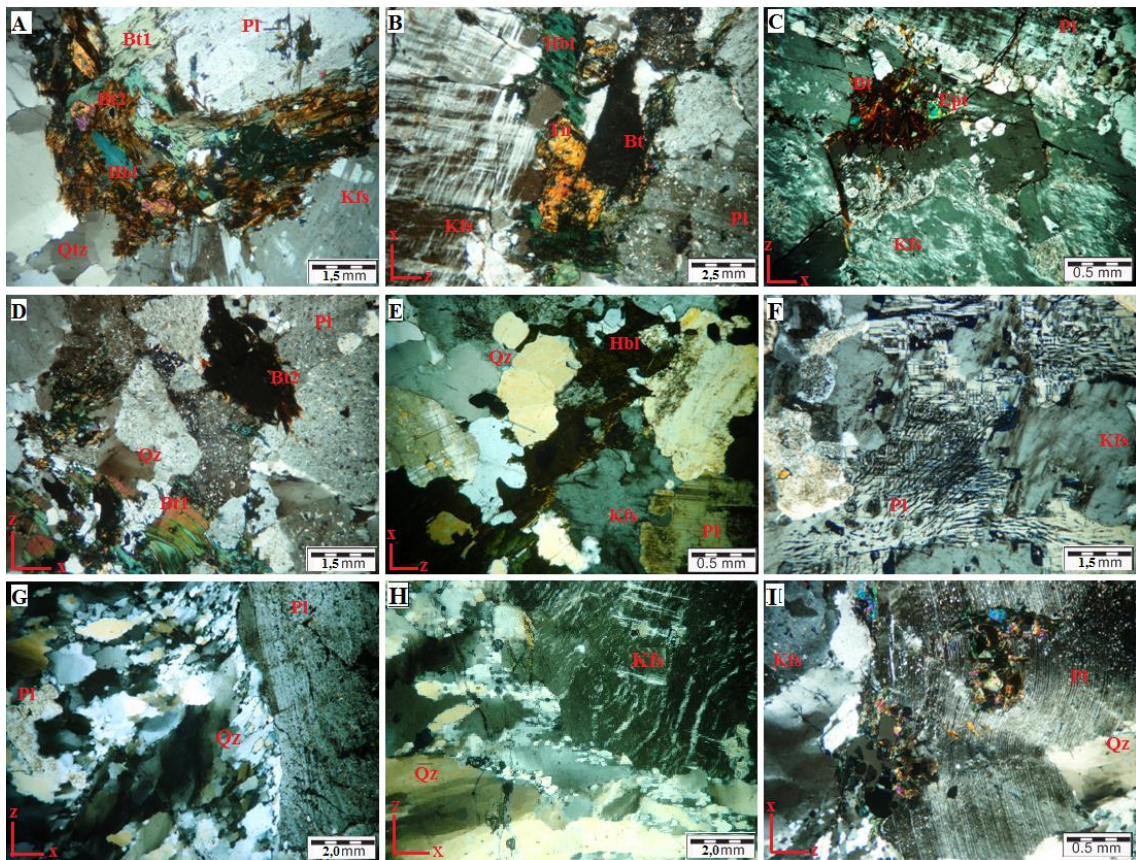
Fig. 7. Photomicrographs of altering minerals and strain mechanisms in Moderna granite: A) fibrous biotite (Bt1), corroded at the edges, and second generation of acicular biotite (Bt2) filling interstices; modified amphibole for chlorite, subhedral epidote, allanite, anhedral quartz (Qtz) with undulose extinction, K-feldspar (Kfs) and plagioclase (Pl) internally deformed (MO17); (B) K-feldspar (Kfs) with planar sliding, altered plagioclase (Pl) with undulose extinction; altered hornblende (Hbl) and biotite (Bt) associated with euhedral titanite (Tn) (MO34); (C) Plagioclase (Pl) and K-Feldspar with planar sliding and fractures filled by acicular biotite and epitope (Ept)

(MO20); (D) Biotite (Bt1) folded, altered to sericite, and biotite (Bt2) associated with epidote, chloritized hornblende and hematite, in altered to muscovite plagioclase (Pl) and quartz (Qtz) with undulose extinction (MO34); (E) anhedral hornblende (Hbl), with lobed boundaries, K-feldspar (Kfs) with undulose extinction and plagioclase (Pl) cusp contact with folded mechanical twining and stretched quartz (Q24); (F) fluidic mirmekite in plagioclase (Pl) and K-feldspar (Kfs) with plastic deformation and undulose extinction (MO24); (G) stretched quartz with planar sliding forming a pressure sheet in folded and fractured plagioclase crystal (Pl) (MO35); (H) stretched quartz (Qtz), flaming perthits in K-feldspar (Kfs) with draging fold (MO34); (I) Kink fold in plagioclase (Pl) with inclusions of hematite, biotite, muscovite and epidote (MO34).

3. SAMPLING AND METHODS

A total of 184 one-inch in diameter cores were sampled using a hand-held drill at 51 stations across the study area (Fig. 2 B). Cores were oriented in-situ with a magnetic compass. In the laboratory, samples were cut into standard specimens of 2.2 cm in height using a diamond-coated wheel saw, providing 796 specimens for magnetic anisotropy measurements (AMS). Statistical treatment and analyses of all measurements were conducted using the ANISOFT 4.2 program (Agico, Czech Republic).

Magnetic susceptibility and its anisotropy were measured at low field (800 A/m, 950 Hz) on a MFK1-FA Kappabridge (Agico, Czech Republic) susceptibiimeter by an automated sample handling system, in which each sample is rotated through three orthogonal planes. Table 1 shows the AMS data which are represented by the magnetic susceptibility ellipsoid with three orthogonal axes: k1 (maximum), k2 (intermediate) and k3 (minimum). Anisotropy ellipsoids were calculated using Jelinek (1977) statistics. The mean bulk susceptibility of each specimen was computed as km = (k1 + k2 + k3)/3. The symmetry of the magnetic ellipsoid is represented by the T parameter (Jelínek, 1981), defined as T = (2 ln (k2/k3) / ln (k1/k3) − 1). It varies from −1 (prolate ellipsoid) through 0 (neutral or triaxial ellipsoid) to +1 (oblate ellipsoid). The degree of anisotropy is indicated by:

$$Pj = \exp\sqrt{2\sum_i(\ln k_i/k_m)^2}$$, where I = 1 to 3 (Jelínek, 1981).

The magnetic mineralogy was investigated through isothermal remanent magnetization (IRM) acquisition curves and thermomagnetic profiles. Both experiments were carried out using selected Km representative specimens from each rock units. Isothermal remanent magnetization data were obtained using a JR6A magnetometer and a pulse magnetizer MMPM 10. IRM curves were determined from 0 up to 2000 mT, at 10 mT intervals. The data was analyzed using cumulative log Gaussian (CLG) curves (Kruiver et al., 2001). Thermomagnetic curves, showing the variation of magnetic susceptibility (k) with temperature, were obtained using a KLY-4S Kappabrigde (Agico, Czech Republic) susceptometer coupled to CS3 furnaces. At each 2 ° C temperature variation, the susceptibility is recorded in a cycle ranging from 20 ° to 750 ° C (the heating cycle) and returns to 20 ° C (the cooling cycle) at a constant magnetic field H= 250 A.

The measured data were processed using the program Cureval 8 (Agico, Czech Republic). All rock-magnetic analyses were performed at the Laboratório de Paleomagnetismo, of the Instituto de Astronomia, Geofísica e Ciências atmosféricas (IAG) of the Universidade de São Paulo (USP). Subsequently the results were related and compared to the petrographic and structural data of the granitic units orientated according classical criteria (e.g. Fossen, 2010).

4. ANISOTROPY OF MAGNETIC SUSCEPTIBILITY

4.1. Magnetic mineralogy

In metallographic analyzes under microscope, Martins Pereira granite show 5% to 10%, in volume, of subhedral to anhedral magnetite individual crystals up to 1,0 mm in size or in clusters, associated with hornblende and biotite. It occurs commonly stretched and folded in hematite solid solution in deformed bands with mylonitic texture silicates (Fig. 8 B). Pyrrhotite (Fig. 8 B) occurs strictly while pyrite and chalcopyrite are common. The Caroebe Granite presents between 1% and 5% of magnetite, which occurs as euhedral to subhedral crystals with 0.2 mm in size forming aggregates. It is characterized by the presence of heterogeneous dark gray stains like patina in the crystal, indicative of localized oxidation to the metastable phase (maghemite; Fig. 8 C). Also occurs anhedral hematite crystals associated with hornblende and biotite crystals edge alteration. In Moderna Granite, magnetite occurs between 1% and 4% in volume, as isolated subhedral crystals, usually altered for maghemite. Fine hematite (<1%) occurs as isolated crystals or associated with hornblende and biotite altered, epitote and titanite, representing a paragenesis related to plastic strain mechanisms (Fig. 7). In Moderna Granite affected by shear zones, euhedral magnetite up to 1 mm in size is found with poiquilític texture in aggregates associated to biotite and hornblende (Fig. 8 D).

Table 1. ASM parameters obtained for the granites analyzed by sampled outcrop.

Rock unit	Site	X	Y	n	Km (mSI)	Pj	T	K1 Dec	K1 Inc	α1	K2 Dec	K2 Inc	α2	K3 Dec	K3 Inc	α3
MO	MO1	817256	116621	10	0,38	1.076	-0,15	302	59	10.4	208	2	30	117	31	30
MO	MO3	815717	116970	6	3,17	1.102	0,19	264	67	27,4	72	23	28	164	4	14
MO	MO4	815145	117029	10	0,09	1.026	0,268	232	60	29,2	51	30	29.6	141	0	21,7
MO	MO5	814894	117162	5	1,36	1.104	0,14	232	36	26.1	71	52	14.6	329	9	26.2
MO	MO6	813530	118231	16	1,42	1.079	0,244	106	69	14	224	16	18.9	199	1	14,2
MO	MO7	814992	116808	5	0,1	1.033	-0,381	223	61	15,1	70	21	28.9	132	1	32,7
MO*	MO8	814174	114963	13	10,3	1.102	-0,129	287	69	21,5	39	15	23	135	19	12,1
MO	MO9	817097	116696	10	0,3	1.072	0,08	28	76	22,8	269	7	25.3	175	12	22
MO	MO11	815414	117084	11	2,22	1.084	0,24	254	64	21,3	63	25	24.8	152	6	18,4
MO*	MO13	814938	113281	13	4,08	1.121	0,455	275	69	23,1	34	7	21.9	6	1	13,3

Rock unit	Site	X	Y	n	Km (mSI)	Pj	T	K1 Dec	K1 Inc	α1	K2 Dec	K2 Inc	α2	K3 Dec	K3 Inc	α3
MO*	MO14	815025	113359	6	18,8	1.069	0,123	228	55	11,5	62	38	8.9	334	11	23,9
MO	MO15	814992	117513	5	1,04	1.080	0,29	183	20	31,3	276	8	30,1	27	69	12,7
MO	MO16	815381	117714	9	0,72	1.056	0,07	287	66	26,6	77	21	26,7	172	11	12,4
MO	MO18	815213	117645	9	1,04	1.055	0,3	76	79	26,8	260	11	26,7	170	1	17,6
MO	MO19	815140	117599	9	0,95	1.060	0,22	257	13	19,2	168	8	20,1	46	75	16,8
MO**	MO22	820083	115042	15	8,59	1.144	0,63	301	68	24,1	109	21	24,1	200	4	13,9
MO**	MO40	821205	117955	8	8,38	1.228	0,608	112	70	21,4	245	14	21,7	338	14	9,1
MO**	MO41	820995	117945	13	11,2	1.084	-0,217	292	33	9,9	88	54	22,6	194	11	22,8
MO**	MO44	819687	114549	15	19,7	1.108	-0,409	276	66	6,5	174	5	19,4	82	24	19,3
MO	MO45	819594	113469	8	0,79	1.162	0,167	280	12	17,2	184	27	19	32	60	18,7
MO	MO51	813296	118459	11	3,77	1.082	0,434	139	78	25	307	12	28,8	38	2	28,1
MO	MO56	817767	115904	8	0,05	1.074	0,245	4	77	11,2	225	10	24,8	133	8	23,6
MO	MO57	817730	116049	10	2,32	1.071	0,143	18	79	28,2	114	1	28,9	204	10	19
MO	MO58	817874	115694	15	3,87	1.061	0,408	83	73	29	257	17	29	348	2	17
MO	MO59	818014	115409	14	0,35	1.087	0,194	207	82	18,5	71	6	18,8	341	6	14,3
MO	MO60	818040	115111	10	0,78	1.095	0,307	176	86	20,7	75	1	21	345	4	18
MO	MO61	818110	116007	10	0,85	1.072	0,444	106	72	20,4	275	18	22,1	6	3	19
MO	MO65	816050	117390	16	0,64	1.074	0,086	215	64	28,7	78	20	28,8	341	16	28,3
MO	MO66	815650	117550	9	0,72	1.051	0,304	226	51	29	328	11	29	66	37	17
MO	MO67	815223	117417	10	1,48	1.074	-0,112	237	55	12,6	109	24	27	7	24	27
MO	MO68	815058	117554	11	0,67	1.083	0,22	15	33	19,4	258	35	21,5	135	38	19
CA*	MO31	820583	116926	10	2,31	1.096	-0,36	292	64	5,9	78	22	11,9	173	13	12,3
CA	MO2	816660	116747	12	1,04	1.069	-0,15	38	66	28,2	143	7	28.4	237	23	14.6
CA	MO10	816081	116813	10	0,51	1.035	-0,15	352	78	15	243	11	28.1	151	11	29,2
CA	MO39	821278	118727	17	6,9	1.234	-0,48	78	10	3,7	261	80	7,9	168	1	7,9
CA	MO42	821054	117544	21	6,14	1.114	0,567	274	35	22,7	44	43	22,5	163	28	12,7
CA	MO43	821172	115431	13	2,44	1.088	-0,182	254	36	16,3	73	54	33,3	164	0,1	23,5
CA	MO50	818574	113530	12	6,14	1.091	-0,065	90	10	13,7	186	28	13,8	342	60	14,8
CA	MO62	818166	116288	15	6,66	1.089	-0,1	311	63	11,6	98	34	20,9	194	14	21,8
CA	MO63	818272	116102	10	4,3	1.090	0,144	15	77	22,6	268	4	24,9	177	12	16,1
CA	MO64	819839	115836	15	6,6	1.095	0,44	253	37	23,2	77	53	23,1	344	2	10,5
MP	MO12	812880	114362	10	5,72	1.041	-0,173	128	74	25,7	296	16	28,7	27	3	29
MP	MO29	817888	112776	15	14	1.143	-0,056	125	22	22,1	30	13	27,9	272	64	21,1
MP	MO46	817144	111617	14	2,02	1.053	0,234	238	45	23,6	129	18	27,8	24	40	28,6
MP	MO47	817586	111337	11	4,5	1.133	0,089	137	10	23,4	231	23	23,5	24	65	15,9
MP	MO48	817850	111718	10	11,9	1.260	-0,12	152	20	17,8	52	25	28,4	275	57	27,7
MP	MO49	818023	112122	10	9,93	1.166	-0,176	320	24	13,2	69	36	17	204	44	16,7
MP	MO52	812775	119807	12	9,67	1.113	0,354	188	69	21	285	3	21,6	16	21	6,9
MP	MO53	814110	120837	10	13,5	1.136	0,635	261	32	12,7	90	58	12,6	354	4	8,6
MP	MO54	813497	120389	13	9,56	1.090	0,481	150	65	24,5	269	12	24,5	3	21	10,3
MP	MO55	813084	120110	13	13,4	1.147	0,621	224	50	21,5	92	30	21,3	345	25	14,9

MO: Moderna Granite; MO * Moderna granite - facies Magnetite-granite; MO **: Moderna granite in shear zone; CA: Caroebe Granite Jaburuzinho facies; CA *: Caroebe Granite Alto Alegre facies; MP: Martins Pereira Granite; n: number of specimens; X and Y: coordinates (in m) on grid WGS_84 UTM (zone 20 N); K_{bulk}: magnetic susceptibility (in 10-3 SI); Pj: degree of anisotropy; T: shape parameter; Dec: declination; Inc: inclination; K1 and

K3: major and minor axes of the ASM ellipsoid (K1: magnetic lineation and K3: magnetic foliation pole); α1 and α3: dimension (in degrees) of the ellipsoid confidence angle expressing the individual dispersion of each ASM measurement.

4.1.1 Isothermal Remanent Magnetization and Thermomagnetometry

methods

The magnetic properties of the minerals responsible for the magnetic susceptibility of the described rock units were analyzed in terms of thermomagnetic behavior and of the remaining magnetization under constant temperature. 20 samples were selected based on the magnetic susceptibility (K) results obtained for each analyzed specimen and were subdivided into three groups: i) samples with K <4 mSI; (ii) samples with K between 4 and 10 mSI; and iii) samples with K> 10 mSI. The analytical results of MRI and thermomagnetic are shown in graphic form (Fig. 8) and the magnetic markers identified are characterized by:

i) low coercivity indicated by the rapid change of the magnetic susceptibility until the applied magnetic field near 200 militeslas, with a plateau formation with slight susceptibility variations, without reaching total saturation, indicating the presence of coercive minerals like hematite. (Fig. 8 A-C). The Heating cycle describes rough thermomagnetic curves with slight decrease of the magnetic susceptibility until the magnetization capacity falls at 580 °C, without reaching the total magnetic randomization, and unchanged cooling cycle, indicatives of the mineral association observed in low Km Moderna granite, constituted by hornblende and biotite altered with generation of hemathitic exsolutions (Fig. 8 A).

ii) IRM curves showing magnetic saturation and continuous thermomagnetic curves with varying susceptibility in the range of 250 - 400 °C and loss of magnetization at 580 °C, defined by a fall exhibiting curvature change without reaching total magnetic randomization and cooling cycle with reduced magnetic susceptibility (Fig. 8C), is interpreted as titanomagnetite in deformed Moderna granite (Fig. 8 D). The asymptotic drop at the Curie point, together with the total randomization of the magnetic susceptibility, indicates the presence of pure magnetite (Magnetite-granite, Fig. 8D).

iii) Magnetite-hematite association, exhibits IRM with slight oscillations in the curve plateau, as well as the thermomagnetic behavior is represented by increase of the susceptibility near Curie temperature indicated by curvature in the heating cycle (Fig. 8 B).

iv) From the IRM curves and thermomagnetic behavior, pyrrhotite is identified with a light and

continuous magnetization capacity without reaching magnetic saturation in the IRM curve. In the heating cycle there it has an increase before abrupt drops of susceptibility at 250 ° C and 580 ° C (Dunlop, 2014; Dunlop & Özdemir, 2007; Fig. 8 B).
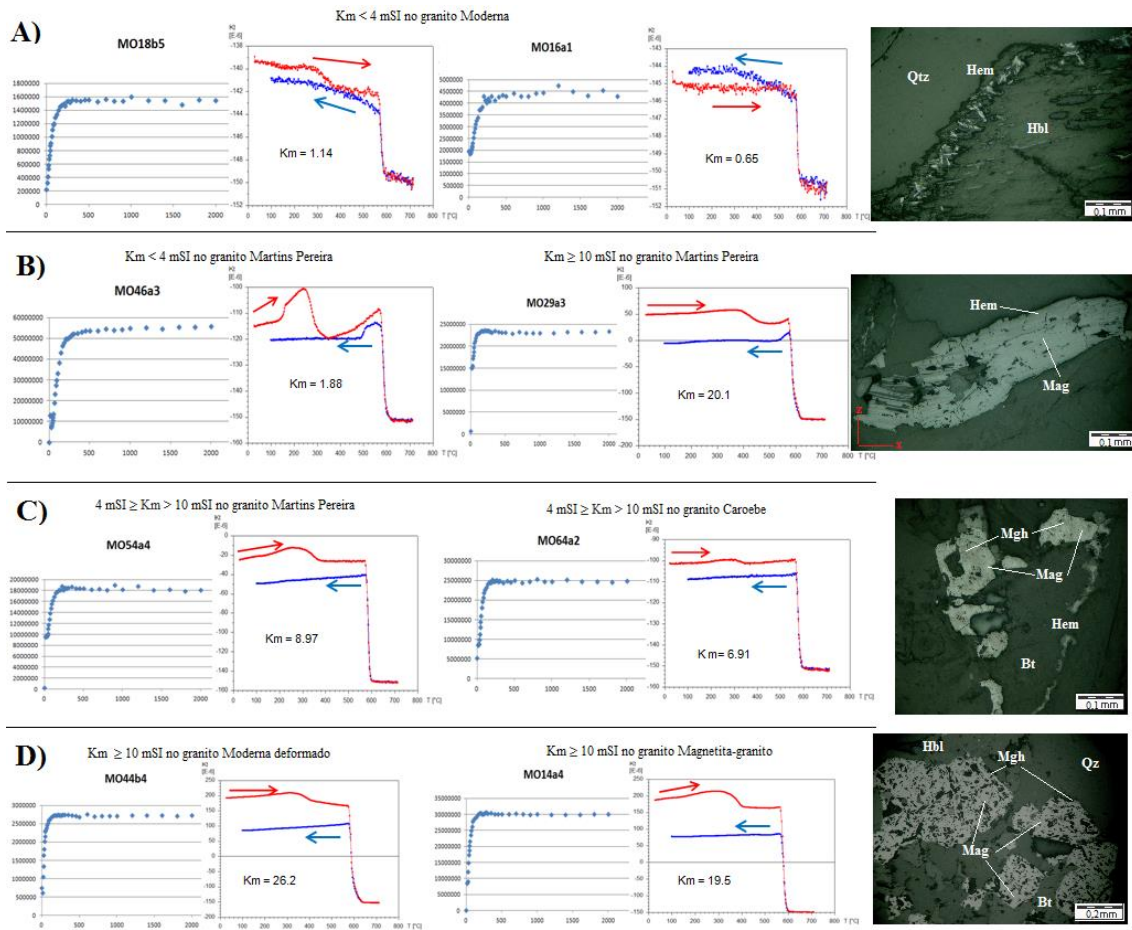
Fig. 8. curves of IRMI in blue points, heating thermomagnetic in red and blue cooling thermomagnetic, and photomicrographs representative of groupings of samples based on the magnetic susceptibility values, per unit of rock: A) Modern granite, hematite (Hem) in hornblende exosolutions (Hbl); B) Martins Pereira granite, hematite (Hem) as altered deformation magnetite crystal (Mgm) stretched by dextral shear; C) values of Km between 4 and 10 mSI, magnetite (Mag) subhedral crystals altered to maghemite (Mgh) and hematite (Hem) filling biotite fracture; D) values of Km greater than 10 mSI, euhedral poiquilithic magnetite crystals (Mag) modified to maghemite (Mgh).

4.2. AMS scalar parameters

The studied granites anisotropy of magnetic susceptibility (Km) and its geometric characteristics: degree of anisotropy (Pj) and shape parameter (T), of the magnetic ellipsoids representative of the organization of each outcrop analyzed magnetic mineral markers are shown in Fig. 9 A.

The average magnetic susceptibility Km represents the contributions of the ferromagnetic, paramagnetic and diamagnetic mineral phases present in the rock (Hrouda, 1993). Considering all the specimens analyzed by outcropping, the Km values vary from 0.05 mSI to 19.70 mSI.

The lowest values are correlated to Moderna Granite (62% of the samples), where 71% is between 0.05 and 3, 90 mSI (Fig. 9 B). When it presents mylonite texture (8%), the magnetic susceptibility is considerably higher and the values of Km vary between 8.38 and 19.70 mSI. The facies Magnetite-granite (5%) presents values of Km also high, between 4 and 18 mSI. The Caroebe Granite (19% of the samples) presents heterogeneous and intermediates values, all of them between 0.5 and 6.5 mSI, being that the highest anisotropy rates are related to the rocks closest to the Martins Pereira granite (19%), which presents values of Km between 4 and 14 mSI.
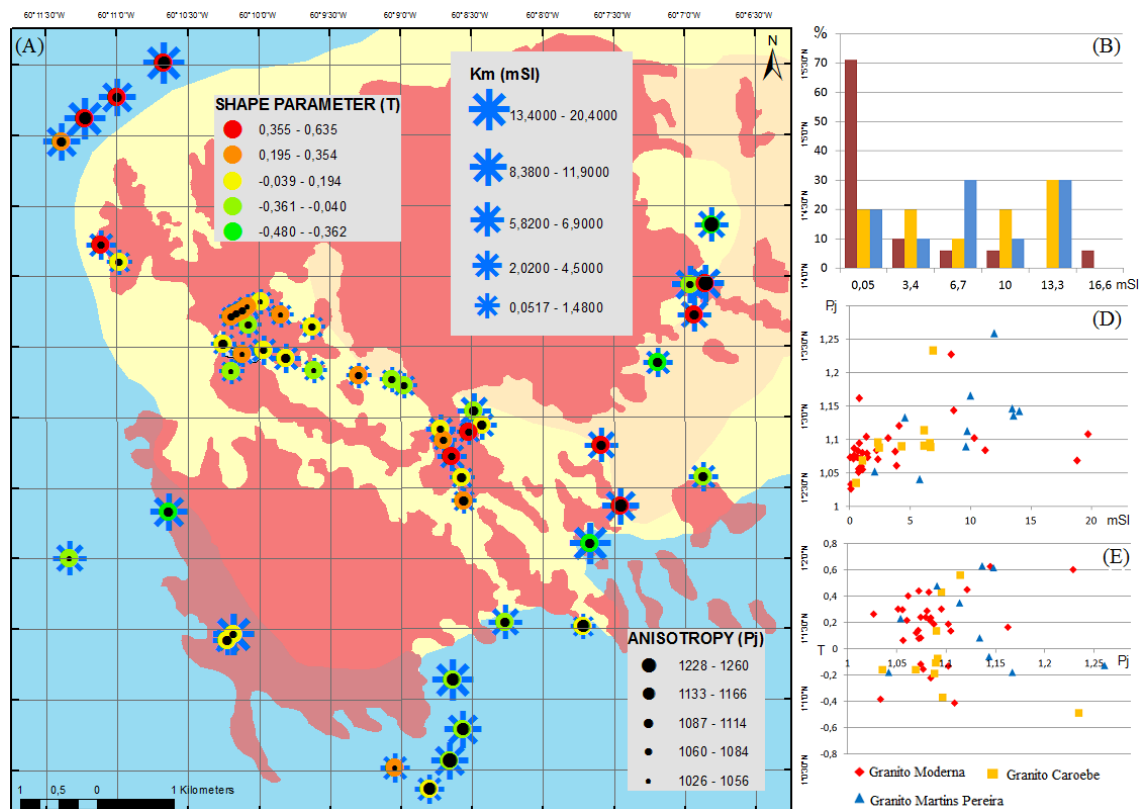
Fig. 9. Distribution of magnetic susceptibility (Km) in the study area at each respective sampling point, represented by blue asterisks with size proportional to the values of km; the anisotropy distribution (Pj) is represented by black circles with size proportional to the values of Pj; and the shape parameter (T) is represented in color scale, where the blue hue refers to the more linear (prolathic) magnetic ellipsoids shape (negative values) and the reddish tones to ellipsoids with more planar (oblathic) shape (positive values). (B) frequency diagram of the magnetic susceptibility values (Km) of the sampled rock units. (C) relation between magnetic susceptibility (Km) and the degree of eccentricity (Pj) of the magnetic ellipsoid; (D) relationship between anisotropy (Pj) and the shape parameter (T) in the sampled rock units.

The direct relation of dependence between the values of magnetic susceptibility Km and degree of anisotropy Pj.for each lithological unit is represented in Fig. 9 C. Similar to the susceptibility, Moderna Granite presents the lowest magnetic ellipsoid degrees of anisotropy, while Martins Pereira Granite presents the largest. The anisotropy in Moderna Granite varies from 3% to 16%, with planar shape defined by the parameter T in 53% of samples and linear shape in 10%. The Caroebe Granite presents an anisotropy varying between 3% and 35%, being that 14% have a

linear form and 6% in a planar. Martins Pereira granite registers Pj between 4% and 26%, where 10% are planar and 8% linear (Fig. 9 D).

4.3. AMS directional data and magnetic fabric

The directional parameters of the AMS: K1-magnetic lineation and K3 magnetic foliation pole (Table 1), define the magnetic fabric of the rocks sampled with statistical quality. This quality is marked by the value of $\alpha 1$ and $\alpha 3$, which represent, respectively, the angular variations of the confidence cone (2σ) between k1 and k3 average direction and the individual directions of the analyzed specimens. When $\alpha 1$ and $\alpha 3 \leq 30$ ° the axis orientation obtained for the analyzed ellipsoid is considered well defined (Jelínek, 1978), otherwise they are considered dispersed and are discarded.

Only one sample (MO15) gave the $\alpha 1$ value slightly higher than 30º. The AMS diretional data are presented on map and on lower hemisphere stereographic projections (Fig 10).
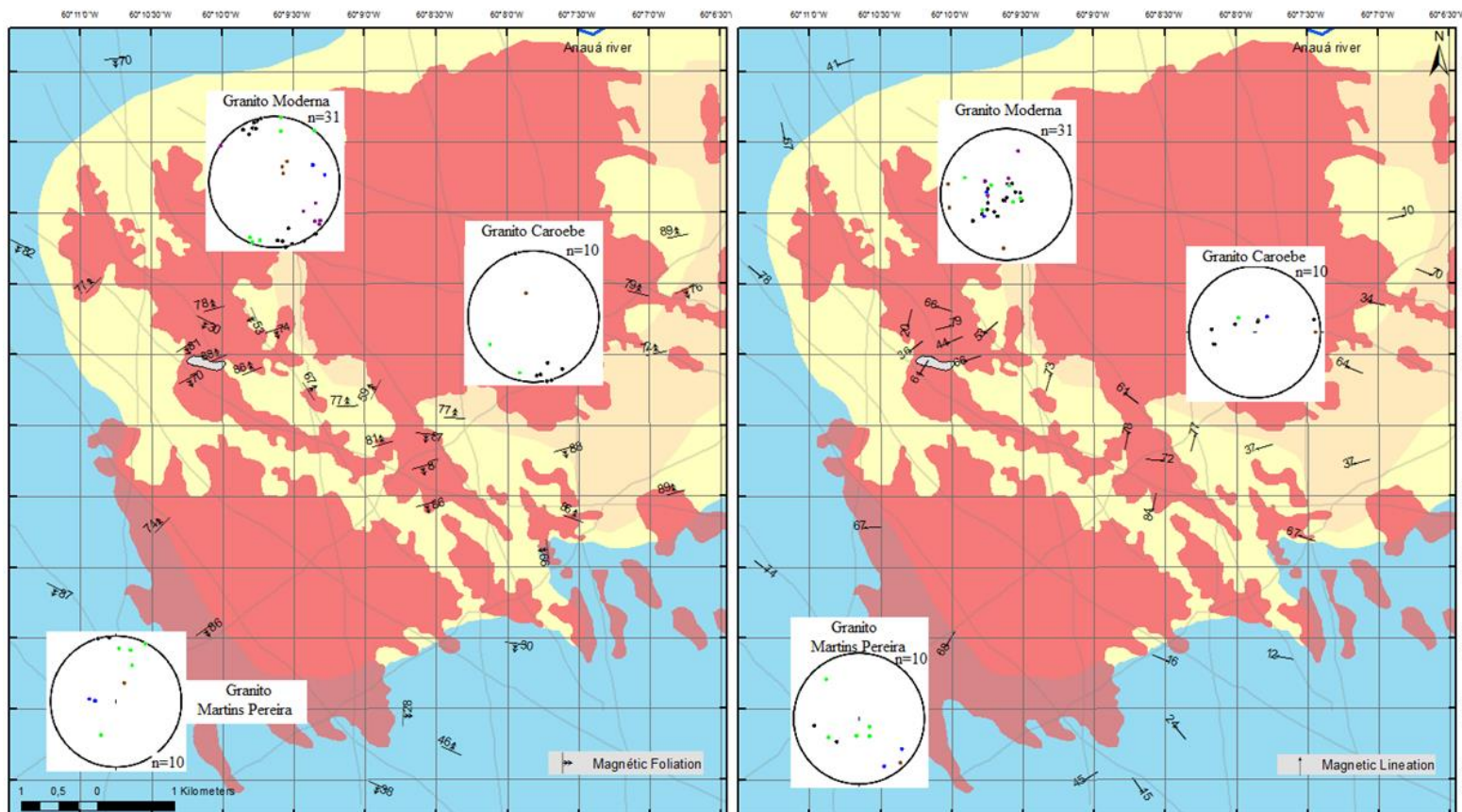
Fig. 10. The magnetic fabric orientation obtained for each unit of sampled rock with respectively stereogram plots.

The magnetic fabric in the Martins Pereira Granite is comparatively more heterogeneous and exhibits dominant E-W trend with elevated S plunge and high rake magnetic lineation with preferential plunge to SE. Caroebe Granite presents mainly WSW-ENE magnetic fabric orientation with high N-dip and magnetic line with high angle plunge to NW. The orientation

of the Moderna Granite magnetic fabric shows a NE-SW (35%) trend with high dip for N or S and down-dip magnetic lineation, a second sub-verticalized SE-NW (20%) orientation presents high rake magnetic lineation and some few fabrics are subhorizontal with W-dip.

Mylonitic foliation resulting from the combination of different deformation processes, pegmatitic dikes and hydrothermal veins are observed deformation structures that contribute to the determination of identified shear zones (Fig. 12). These shear zones exhibit sinuous and discontinuous structures where the deformation is mainly ductile and localized. In the Martins Pereira Granite, stretched quartz and feldspar crystals were observed (Fig. 3B), which define proto to meso-mylonitic foliation with high dips (around 65°) and WNW-ESE direction and, subordinated, SE-NW proto-mylonitic foliation of high dips. Caroebe granite records the main ENE-WSW shear direction (Fig. 5 A B) with high dips (around 70°), parallel to the magmatic foliation of the rock; it also records NE-SW and NW-SE directions with high dips. Moderna granite features stretched quartz crystals and aligned mafic minerals that define proto mylonitic foliation (Fig. 6B) with SE-NW main direction and SW-NE subordinate direction, both with high dips (around 75°). The kinematics of the structures are predominantly dextral in all mapped area, regardless of the shear zone or rock unit in which it propagates.
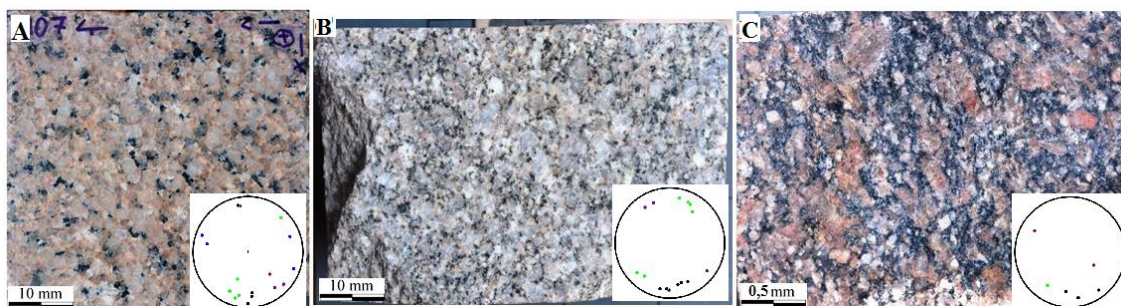
Fig. 11. Magmatic foliation So measured in the rock units identified in the field. A) Moderna Granite, n = 17; B) Caroebe Granite, n = 16; C) Martins Pereira Granite, n = 6.

Dykes of granitic composition with medium to fine texture and thicknesses between 0.5 cm and 60 cm occurs oriented subparalel to the mylonitic foliation and occasionally parallel to the magmatic foliation. The main direction is recorded around NNW-SSE axis with high inclinations (around 70 °) in all mapped rock units (Fig. 12). These dikes are preferably concentrated in the contact zones between the mapped granites. Quartz veins are more present in the surrounding areas of the identified shear zones. These quartz veins show width between 0.5 cm and 80 cm and occur subparallel to the granitic dikes.
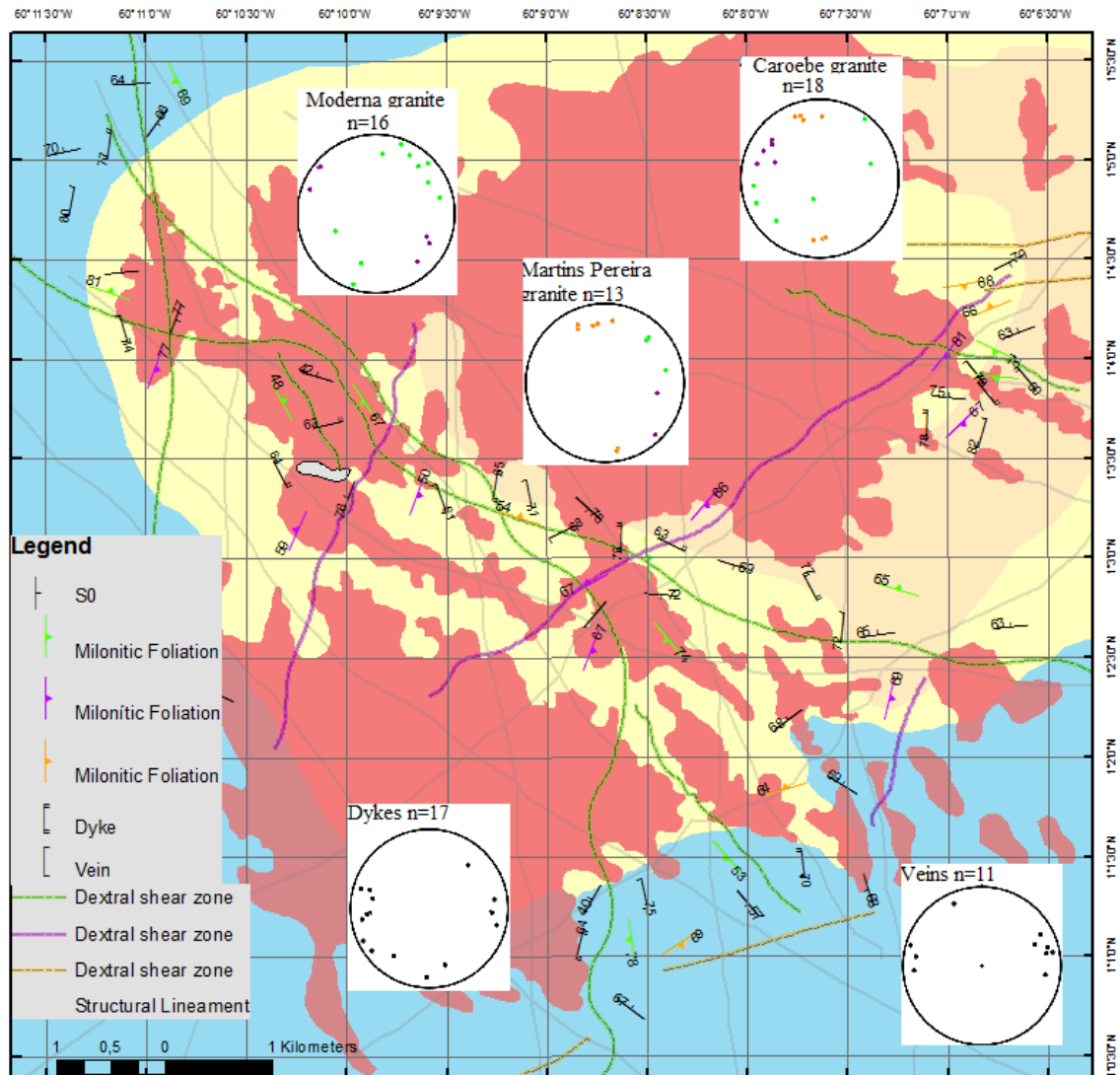
Fig. 12. Study area structural map with the stereographic projections of field - measured mylonitic foliations, dikes and veins.

4. DISCUSSION

The motivation to carry out the present research had as its starting point the works of Santos et al., (1997) e Almeida (2006), that describing Moderna granite as A-type, with plutonic accommodation controlled by NW-SE regional structures (Almeida & Macambira, 2007), related to the 1.81-1.79 Ga A-type Madeira intrusive magmatism, although Moderna granite is spatially related to the Caroebe calc-alkaline granite, generated in a collisional tectonic environment, while Madeira granite presents controlled accommodation by regional NE-SW structuring (Siachoque et al 2017). The tectonic context of Moderna Granite emplacement is intraplate interpreted based, mainly, on geochronological data (Santos et al., 1997) and on the A-type classification, which relates this type of granite to intraplate tectonics environments and distensive tectonic regime (Barbarin, 1999, Eby, 1992, Whalen et al., 1987, Loiselle & Wones,

1979. Collins et al., 1992; Bonin et al 2007; Karsli et al., 2012; Martin et al., 1994; Zhao et al., 2008; Dall'agnol et al., 2005). In spite of the geochemical signature of these granites can be more related to the magma source than the intraplate geotectonic environment (Almeida, 2006). Field evidences show that Caroebe Granite is intrusive in Martins Pereira Granite. Sometimes tectonic contact and assimilation features are also observed. The contact between Moderna and Caroebe granites is intrusive-transitional, and the contact between Moderna and Martins Pereira granites is materialized by Magnetite-granite facies of Moderna granite, and by late hydrothermal amethyst mineralized veins. The crustal discontinuity generated by the contact between the Caroebe and Martins Pereira granites serves as a duct for the Moderna Granite rise, which in contact with the cooler Martins Pereira granite crystallizes the Magnetite-granite facies. In the Moderna-Caroebe contact zone, a mixing process is associated with a metasomatic alteration and plastic deformation. Rheological contrast between pluton - host rock was only observed in the occurrence of xenoliths of the Cauarane Group, some partially assimilated, in the Moderna Granite domain. Although the Moderna Granite shows intrusive contact with Cauarane Group. Martins Pereira and Caroebe granites do not present the same relation in the study area. This is due to the more upright and shallow character of the Moderna Granite intrusion.

Magnetic and petrographic analyzes show that magnetite is the main magnetic phase in the three rock units analyzed. Secondary oxides, mainly hematite, have been identified in Moderna granite, associated with altered magnetite or mafic silicates generally oriented. In this sense, the late hydrothermal alteration is probably responsible (Siachoque et al., 2016) for the low values of magnetic susceptibility in Moderna Granite. Petrographic analyzes confirm that iron oxide crystals associated with epidote-titanite and biotite-chlorite crystallize in the final stages of metassomatism. The presence of secondary minerals, such as chlorite and epidote, differentiated mineral magnetic markers such as pyrrhotite, and magnetite to maghemite alteration, would explain the low magnetic susceptibility in some sites of the pluton.

The presence of pyrrhotite in Martins Pereira granite adjacent to Moderna granite must be related to late-magmatic fluids that forms amethyst veins and pegmatite dykes associated with Moderna magmatism. The occurrence of a subordinate mineral association (hornblende, secondary biotite, hematite, epitote, titanite and allanite) in Moderna Granite, associated with plastic deformation features, demonstrates reddish (Fe-Ti hydroxides?) hydrotermal alteration affecting Moderna Granite. The plutonism associated with this alteration was not identified and shows no relation with mafic clots (Almeida, 2006) that occur in the region. This alteration event can be concomitant with the plastic deformation, once it do not modify the granites

magnetic and magmatic fabrics.

The fabric patterns

In all granites analyzed was observed preferential shape orientation of silicates, producing magmatic foliation So generated in a plastic regime of deformation. When oriented obliquely to So, the minerals are deformed by ductile shear zones, generated by local variations in the flow direction, with dragging folds in restricted deformation bands. When the silicates are oriented subparallel to So, only occurs size reduction without development of planar structure in solid state deformation. Strain mechanisms show foliations recorded under high temperature, with subverticalized dominant trend in the range of 080 ° -120 °. Such evidence suggests that the different granitic units were placed at crustal levels of depth and pressure dominated by the plastic deformation regime (Vernon et al., 2004).

Solid state deformation is reflected in the presence of features of dynamic recrystallization, edge migration, planar sliding, subgrain rotation and folded twining, which, in the field, is identified with a subparallel orientation to the magmatic foliation. These strain mechanisms represent the crystalline deformation after the crystallization limit (Vernon et al., 2004) and reveal the continuity of the deformation of the granitic body from the initial to the final stages of the emplacement (Stipp et al., 2002; Tullis et al. Yund, 1991; Vernon et al., 2004).

Magnetic fabric

The AMS results and microtexture analyzes combined with geological field data revealed that the magnetic fabric and the magmatic fabric are parallel, and maintain a similar dominant trend orientation in the three granites analyzed. The fabrics of the plutons were developed at high temperature and the magnetic fabric, marked mainly by magnetite, was only locally modified by solid state imposed deformation on Martins Pereira granite. Microstructures identified in Moderna granite are attributed to magmatic crystallization processes related to crystalline phases and mineral aggregates that do not exhibit evidence of change in grain shape during cooling (Vernon & Paterson, 2008). Granitic emplacement subjected to plastic deformation develops characteristics as aggregates of fragmented minerals by grain size reduction (Kilian et al., 2011), grain boundary migration by intracrystalline sliding at high temperature (Passchier & Trouw, 2005) and preferential shape orientation (Stipp et al., 2002).

The absence of expressive solid-state deformation structures (except the punctual regions affected by shear zones) suggests that the Moderna granite mineral fabric was formed during the crystallization processes, although poorly developed ASM fabrics observed in granite intrusions are commonly obliterated by late to post-magmatic hydrothermal alteration events (Archanjo et al., 2009; Nédélec et al., 1994, 2015; Price et al., 1998) As presented by Archanjo

et al. (2009) for the alkaline Merouca granite, localized and restricted dispersion of the AMS axes in the Moderna granite magnetic fabric may be related to a hydrothermal event that punctually affected the Caroebe batholith after the placement of Moderna granite, mainly in regions deformed by shear zones.

During a pluton emplacement under regional tectonic control, is commom dispersion in the orientation of primary fabric and recording of two orientations, Similar features are observed in the granitic units analyzed, despite the preferred orientation of the well-defined fabric. This dispersion is related to the development of foliation in granite still with plastic behavior (close to solidus state). With constant stresses and temperature decrease, the magnetite in the rock rotates as a rigid body, accommode itself as a deformation active marker and, consequently, under the tectonic control, displays obliquous to high axial ratio silicates passive markers. Intracrystalline strain is accommodated by these silicates through planar slides, subgrain rotation, and boundary migration. Passchier (1997) proposes that these different deformations may result in obliquity of the organization of the magnetic and silicate (magmatic) fabric. In flow bands and mylonite deformation all minerals tend to settle in alignment. Since the fabric is solid state, the deformation compartmentalizes and develop localized shear zones that accommodate the solid state deformation (Žák & Patterson 2009, Vigneresse 2014; Patterson 2018).

The ASM reveals mainly planar magnetic fabric with dominant ENE trend with high to subvertical dips for the three plutons. The ASM data shows also high rake magnetic lineation with subvertical plunge, suggesting that mass transport during plutonic positioning was by vertical magmatic flow (McNulty et al., 2000), and the high-angle magnetic lineation was fixed during the upward movement of the magma along the feeding zone (Vigneresse & Bouchez, 1997; Bouchez, 2000), mainly in Moderna granite. A subordinate fabric spreads to SE-NW with SW dips and low-angle magnetic lineation, suggests a transcurrent component performance during the accommodation, although the consistency of the magnetic fabric indicates that there have been no significant changes in efforts orientation of the over time. The fabric stability in the three plutons represents the continuity of the active regional shortening component NW-SE in the range plutons emplacements.

Plutonic emplacement model

Although different ages for the placement of Martins Pereira (1.96-1.97 Ga), Caroebe (1.89-1.90 Ga) and Moderna (1.81 Ga) plutons are reported in literature, sin-kinematic placement conditions under same orientation tectonic field were identified for the three plutons, despite the long-time interval. In this sense, the emplacement mechanisms and primary fabric in the

studied granites highlights the need to refine the crystallization ages of Moderna granite. Affections to the U-Pb isotopic system in zircon by intense hydrothermal alteration in Moderna granite can be pointed out as the cause of this discrepancy of ages between the ages reported in the literature and the syn-kinetic placement mechanisms in a transpressive regime for the three rock units presented here (Fig 13). It is postulated, therefore, orogenic conditions for the placement of Moderna granite, whether these conditions associated with a distal orogeny (Ahall et al., 2000) Cauaburí (Almeida et al 2013) or, according to the structural, petrographic and magnetic results, to the orogeny (Almeida 2006). that controlled the emplacement of calc-alkaline Martins Pereira and Caroebe granites. The tectonic conditions for the Moderna Granite emplacement may be related to the Cauaburi Orogeny (author) in the Rio Negro Province (far away ~300km to west), based on the distal orogeny model (author). For the Martins Pereira and Caroebe granites, reinforced by strucutural, petrographic and magnetic data, orogenic and post-orogenic settings, respectively, may be controlled the plutons emplacement.
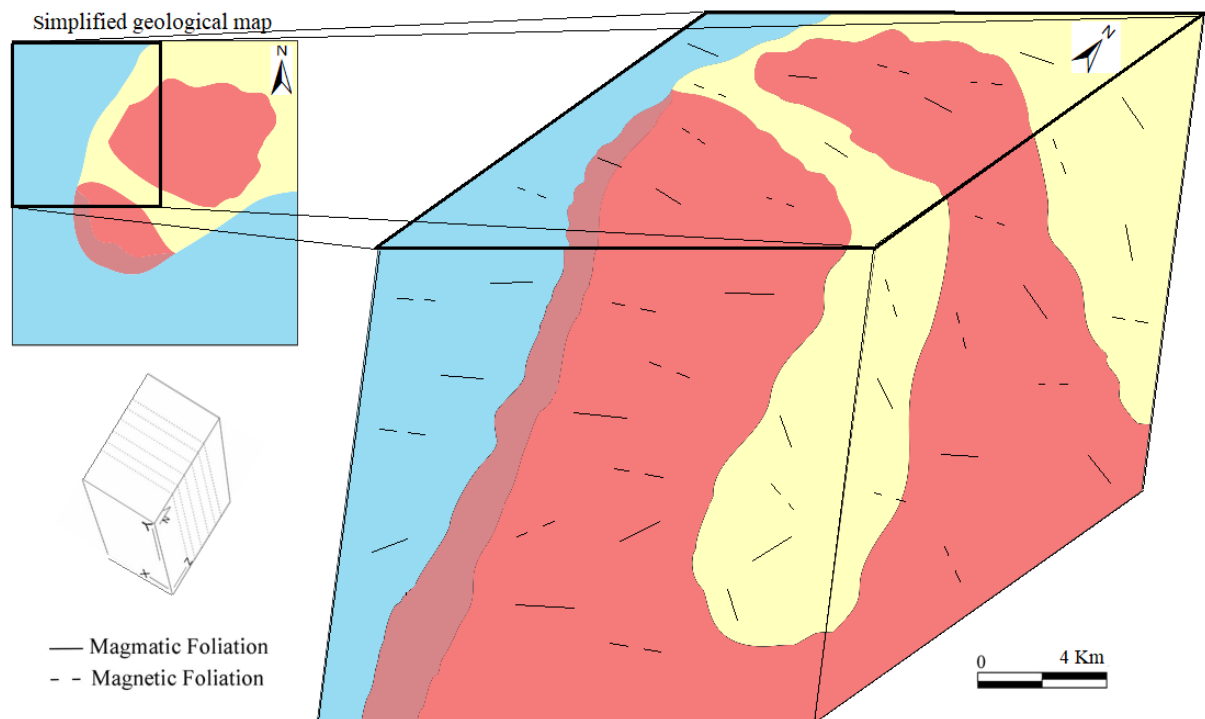

Fig. 13 Moderna granite emplacement model.

5. CONCLUSIONS

Field structural data combined with petrographic and AMS data support the interpretations about Moderna Granite emplacement, which exhibits distinct reddish coloration due to punctual hydrothermal alteration processes associated with late plastic deformation. It was verified that

the magmatic fabric of the three analyzed granite units, defined by the preferred shape orientation of felsic minerals, presents the same orientation of the magnetic fabric defined by iron oxides associated with aggregates of mafic oriented minerals in both rock units. The orientation of the fabrics is due to the tectonic field, with shortening in the NW-SE direction, which controlled the placement of the three distinct granite units identified in the study area, despite the temporal distance between the crystallizations of them. What characterizes the Moderna granite emplacement as sin kinematic, under crustal conditions similar to the adjacent granites, controlled by NE-SW dextal transpressives structures, in agreement with the regional structural framework. Pointwise shear zones, orientated sub-parallel to magmatic foliation, demonstrate the persistence of the effort field at the end of the plutonic emplacement, while discrete posterior, subvertical NW-SE shear zones, deform rock units restricted portions in solid state.

REFERENCES

ÅHÄLL K.I., CONELLY J.N., BREWER T.S. 2000. Episodic rapakivi magmatism due to distal orogenesis?: Correlation of 1.69-1.50 Ga. orogenic and inboard, "anorogenic" events in the Baltic Shield. Geology, vol. 28: 823-826 p.

ALMEIDA, F.F.M., HASUI, Y., de BRITO NEVES, B.B., FUCK, R.A. 1981, Brazilian structural provinces: an introduction. Earth-Science Reviews 17;: 1–29 p.

ALMEIDA, F.F.M.D., BRITO, N., De, B.B., DAL RÉ CARNEIRO, C. 2000, The origin and evolution of the South American Platform. Earth-Science. Reviews 50 :77–111 p.

ALMEIDA, M.E.; MACAMBIRA M.J.B., FARIA M.S.G. de. 2002 A Granitogênese Paleoproterozóica do Sul de Roraima. In: CONGRESSO BRASILEIRO DE GEOLOGIA, 41,. Anais..., SBG, p 434.

ALMEIDA, M. 2006. Evolução geológica da porção centro-sul do Escudo das Guianas com base no estudo geoquímico, geocronológico e isotópico dos granitóides Paleoproterozóicos do sudeste de Roraima, Brasil. Pará: Universidade federal do Pará. Tese de Doutorado.. 241 P.

ALMEIDA, M.E, MACAMBIRA, M.J.B., OLIVEIRA, E.C. 2007 Geochemistry and zircon geochronology of I-type high-K calc-alkaline and S-type granitoid rocks from south-eastern Roraima, Brazil: Orosirian collisional magmatism evidence (1.97-1.96Ga) in central portion of Guyana Shield. Prec. Res., 155,. p. 69-97.

ALMEIDA, M.E., MACAMBIRA, M.J.B., VALENTE, S.d.C. 2008, New geological and single-zircon Pb evaporation data from the Central Guyana Domain, southeastern Roraima, Brazil: tectonic implications for the central region of the Guyana Shield. Journal of South American Earth Sciences,. 26:318–328p.

ALMEIDA, M.E., MACAMBIRA, M.J.B., SANTOS, J.O.S., NASCIMENTO, R.S.C., PAQUETTE, J.L., 2013. Evoluçao crustal do noroeste do Cráton Amazônico (Amazonas,

Brasil) baseada em dados de campo, geoquímicos e geocronologicos. In: SBG/Núcleo Norte, Simposio de Geologia da Amazônia, 13, Belem. Anais 1 – 4.

ARCHANJO, C. J., DA SILVA, E. R., & CABY, R. 1999. Magnetic fabric and pluton emplacement in a transpressive shear zone system: the Itaporanga porphyritic granitic pluton (northeast Brazil). Tectonophysics, 312(2), 331-345.

ARCHANJO, C.J., LAUNEAU, P., HOLLANDA, M.H.B.M., MACEDO, J.W.P., LIU, D., 2009. Scattering of magnetic fabrics in the Cambrian alkaline granite of Meruoca (Ceará state, northeastern Brazil). International Journal of Earth Sciences 98:1793–1807. http://dx.doi.org/ 10.1007/s00531-008-0342-z.

BARBARIN, B., 1999. A review of the relationships between granitoids types, their origins and their geodynamic environments. Lithos 46, 605–626.

BASTOS NETO, A.C., PEREIRA, V.P., RONCHI, L.H., DE LIMA, E.F., FRANTZ, J.C., 2009. The world-class Sn, Nb, Ta, F (Y, REE, Li) deposit and the massive cryolite associated with the albiteenriched facies of the madeira A-type granite, Pitinga Mining District, Amazonas State, Brazil. Canadian Mineralogist 47:1329–1357. http://dx.doi.org/10.3749/ canmin.47.6.1329.

BEAUMONT. C., NGUYEN. M. H., JAMIESON. R. A., ELLIS. S. 2006. Crustal flow modes in large hot orogens. *From:* LAW,R. D., SEARLE,M. P. & GODIN,L. (eds) *Channel Flow, Ductile Extrusion and Exhumation in Continental Collision Zones.* Geological Society, London, Special Publications, 268, 91-145. 0305-8719/06l$15.00. 9. The Geological Society of London .

BETTENCOURT, J.S., JULIANI, C., XAVIER, R.P., MONTEIRO, L.V.S., BASTOS NETO, A.C., KLEIN, E.L., ASSIS, R.R., LEITE, W.B., MORETO, C.P.N., FERNANDES, C.M.D., PEREIRA, V.P., 2015. Metallogenetic systems associated with granitoid magmatism in the Amazonian Craton: an overview of the present level of understanding and exploration significance. Journal of South American Earth Sciences http://dx.doi.org/10.1016/j.jsames.2015.11.014.

BOLLE, O., DIOT, H., DUCHESNE, J.C., 2000. Magnetic fabric and deformation in charnockitic igneous rocks of the Bjerkreim–Sokndal layered intrusion (Rogaland, Southwest Norway). Journal of Structural Geology 22:647–667. http://dx.doi.org/10.1016/ S0191-8141(99)00183-2.

BOLLE, O., TRINDADE, R.I.F., LUC BOUCHEZ, J., DUCHESNE, J.-C., 2002. Imaging downward granitic magma transport in the Rogaland Igneous Complex, SW Norway. Terra Nova 14: 87–92. http://dx.doi.org/10.1046/j.1365-3121.2002.00393.x.

BONIN, B., 1986. Ring Complex Granites and Anorogenic Magmatism. North Oxford Academic Pub, London.

BONIN, B., 2007. A-type granites and related rocks: evolution of a concept, problems and prospects. Lithos 97 (1–2), 1–2.

BORRADAILE, G.J., & HENRY, B. 1997. Tectonic applications of magnetic susceptibility and its anisotropy. Earth-Science Review. 42, 49–93.

BORRADAILE, G. J., & JACKSON, M. 2004. Anisotropy of magnetic susceptibility (AMS):

magnetic petrofabrics of deformed rocks. Geological Society, London, Special Publications, 238(1), 299-360.

BOUCHEZ, J.L. 1997. Granite is never isotropic: an introduction to AMS studies in granitic rocks. In: Bouchez, J.L., Hutton, D.H.W., & Stephens, W.E. (Ed.). Granite: from segregation of melt to emplacement fabrics, Dordrecht: Kluwer Academic Publishers.

BOUCHEZ, J.L., 2000. Anisotropie de susceptibilité magnétique et fabrique des granites. Comptes Rendus de l'Académie des Sciences-Series IIA-Earth and Planetary Science 330 (1), 1–14.

BROWN, M., & SOLAR, G. S. 1998. Granite ascent and emplacement during contractional deformation in convergent orogens. Journal of Structural Geology, 20(9), 1365-1393.

CARNEIRO, M. C. R., NASCIMENTO, R. S. C., ALMEIDA, M. E., SALAZAR, C. A., TRINDADE, I. R., RODRIGUES, V. O. 2017. The Cauaburi magmatic arc: Litho-stratigraphic review and evolution of the Imeri Domain, Rio Negro Province, Amazonian Craton. journal of South American Earth Sciences, 77. 310 -326.

CASTRO, A., 1986. Structural pattern and ascent model in the central Extremadura Batholit, Hercynian Belt, Spain. J. Struct. Geol. 8, 633–645.

COLLINS, W.J., BEAMS, S.D., WHITE, A.J.R., CHAPPELL, B.W., 1992. Nature and origin of A-type granites with particular reference to southeastern Australia. Contributions to Mineralogy and Petrology 80, 189–200.

COSTI, H.T., DALL'AGNOL, R., MOURA, C.A.V. Geology and Pb-Pb geochronology of Paleoproterozoic volcanic and granitic rocks of the Pitinga Province, Amazonian craton, northern Brazil. International Geology Review, 2000. 42 : p 832-849.

CPRM. 2000. Programa Levantamentos Geológicos Básicos do Brasil. Caracaraí, Folhas NA.20-Z-B e NA.20-Z-D (integrais), NA.20-Z-A, NA.21-Y-A, NA.20-Z-C e NA.21-Y-C (parciais). Escala 1:500.000. Estado de Roraima. Manaus, CPRM, p 157 (em CD-ROM).

CPRM. 2003. Programa Levantamentos Geológicos Básicos do Brasil. Geologia, Tectônica e Recursos Minerais do Brasil: sistema de informações geográficas - SIG. Rio de Janeiro. CPRM, Mapas. Escala 1:2.500.000. (em 4 CDs-ROM).

CPRM. 2006. Programa Integração, Atualização e Difusão de Dados da Geologia do Brasil: Subprograma Mapas Geológicos Estaduais. Geologia e Recursos Minerais do Estado do Amazonas. Manaus, CPRM/CIAM-AM, Escala 1:1.000.000. Texto explicativo, p 148 (em CD-ROM).

DALL'AGNOL R., TEIXEIRA N.P.R., RÄMÖ O.T., MOURA C.A.V., MACAMBIRA M.J.B., OLIVIRA D.C. 2005. Petrogenesis of the Paleoproterozoic rapakivi, A-type granites of the Archaean CarajásMetallogenic Province. Lithos,. vol. 80: p 101-129.

DUNLOP, D.J., ÖZDEMIR, Ö., 2007. Magnetizations in rocks and minerals. Treatise on Geophysics:pp. 277–336 http://dx.doi.org/10.1016/B978-044452748-6.00093-6.

Dunlop, D.J., 2014. High-temperature susceptibility of magnetite: a new pseudo-singledomain effect. Geophysical Journal International 199:707–716. http://dx.doi.org/10. 1093/gji/ggu247.

EBY N. 1992, Chemical subdivision of the A-type granitoids: Petrogenetic and tectonic

implications. Geology, vol. 20: 641-644.

EVANS, D. A. D. 2013. Reconstructing pre-Pangea supercontinents. Geological Society of America Bulletin, 125: 1735-1751.

FERRÉ, E.C., WILSON, J., GLEIZES, G., 1999. Magnetic susceptibility and AMS of the Bushveld alkaline granites, South Africa. Tectonophysics 307:113–133. http://dx.doi.org/10. 1016/S0040-1951(99)00122-5.

FOSSEN, H., TIKOFF, B., & TEYSSIER, C. 1994. Strain modeling of transpressional and transtensional deformation. Norsk Geologisk Tidsskrift, 74(3), 134-145.

FOSSEN, H., & TIKOFF, B. 1998. Extended models of transpression and transtension, and application to tectonic settings. Geological Society, London, Special Publications, 135(1), 15-33.

FRAGA, L.M., MACAMBIRA, M.J.B., DALL'AGNOL, R., COSTA, J.B.S. 2009. 1.94–1.93 Ga charnockitic magmatism from the central part of the Guyana Shield, Roraima, Brazil: single-zircon evaporation data and tectonic implications. Journal of South American Earth Sciences, 27, p 247–257.

GLEIZES, G., NÉDÉLEC, A., BOUCHEZ, J.L., AUTRAN, A., & ROCHETTE, P. 1993. Magnetic susceptibility of the Mont-Louis Andorra ilmenite-type granite (Pyrenees): a new tool for the petrographic characterization and regional mapping of zoned granite plutons. Journal Geophysics Research. 98(3): 4317-4331.

HROUDA, F., 1982. Magnetic anisotropy of rocks and its application in geology and geophysics. Geophysical Surveys 5:37–82. http://dx.doi.org/10.1007/ BF01450244.

HROUDA, F., 1993. Theoretical models of magnetic anisotropy to strain relationship revisited. Physics of the Earth and Planetary Interiors 77:237–249. http://dx.doi.org/ 10.1016/0031-9201(93)90101-E.

INGRAM, G.M., HUTTON, D.H.W., 1994. The Great Tonalite Sill: Emplacement into a contractional shear zone and implications for Late Cretaceous to Early Eocene tectonics in southeastern Alaska and British Columbia. Geol. Soc. Am. Bull. 106, 715–728.

JELINEK, V., 1977. The Statistical Theory of Measuring Anisotropy of Magnetic Susceptibility of Rocks and Its Application. Jelínek, V., 1978. Statistical processing of anisotropy of magnetic susceptibility measured on groups of specimens. Studia Geophysica et Geodaetica 22:50–62. http://dx.doi. org/10.1007/BF01613632.

JELÍNEK, V., 1981. Characterization of the magnetic fabric of rocks. Tectonophysics 79: T63–T67. http://dx.doi.org/10.1016/0040-1951(81)90110-4.

JOHANSSON, A., 2009. Baltica, Amazonia and the SAMBA connection —1000 million years of neighbourhood during the Proterozoic? Precambrian Res. 175, 221–234

KARSLI, O., CARAN, Ş., DOKUZ, A., ÇOBAN, H., CHEN, B., KANDERMIR, R., 2012. A-type granitoids from the Eastern Pontides, NE Turkey: Records for generation of hybrid A-type rocks in a subduction-related environment. Tectonophysics 530–531, 208–224.

KILIAN, R., HEILBRONNER, R., STÜNITZ, H., 2011. Quartz grain size reduction in a granitoid rock and the transition from dislocation to diffusion creep. Journal of Structural

Geology 33:1265–1284. http://dx.doi.org/10.1016/j.jsg.2011.05.004.

KRUIVER, P.P., DEKKERS, M.J., HESLOP, D., 2001. Quantification of magnetic coercivity components by the analysis of acquisition curves of isothermal remanent magnetisation. Earth and Planetary Science Letters 189:269–276. http://dx.doi.org/10.1016/S0012- 821X(01)00367-3.

LOISELLE, M.C., WONES, D.R., 1979. Characteristics and origin of anorogenic granites. Abstracts papers to be presented at the Annual Meetings of the Geological Society of America and Associated Societies, San Diego, CA 11, 468.

MARTIN, H., BONIN, B., CAPDEVILA, R., JAHN, B.M., LAMEYRE, J., WANG, Y., 1994. The Kuiqi peralkaline granitic complex (SE China): petrology and geochemistry. Journal of Petrology 35, 983–1015.

MCNULTY, B.A., TONG, W., TOBISCH, O.T., 1996. Assembly of a dike-fed magma chamber: the Jackass Lakes pluton, central Sierra Nevada, California. Bulletin of the Geological Society of America 108:926–940. http://dx.doi.org/10.1130/0016-7606(1996)108b0926: AOADFMN2.3.CO;2.

MCNULTY, B.A., TOBISCH, O.T., CRUDEN, A.R., GILDER, S., 2000. Multistage emplacement of the Mount Givens pluton, Central Sierra Nevada batholith, California. Bulletin of the Geological Society of America 112:119–135. http://dx.doi.org/10.1130/0016-7606(2000)112b119:MEOTMGN2.0.CO;2.

NÉDÉLEC, A., PAQUETTE, J.-L., BOUCHEZ, J.-L., OLIVIER, P., RALISON, B., 1994. Stratoid granites of Madagascar: structure and position in the Panafrican orogeny. Geodinamica Acta 7: 48–56. http://dx.doi.org/10.1080/09853111.1994.11105258.

NÉDÉLEC, A., TRINDADE, R., PESCHLER, A., ARCHANJO, C., MACOUIN, M., POITRASSON, F., BOUCHEZ, J.- L., 2015. Hydrothermally-induced changes in mineralogy and magnetic properties of oxidized A-type granites. Lithos 212–215:145–157. http://dx.doi.org/10.1016/j.lithos. 2014.11.007.

OLIVEIRA, D.C., NEVES, S.P., TRINDADE, R.I.F., DALL'AGNOL, R., MARIANO, G., CORREIA, P.B., 2010. Magnetic anisotropy of the Redenção granite, eastern Amazonian craton (Brazil): implications for the emplacement of A-type plutons. Tectonophysics 493:27–41. http://dx.doi.org/10.1016/j.tecto.2010.07.018.

PASSCHIER, C.W., TROUW, R.A.J., 2005. Microtectonics, second ed. Springer, Berlin, Heidelberg, New York.

PATERSON, S.R., FOWLER, T.K., 1993. Extensional pluton-emplacement models: do they work for large plutonic complexes? Geology 21:781–784. http://dx.doi.org/10.1130/0091-7613(1993)021b0781:EPEMDTN2.3.CO.

PATERSON, S. R, ARDILL K., VERNON R. ZÁK J. 2018. A review of mesoscopic magmatic structures and their potential for evaluating the hypersolidus evolution of intrusive complexes. Journal of structural Geology.

PETFORD, N., KERR, R.C., LISTER, J.R., 1993. Dike transport of granitoid magmas. Geology 21:845–848. http://dx.doi.org/10.1130/0091-7613(1993)021b0845:DTOGMN2.3.CO;2.

PITCHER, W.S., 1979. The nature, ascent and emplacement of granitic magmas. Journal of the Geological Society 136:627–662. http://dx.doi.org/10.1144/gsjgs.136.6.0627.

PRICE, J., HOGAN, J.P., GILBERT, M.C., PAYNE, J.D., 1998. Surface and near-surface investigation of the alteration of the Mount Scott Granite and geometry of the Sandy Creek Gabbro Pluton, Hale Spring Area, Wichita Mountains, Oklahoma. In: Hogan, J.P., Gilbert, M.C. (Eds.), Central North America and Other Regions 12. Kluwer Academic Publisher, Basement Tectonics, pp. 79–122.

REIS, N.J.; FRAGA, L.M.; FARIA, M.S.G. DE; ALMEIDA, M.E. 2003. Geologia do Estado de Roraima. Géologie de la France, 2-3: 71-84..

ROSENBERG CL, HANDY MR. 2005. Experimental deformation of partially melted granite revisited: implications for the continental crust. Journal of Metamorphic Geology, vol.23: 19-28: 19-28.

SANTOS J.O.S. DOS, SILVA L.C., FARIA M.S.G. DE, MACAMBIRA, M.J.B. 1997. Pb-Pb single crystal, evaporation isotopic study on the post-tectonic, sub-alkalic, A-type Moderna granite, Mapuera intrusive suite, State of Roraima, northern Brazil. In: SYMPOSIUM OF GRANITES AND ASSOCIATED MINERALIZATIONS, 2, Salvador,. Extended Abstract…, SBG, p.273-275.

SANTOS, J.O.S., HARTMANN, L.A., GAUDETTE, H.E., GROVES, D.I., MCNAUGHTON, N.J., FLETCHER, I.R., 2000. A new understanding of the provinces of the Amazon Craton based on integration of field mapping and U–Pb and Sm–Nd geochronology. Gondwana Research 3: 453–488. http://dx.doi.org/10.1016/S1342-937X(05)70755-3.

SANTOS, J.O.S., 2003. Geotectonics of the Guyana and Central-Brazil shields. In: Bizzi, L.A., Schobbenhaus, C., Vidotti, R.M., Gonçalves, J.H. (Eds.), Geology, Tectonics, and Mineral Resources of Brazil, pp. 169–226.

SIACHOQUE A., SALAZAR, C. A., TRINIDADE, R. 2016. Emplacement and deformation of the A-type Madeira granite (Amazonian Craton, Brazil).Lithos, accepted 18 oct. 2016.

STIPP, M., STUNITZ, H., HEILBRONNER, R., SCHMID, S.M. 2002. Dynamic recrystallization of quartz: correlation between natural and experimental conditions. Geological Society, London, Special Publications 200:171–190. http://dx.doi.org/10.1144/GSL.SP.2001.200.01.11.

TARLING, D. H. & HROUDA, F. (eds) 1993. The Magnetic Anisotropy of Rocks. London: Chapman & Hall. 217 pp.

TIKOFF, B., SAINT BLANQUAT, M., 1997. Transpressional shearring and strikeslip partitioning in the Late Cretaceous Sierra Nevada magmatic arc, California. Tectonics 16, 442–459.

TULLIS, I. & YUND, R.A. 1977. Experimental deformation of dry Westerly granite. J. Geophys. Res., 82: 5.705-5.718.

VALÉRIO, C.D.S., SOUZA, V.D.S., MACAMBIRA,M.J.B. 2009. The 1.90–1.88 Ga magmatism in the southernmost Guyana Shield, Amazonas, Brazil: geology, geochemistry, zircon geochronology, and tectonic implications. Journal of South American Earth Sciences 28: p 304–320.

VALLE AGUADO, B., AZEVEDO, M. R., NOLAN, J., MEDINA, J., COSTA, M. M., CORFU, F., & CATALÁN, J. M. 2017. Granite emplacement at the termination of a major Variscan transcurrent shear zone: The late collisional Viseu batholith. Journal of Structural Geology, 98, 15-37.

VERNON, R.H., JOHNSON, S.E., MELIS, E.A., 2004. Emplacement-related microstructures in the margin of a deformed pluton: the San José tonalite, Baja California, México. Journal of Structural Geology 26:1867–1884. http://dx.doi.org/10.1016/j.jsg.2004.02.007.

VERNON, R.H., PATERSON, S.R., 2008. How late are K-feldspar megacrysts in granites? Lithos 104:327–336. http://dx.doi.org/10.1016/j.lithos.2008.01.001.

VIGNERESSE, J.L., BOUCHEZ, J.L., 1997. Successive granitic magma batches during pluton emplacement: the case of Cabeza de Araya (Spain). Journal of Petrology 38:1767–1776. http://dx.doi.org/10.1093/petroj/38.12.1767.

VIGNERESSE, J.L., CLEMENS, J.D., 2000. Granitic magma ascent and emplacement: neither diapirism nor neutral buoyancy. Geological Society, London, Special Publications 174: 1–19. http://dx.doi.org/10.1144/GSL.SP.1999.174.01.01.

VOICU G., BARDOUX M., STEVENSON R., Lithostratigraphy, geochronology and gold metallogeny in the northern Guiana Shield, South America: a review. 2001. Ore Geol. Rev., 18, p 211-236.

WHALEN, J.B., CURRIE, K.L., CHAPPELL, B.W., 1987. A-type granites: geochemical characteristics, discrimination and petrogenesis. Contributions to Mineralogy and Petrology 95 (4), 407–419.

WILSON, J., FERRE, E.C., LESPINASSE, P., 2000. Repeated tabular injection of high-level alkaline granites in the eastern Bushveld, South Africa. Journal of the Geological Society 157, 1077–1088.

ŽÁK, J., VERNER, K., KLOMÍNSKÝ, J., CHLUPÁČOVÁ, M., 2009. "Granite tectonics" revisited: insights from comparison of K-feldspar shape-fabric, anisotropy of magnetic susceptibility (AMS), and brittle fractures in the Jizera granite, Bohemian Massif. International Journal of Earth Sciences 98:949–967. http://dx.doi.org/10.1007/s00531-007-0292-x

ŽÁK, J., PATERSON, S.R., 2009. Magmatic erosion of the solidification front during reintrusion: the eastern margin of the Tuolumne batholith, Sierra Nevada, California. Int. J. Earth Sci. (Geol Rundsch) 99 (4), 801–812. http://dx.doi.org/10.1007/s00531-009-0423-7.

ŽÁK, J., VERNER, K., HOLUB, F. V., KABELE, P., CHLUPÁČOVÁ, M., & HALODOVÁ, P. 2012. Magmatic to solid state fabrics in syntectonic granitoids recording early Carboniferous orogenic collapse in the Bohemian Massif. Journal of Structural Geology, 36, 27-42.

ZHAO, X.F., ZHOU, M.F., LI, J.W.,WU, F.Y., 2008. Association of Neoproterozoic A- and I-type granites in South China: Implications for generation of A-type granites in a subduction-related environment. Chemical Geology 257, 1–15

5   CONSIDERAÇÕES FINAIS

As conclusões do trabalho são baseadas em interpretações bem embasadas sobre os resultados da pesquisa, criteriosamente executada, a partir da aplicação da metodologia recomendada, diante do problema geológico apresentado, embora possam ser questionadas e até inviabilizadas, principalmente em se tratando de crosta Paleoproterozóica e de Amazônia.

Os processos de alteração hidrotermal aos quais foi submetido o Granito Moderna, podem não só modificar composição mineralógica, texturas, foliações e gerar anomalias à resposta geofísica, como também fornecem características distintivas às rochas alteradas, como é distintamente vermelho o Granito Moderna.

O Granito Moderna tipo, aflorante na Serra da Antena, pode ter sua intrusão associada à descontinuidade litológica existente entre os granitos Martins Pereira e Caroebe, com direção aproximada N-S na área de estudo, segundo a qual se dispõe a Serra da Antena. Os lineamentos estruturais E-W já existentes, permitiram que o magmatismo se propagasse para leste, encaixado em descontinuidades tectônicas crustais. Fato que se reflete no Granito Moderna pálido encontrado a sudeste da Serra da Antena, em contato progressivo e difuso com o Granito Caroebe, onde, assim como na aparência da rocha, a resposta geomorfológica não é tão distinta. Já o Granito Matins Pereira, mais antigo e consolidado, a sudoeste, não permitiu essa propagação. Esse contato é marcado pela fácies Magnetita-granito do Granito Moderna.

Dois corpos alongados NW-SE revelam-se um único pluton alongado NE-SW interceptado por zona de cisalhamento NW-SE. A disposição espacial do Granito Moderna tem relação com seu fluxo magmático, orientado predominantemente ENE-WSW, com obliterações locais decorrentes de zonas de cisalhamento dúcteis. Deformação em estado sólido é observada principalmente nas rochas encaixantes.

De acordo com os dados apresentados, o Granito Moderna demostra ter uma relação genética-estrutural limitada com a orogenia que formou os granitos adjacentes. Pode, portanto, ser entendido como resultado de pontual magmatismo associado à reativação de zonas de cisalhamento e alterações metassomáticas em um ambiente pós-orogênico. Esses eventos, por sua vez, podem ter relação com orogenias distais ou demais processos responsáveis por instabilidades crustais oriundas da amalgamação das províncias ocidentais do Cráton Amazônico. Por outra ótica, o magmatismo Moderna pode também ser entendido como um dos últimos pulsos magmáticos relacionados a uma orogênese Orosiriana, com mais de 150 milhões de anos de duração, controlada por campos de tensão com diferentes orientações, responsável pelo arcabouço litológico-estrutural da porção central do Escudo das Guianas.

6. REFERÊNCIAS BIBLIOGRÁFICAS

Abreu, R. L. Mapa do Estado de Roraima; 30 de abril de 2006. Disponível em: <https://commons.wikimedia.org/wiki/File:Roraima_MesoMicroMunicip.svg>. Acessado em 23 de janeiro de 2017.

Åhall K.I., Conelly J.N., Brewer T.S.; Episodic rapakivi magmatism due to distal orogenesis?: 2000 Correlation of 1.69-1.50 Ga. orogenic and inboard, "anorogenic" events in the Baltic Shield. Geology, vol. 28: 823-826 p.

Almeida, F.F.M., Hasui, Y., de Brito Neves, B.B., Fuck, R.A. 1981. Brazilian structural provinces: an introduction. Earth-Science Reviews 17;: 1–29 p.

Almeida, M.E.; Fraga, L.M.B.; Macambira, M.J.B. 1997. New geochronological data of calc-alkaline granitoids of Roraima State, Brazil. In: SOUTH-AMERICAN SYMPOSIUM ON ISOTOPE GEOLOGY, 1,. Extended Abstract, IG/USP, p.34-37.

Almeida, F.F.M.D., Brito, N., De, B.B., Carneiro, C. 2000, The origin and evolution of the South American Platform. Earth-Science. Reviews 50 :77–111 p.

Almeida, M.E.; Macambira M.J.B., Faria M.S.G. de. A 2002. Granitogênese Paleoproterozóica do Sul de Roraima. In: CONGRESSO BRASILEIRO DE GEOLOGIA, 41,. Anais..., SBG, p 434.

Almeida, M. 2006. Evolução geológica da porção centro-sul do Escudo das Guianas com base no estudo geoquímico, geocronológico e isotópico dos granitóides Paleoproterozóicos do sudeste de Roraima, Brasil. Pará: Universidade federal do Pará. Tese de Doutorado.. 241 P.

Almeida, M.E, Macambira, M.J.B., Oliveira, E.C. 2007. Geochemistry and zircon geochronology of I-type high-K calc-alkaline and S-type granitoid rocks from south-eastern Roraima, Brazil: Orosirian collisional magmatism evidence (1.97-1.96Ga) in central portion of Guyana Shield. Prec. Res., 155,. p. 69-97.

Almeida, M.E., Macambira, M.J.B., Valente, S.d.C., 2008. New geological and single-zircon Pb evaporation data from the Central Guyana Domain, southeastern Roraima, Brazil: tectonic implications for the central region of the Guyana Shield. Journal of South American Earth Sciences,. 26:318–328p.

Almeida, M.E., Macambira, M.J.B., Santos, J.O.S., Nascimento, R.S.C., Paquette, J.L., 2013. Evoluçao crustal do noroeste do Craton Amazonico (Amazonas, Brasil) baseada em dados de campo, geoquímicos e geocronologicos. In: SBG/Núcleo Norte, Simposio de Geologia da Amaz onia, 13 , Belem. Anais 1 e4.

Amaral, G. 1974. Geologia Pré-Cambriana da Região Amazônica. PhD thesis, Universidade de São Paulo, Instituto de Geociências.

Amaral, G. 1984. Provincia Tapajós e Rio Branco. In: Almeida, F.F.A & Hasui, Y. (eds.) O Précambriano do Brasil. São Paulo: Edgar Blucher Ltda., pp. 6-35.

Archanjo, C.J., Launeau, P. & Bouchez, J.L., 1995. Magnetite fabric vs. magnetite and biotite shape fabrics of the magnetite-bearing granite pluton of Gameleiras (Northeast Brazil). Physics of the Earth and Planetary Interiors, 89, 63–75.

Archanjo, C. J., Da Silva, E. R., & Caby, R. 1999. Magnetic fabric and pluton emplacement in a transpressive shear zone system: the Itaporanga porphyritic granitic pluton (northeast Brazil). Tectonophysics, 312(2), 331-345.

Archanjo, C. J., Trindade, R. I., Bouchez, J. L., & Ernesto, M. 2002. Granite fabrics and regional-scale strain partitioning in the Seridó belt (Borborema Province, NE Brazil). Tectonics, 21(1). 3-14.

Archanjo, C.J., Launeau, P., Hollanda, M.H.B.M., Macedo, J.W.P., Liu, D., 2009. Scattering of magnetic fabrics in the Cambrian alkaline granite of Meruoca (Ceará state, northeastern Brazil). International Journal of Earth Sciences 98:1793–1807. http://dx.doi.org/ 10.1007/s00531-008-0342-z.

Arzi, A.A., 1978. Critical phenomena in the rheology of partially melted rocks. Tectonophysics 44, 173–184.

Barbarin, B., Didier, J. 1992. Genesis and evolution of mafic microgranular enclaves through various types of interaction between coexisting felsic and mafic magmas. Transactions of the Royal Society of Edinburgh: Earth Sciences 83: 145-153.

Barbarin, B., 1990. Plagioclase xenocrysts and mafic magmatic enclaves in some granitoids of the Sierra Nevada Batholith, California.Journal of Geophysical Research B95, 17747 -17756.

Barbarin, B., 1999. A review of the relationships between granitoids types, their origins and their geodynamic environments. Lithos 46, 605–626.

Barron, C.N. 1966. Notes on the Stratigraphy of Central British of Guyana.In: ConferenciaGeologicaInterguianas, 6. BelCm,1966. Anais. BelCm, Pard, Brazil. Departamento Nacional da Produqz Mineral. Avulso, v. 41, pp. 121-126.

Barros, C.E.M.; Barbey, P.; Boullier, A.M. 2001. Role of magma pressure, tectonic stress and crystallization progress in the emplacement of syntectonic granites. The A-type estrela Granite Complex (Carajás Mineral Province, Brazil). Tectonophysics, 343: 93-109.

Bastos Neto, A.C., Pereira, V.P., Ronchi, L.H., De Lima, E.F., Frantz, J.C., 2009. The world-class Sn, Nb, Ta, F (Y, REE, Li) deposit and the massive cryolite associated with the albiteenriched facies of the madeira A-type granite, Pitinga Mining District, Amazonas State, Brazil. Canadian Mineralogist 47:1329–1357. http://dx.doi.org/10.3749/ canmin.47.6.1329.

Bastos Neto, A.C., Ferron, J.T.M.M., Chauvet, A., Chemale, F., de Lima, E.F., Barbanson, L., Costa, C.F.M., 2014. U–Pb dating of the Madeira Suite and structural control of the albite-enriched granite at Pitinga (Amazonia, Brazil): evolution of the A-type magmatism and implications for the genesis of the Madeira Sn–Ta–Nb (REE, cryolite) world-class deposit. Precambrian Research 243:181–196. http://dx.doi.org/10.1016/j. precamres.2013.12.021.

Bergantz, G.W., Schleicher, J.M., Burgisser, A., 2017. On the kinematics and dynamics of crystal-rich systems. J. Geophys. Res. Solid Earth 122.

Bettencourt, J.S., Juliani, C., Xavier, R.P., Monteiro, L.V.S., Bastos Neto, A.C., Klein, E.L., Assis, R.R., Leite, W.B., Moreto, C.P.N., Fernandes, C.M.D., Pereira, V.P., 2015. Metallogenetic systems associated with granitoid magmatism in the Amazonian Craton: an overview of the present level of understanding and exploration significance. Journal of South American Earth Sciences http://dx.doi.org/10.1016/j.jsames.11.014.

Bolle, O., Diot, H., Duchesne, J.C., 2000. Magnetic fabric and deformation in charnockitic igneous rocks of the Bjerkreim–Sokndal layered intrusion (Rogaland, Southwest Norway). Journal of Structural Geology 22:647–667. http://dx.doi.org/10.1016/ S0191-8141(99)00183-2.

Bolle, O., Trindade, R.I.F., Luc Bouchez, J., Duchesne, J.-C., 2002. Imaging downward granitic magma transport in the Rogaland Igneous Complex, SW Norway. Terra Nova 14: 87–92. http://dx.doi.org/10.1046/j.1365-3121.2002.00393.x.

Bonin, B., 1986. Ring Complex Granites and Anorogenic Magmatism. North Oxford Academic Pub, London.

Bonin, B., 2007. A-type granites and related rocks: evolution of a concept, problems and prospects. Lithos 97 (1–2), 1–2.

Borradaile, G.J., Jackson, M., 2004. Anisotropy of magnetic susceptibility (AMS): magnetic petrofabrics of deformed rocks. Geological Society, London, Special Publications 238: 299–360. http://dx.doi.org/10.1144/GSL.SP.2004.238.01.18.

Borradaile, G.J., Henry, B., 1997. Tectonic applications of magnetic susceptibility and its anisotropy. Earth-Science Reviews 42:49–93. http://dx.doi.org/10.1016/S0012-8252(96)00044-X.

Borradaile G. J., Werner T. 1994. Magnetic anisotropy of some phyllosilicates. Tectonophysics, vol. 235, issue 3,

pp 233 – 248

Bouchez, C.L.; Delas, C.; Gleizes, G.; Nédélec, A. 1992. Submagmatic microfractures in granites. Geology, vol. 20: 35-38.

Bouchez, J. 1997. Granite is never isotropic: an introduction to AMS studies in granitic rocks. In: Bouchez, J.; Hutton, D.; Stephens, W. Granite: from segragation of emplacement fabrics. Dordrecht: Kluwer Academic Publishers, v. 8, p. 95-112.

Bouchez, J.L., 2000. Anisotropie de susceptibilité magnétique et fabrique des granites. Comptes Rendus de l'Académie des Sciences-Series IIA-Earth and Planetary Science 330 (1), 1–14.

Bouchez, J.L., Diot, H., 1990. Nested granites in question: contrasted emplacement kinematics of independent magmas in the Zaër pluton, Morocco. Geology 18:966–969. http://dx.doi.org/10.1130/0091-7613(1990)018b0966:NGIQCEN2.3.CO;2.

Breiter, K., 2012. Nearly contemporaneous evolution of the A- and S-type fractionated granites in the Krušné hory/Erzgebirge Mts., Central Europe. Lithos 151, 105–121.

Brown, M., 2013. Granite: from genesis to emplacement. Bull. Geol. Soc. Am. 125, 1079–1113.

Brown M., Solar G.S. 1998. Shear-zone systems and melts: feedback relations and self-organization in orogenic belts. Journal of Strutural Geology. Vol 20, p. 211-227,.

Brown M. 2001. Orogeny, migmatites and leucogranites: A review Earth Planet. Science, vol. 110 (4):.313-336

Burg J. P., Arbert L., Chaudhry N.M. Dawwod H., Hussain S., Zeilinger G. 2005. Shear strain localization from the upper mantle to the middle crust of the Kohistan Arc (Pakistan). Geological Society, Special Publication 245, pp 34-52.

Burgess, S.D., Miller, J.S., 2008. Construction, solidification and internal differentiation of a large felsic arc pluton: cathedral Peak granodiorite, Sierra Nevada Batholith. Geol. Soc. Lond. Spec. Publ. 304, 203–233.

Caballero, C.I. 2011. La fábrica magnética a partir de la anisotropía de susceptibilidad Magnénica (AMS): sus bases generales y ejemplos como auxiliar para determinar direcciones, fuentes y dinamicas de flujo.Geofisica UNAM. 69p.

Caricchi, L., Annen, C., Rust, A., Blundy, J., 2012. Insights into the mechanisms and timescales of pluton assembly from deformation patterns of mafic enclaves.Journal of Geophysical Research B117, B11206.http://dx.doi.org/10.1029/2012JB009325.

Carvalho Filho, N., Horbe, M.A., Horbe, A.C., 1984. A natureza dos depósitos de cassiterita do setor Madeira, região do Pitinga, Amazonas, Brasil. Anais Do II Simpósio Amazonico, Manaus, DPNPM:pp. 459–466 http://dx.doi.org/10.1016/0375-6742(91)90040-2.

Chappell, B.W., White, A.J.R., 1974. Two contrasting granite types. Pacific Geology 8, 173–174.

Clarke, D.B., Clarke, G.K.C., 1998. Layered granodiorites at chebutco head, South mountain batholith, Nova Scotia. J. Struct. Geol. 20, 1305–1324.

Collins, W.J., Beams, S.D., White, A.J.R., Chappell, B.W., 1992. Nature and origin of A-type granites with particular reference to southeastern Australia. Contributions to Mineralogy and Petrology 80, 189–200.

Cordani, U.G. & Brito Neves, B.B. The Geologic Evolution of South America During the Archean and Early Proterozoic. Revista Brasileira de Geociências, 12 (1-3): 78- 88. 1982.

Cordani, U.G.; Tassinari; C.G.C.; Teixeira, W.; Basei, M.A.S.; Kawashita, K. 1979. Evolução tectônica da Amazônia com base nos dados geocronológicos. In: CONGRESO Geológico Chileno, 2. Arica. Anais. Arica, Chile, p.137-138.

Costa, A., Caricchi, L., Bagdassarov, N., 2009. A model for the rheology of particle bearing suspensions and partially molten rocks. Geochem. Geophys. Geosys. 10http://dx.doi.org/10.1029/2008GC002138. Q03010.

Costa, J.B.S. & Hasui, Y. 1997. Evolução Geológica da Amazônia. In: FINEP, SBGNO (Ed.). Geologia da Amazônia. Belém, p. 15-90.

Costa, J.B.S.; Pinheiro, R.V.L; Reis, N.J.; Pessoa, M.R.; Pinheiro, S. da S. 1991.O Hemigraben do Tacutu, uma estrutura controlada pela geometria do Cinturão de Cisalhamento Guiana Central. Geociências, São Paulo, 10:119-130.

Costi, H.T., 2000. Petrology of Rare Metals-, High-F Alkaline Granites: The Example of the Albite Granite From the Pitinga Mine, Amazonas State, Brazil. Federal University of Pará, Belém, Brazil, p. 345 (Doctoral thesis).

Costi, H.T., Dall'Agnol, R., Moura, C.A.V. Geology and Pb-Pb geochronology of Paleoproterozoic volcanic and granitic rocks of the Pitinga Province, Amazonian craton, northern Brazil. International Geology Review, 2000. 42 : p 832-849.

Costi, H.T., Dall'Agnol, R., Borges, R.M.K., Minuzzi, O.R.R., Teixeira, J.T., 2002. Tin-bearing Sodic Episyenites associated with the Proterozoic, A-type Água Boa Granite, Pitinga Mine, Amazonian Craton, Brazil. Gondwana Research 5:435–451. http://dx.doi.org/ 10.1016/S1342-937X(05)70734-6.

Costi, H.T., Borges, R.M.K., Dall'Agnol, R., 2005. Depósitos de estanho da Mina Pitinga, Estado do Amazônas. Caracterização de Depósitos Minerais Em Distritos Mineiros Da Amazônia, p. 475.

Costi, H.T., Dall'Agnol, R., Pichavant, M., Ramo, O.T., 2009. The peralkaline tin-mineralized Madeira cryolite albite-rich granite of Pitinga, Amazonian Craton, Brazil: petrography, mineralogy and crystallization processes. The Canadian Mineralogist 47:1301–1327. http://dx.doi.org/10.3749/canmin.47.6.1301.

CPRM – Serviço Geológico do Brasil. 1999. Roraima Cnetral, folhas NA. 20-X-D (integrais) e folhas NA. 20-XA, NA.21-V-C (Parciais). Escala 1:500.000. Programa de Levantamentos Geológicos Básicos do Brasil Estado de Roraima, Superintendência Regional de Manaus, Brasil, 166 p.

CPRM. 2000. Programa Levantamentos Geológicos Básicos do Brasil. Caracaraí, Folhas NA.20-Z-B e NA.20-Z-D (integrais), NA.20-Z-A, NA.21-Y-A, NA.20-Z-C e NA.21-Y-C (parciais). Escala 1:500.000. Estado de Roraima. Manaus, CPRM, p 157 (em CD-ROM).

CPRM. 2003. Programa Levantamentos Geológicos Básicos do Brasil. Geologia, Tectônica e Recursos Minerais do Brasil: sistema de informações geográficas - SIG. Rio de Janeiro, CPRM, Mapas. Escala 1:2.500.000. (em 4 CDs-ROM).

CPRM 2006. Programa Integração, Atualização e Difusão de Dados da Geologia do Brasil: Subprograma Mapas Geológicos Estaduais. Geologia e Recursos Minerais do Estado do Amazonas. Manaus, CPRM/CIAM-AM,. Escala 1:1.000.000. Texto explicativo, p 148 (em CD-ROM).

Cruden, A., 1990. Flow and fabric development during the diapiric rise of magma. J. Geol. 98, 681–698.

Dall'agnol R., Costi H.T., Leite S.A.A., Magalhães M.S., Teixeira N.P. 1999, Rapakivi granites from Brazil and adjacent areas. Precambrian Research,. vol. 95: p 9-39.

Dall'agnol R., Teixeira N.P.R., rämö O.T., Moura C.A.V., Macambira M.J.B., Olivira D.C. 2005. Petrogenesis of the Paleoproterozoic rapakivi, A-type granites of the Archaean CarajásMetallogenic Province. Lithos,. vol. 80: p 101-129.

Delor, C.; Lafon, J-M; Lahondere, D.; De Roever, E.W.F. ;Fraga, L.M. : Rossi, P. 2001. Paleoproterozoic framework of the Guiana Shield II – continental scale boudinage and ultra-high temperature granulite belt exumation at 2.07-2.05 Ga. In: SIMPÓSIO DE GEOLOGIA DA AMAZÔNIA, 7. Belém. Anais... Belém : SBG, Núcleo Norte. CD-ROM.

Dunlop, D. J., & Özdemir, Ö. 1997. Rock magnetism: fundamentals and frontiers. Cambridge University Press, 572p.

Dunlop, D.J., 2014. High-temperature susceptibility of magnetite: a new pseudo-singledomain effect. Geophysical Journal International 199:707–716. http://dx.doi.org/10. 1093/gji/ggu247.

Dunlop, D.J., Özdemir, Ö., 2007. Magnetizations in rocks and minerals. Treatise on Geophysics:pp. 277–336 http://dx.doi.org/10.1016/B978-044452748-6.00093-6.

Eby N. 1992, Chemical subdivision of the A-type granitoids: Petrogenetic and tectonic implications. Geology, vol. 20: 641-644.

Emslie, R.F., Stirling, J.A.R.. 1993. Rapakivi and related granitoids of the Nain Plutonic Suite: Geochemistry, mineral assemblages and fluid equilibria. CanadianMineralogy,. vol. 31: p 821-847.

Farahat, E.S., Mohamed, H.A., Ahmed, A.F., Mahallawi, M.M.E., 2007. Origin of I- and Atype granitoids from the Eastern Desert of Egypt: Implications for crustal growth in the northern Arabian-Nubian Shield. Journal of African Earth Sciences 49, 43–58.

Faria M.S.G. de, Luzardo R., Pinheiro S. da S. 1999. Litoquímica e petrogênese do Granito Igarapé Azul. In: SBG, Simp. Geol. Amaz., 6, Anais, p. 577-580.

Faria M.S.G. de, Oliveira M.J.R., Luzardo R, Pinheiro S. da S. 1996. Garimpo do Anauá, Sudeste do Estado de Roraima: dados preliminares sobre ocorrência aurífera associada à zona de cisalhamento. In: SBG, Cong. Bras. Geol., 39, Anais, v. 3 p. 316-319.

Faria M.S.G. de, Almeida M.E., Santos J.O.S. dos, Chemale Jr. F. 2003. Evolução Geológica da Região do Alto Rio Anauá - Roraima. In: SBG, Simp. Geol. Amaz., 8, Anais, CD-ROM.

Ferré, E.C., 2002. Theoretical models of intermediate and inverse AMS fabrics. Geophysical Research Letters 29:29–32. http://dx.doi.org/10.1029/2001GL014367.

Ferré, E.C., Wilson, J., Gleizes, G., 1999. Magnetic susceptibility and AMS of the Bushveld alkaline granites, South Africa. Tectonophysics 307:113–133. http://dx.doi.org/10. 1016/S0040-1951(99)00122-5.

Ferron, J.M.T.M., Bastos Neto, A.C., Rolim, S.B.A., 2002. Reconhecimento de uma megaestrutura no distrito mineiro de Pitinga-AM: dados preliminares a partir da aplicação de técnicas de processamento digital de imagens ETM+ Landsat 7. II Simpósio de Vulcanismo, Belém, Brazil, Anais 1, p. 14.

Ferron, J.M.T.M., Neto, A.C.B., de Lima, E.F., Rolim, S., Hoff, R., Umann, L., Minuzzi, O.R.R., 2004. Novos dados geoquímicos de rochas granitóides e vulcânicas paleoproterozóicas do Distrito Mineiro de Pitinga, Amazonas. Congresso Brasileiro de Geologia, 42, Goiânia, SBG (Em CD-ROOM).

Ferron, J.M.T.M., Neto, A.C.B., de Lima, E.F., Costi, H.T., Moura, C.A.V., Prado, M., Pierosan, R., Galarza, M.A., 2006. Geologia e geocronologia Pb–Pb de rochas graníticas e vulcânicas ácidas a intermediárias Paleoproterozóicas da Província Pitinga, Craton Amazônico. Revista Brasileira de Geociencias 36, 499–512.
Ferron, J.M.T.M., Bastos Neto, A.C., Lima, E.F., Nardi, L.V.S., Costi, H.T., Pierosan, R., Prado, M., 2010. Petrology, geochemistry, and geochronology of Paleoproterozoic volcanic and granitic rocks (1.89–1.88 Ga) of the Pitinga Province, Amazonian Craton, Brazil. Journal of South American Earth Sciences 29:483–497. http://dx.doi.org/10.1016/j. jsames.2009.05.001.

Fraga, L. M. B. 2009. 1.94-1.93 Ga charnockitic magmatism from the central parto f the Guyana Shield, Roraiza, Brazil: Single-zircon evaporation data and tectonic implications. Journal of South American Earth Sciences, 27, 247-257.

Fraga, L. M. B. 2002. A Associação Anortosito-Mangerito Granito Rapakivi (AMG) do Cinturão Guiana Central e suas encaixantes paleoproterozóicas: Evolução Estrutural, Geocronologia e Petrologia. Pará: Universidade federal do Pará, p351.

Fossen, H., 2010. Structural Geology. First. ed. Cambridge University Press, New York http://dx.doi.org/10.1007/s13398-014-0173-7.2.

Fossen, H., Tikoff, B. 1998.Extended models of transpression/transtension and application to tectonic settings. In: Holdsworth, R.E., Strachan, R.A., Dewey, J.F. (Eds.), Continental Transpressional and Transtensional Tectonics, Geological Society of London Special Publication, vol. 135, p. 15-33.

Fossen, H., Tikoff, B., Teyssier, C. 1994. Strain modeling of transpressional and transtensional deformation. Norsk Geol. Tidsskr. 74, 134-145.

Frost, C.D., Frost, B.R., 2011. On ferroan (A-type) granitoids: their compositional variability and modes of origin. Journal of Petrology 52 (1), 39–53.

Fuck, R.A., Pimentel, M.M., Machado, N., Daoud, W.E.K., 1993. Idade U–Pb do Granito Madeira, Pitinga (AM) 1993. 4th Congresso Brasileiro de Geoquímica. Resumos expandidos, Brasília, pp. 246–249.

GapaiS, D., Barbarin, B., 1986. Quartz fabric transition in a cooling syntectonic granite (Hermitage Massif, France). Tectonophysics 125, 357e370.

Gapais, D. 1989. Shear strutures within deformed granites: Mechanical and thermal indicators. The geological society of America, 17(12). p. 1144-1147.

Gaudette, H., Olszewski, J., Santos, J. 1996. Geochronologyof precambriam rocks from the northern parto Guiana Shield, Stare of Roraima, Brazil. Journal of South America Earth Sciences, v. 9 (3 e 4), p. 183-195.

Gaudette, H.E. & Olszewski JR., W.J. 1985. Geochronology of the basement rocks, Amazonas Territory, Venezuela, and the tectonic evolution of the western Guiana Shield. Geol. Mijnbouw, 64: 131-143.

Gibbs, A.K. & Barron, C.N. 1993. The geology of the Guyana Shield. Oxford University Press, Oxford, N. York,. p 245.

Glazner, A.F., Bartley, J.M., Coleman, D.S., Gray, W., Taylor, R.Z., 2004. Are plutons assembled over millions of years by amalgamation from small magma chambers? GSA Today 14:4–11. http://dx.doi.org/10.1130/1052-5173(2004)014b0004.

Gleizes, G., Nédélec.,J.L, Bouchez, A., Autran, A., Rochette, P. 1994. Magnetic susceptibility of the Mont-Louis-Andorra ilmenite-type granite (Pyrenees): A new tool for the petrographic characterization and regional mapping of zoned granite plutons. JournalOfGeophysicalResearch, Vol 103,p. 5257-5267

Gourgaud A., Fichaut M., Joron J. L. 1989. Magmatology of Mt. Pelee (Martinique, F.W.I.). I: Magma mixing and triggering of the 1902 and 1929 Pelean nuees ardentes. J. Volc. Geotherm. Res., 38:143-169.

Guilbert, J.M. and Park, C. F. 1986. The Geology of Ore Deposits. W. H. Freeman and Company, New York.

Hasui, Y., HaralyI, N., L. E., Costa, J. B.S. 1993. Megaestruturação pré-cambriana do território brasileiro baseada em dados geofísicos e geológicos. Geociências, São Paulo, v. 12, n. 1, p. 7-31.

Hasui, Y. 1990. Neotectônica e aspectos fundamentais da tectônica ressurgente no Brasil. In: workshop sobre neotectônica e sedimentação cenozóica continental no sudeste brasileiro, Belo Horizonte, 1990. Anais ...Belo Horizonte: SBG/MG, p.1-31.

Hasui, Y., Haralyi., N.L.E., Schobbenhaus F.C. 1984. Elementos geofísicos e geológicos da região amazônica: subsídios para o modelo geotectônico. In: Symposium Amazonico 2, Manaus. Anais., SBG, v. 1, pp. 129-148.

Hutton, D. H. W. 1988. Granirte emplacement mechanisms and tectonic controls: inferences from de deformation studies. Transactions of Royal Society of Edinburgh: Earth Sciences, 79: 245-255.

Hasui, Y. 1996. Evolução geológica da Amazônia In: SIMP. GEOL AMAZ., 5. Belém, 1996. Boletim de resumos expandidos ... Belém, SBG p. 31-34.

He, Z.Y., Xu, X.S., Niu, Y.L., 2010. Petrogenesis and tectonic significance of a Mesozoic granite-syenite-gabbro association from inland South China. Lithos 119, 621–641

Hodych, J.P., Mackay, R.I., English, G.M., 1998. Low-temperature demagnetization of saturation remanence in magnetite-bearing dolerites of high coercivity. Geophysical Journal International 132 (2), 401–411.

Horbe, M., Horbe, A., Teixeira, J., Costi, H.T., 1985. Granito Madeira: petrologia, petroquímica e mineralizações. II Simpósio de Geologia Da Amazônia, Anais, Belem, SBG/NM 3, pp. 284–320.

Horbe, M.A., Horbe, A.C., Costi, H.T., Teixeira, J.T., 1991. Geochemical characteristics of cryolite-tin-bearing granites from the Pitinga Mine, northwestern Brazil—A review. Journal of Geochemical Exploration 40 (1-3), 227–249.

Hrouda, F., 1982. Magnetic anisotropy of rocks and its application in geology and geophysics. Geophysical Surveys 5:37–82. http://dx.doi.org/10.1007/ BF01450244.

Hrouda, F., 1993. Theoretical models of magnetic anisotropy to strain relationship revisited. Physics of the Earth and Planetary Interiors 77:237–249. http://dx.doi.org/ 10.1016/0031-9201(93)90101-E.

Hutton D. H. W. 1988. Granite emplacement mechanisms and tectonic controls: inferences from deformation studies. TRANS R SOC EDINBURGH 79, 245–55

Irvine, T.N., 1977, Origin of chromite layers in the Muskox intrusion and other stratiform intrusions: A new interpretation: Geology, v. 5, p. 273–277, doi: 10.1130/0091-7613(1977)5,273:OOCLIT.2.0.CO;2.

Jackson, M., 1991. Anisotropy of magnetic remanence: a brief review of mineralogical sources, physical origins, and geological applications, and comparison with susceptibility anisotropy. Pure and Applied Geophysics PAGEOPH 136:1–28. http://dx.doi. org/10.1007/BF00878885.

Jamieson R A, Unsworth JM, Harris BW N, Rosenberg CL, Karel Schulmann k. 2011. Crustal Melting and the Flow of Mountains. ELEMENTS, VOL. 7: 253–260.

Janelik, V. 1981. Characterization of the magnetic fabric of rocks.Tectonophysis, vol.79: T63-T67..

Jelinek, V., 1977. The Statistical Theory of Measuring Anisotropy of Magnetic Susceptibility of Rocks and Its Application. Jelínek, V., 1978. Statistical processing of anisotropy of magnetic susceptibility measured on groups of specimens. Studia Geophysica et Geodaetica 22:50–62. http://dx.doi. org/10.1007/BF01613632.

Jiang, Y.H., Zhao, P., Zhou, Q., Liao, S.Y., Jin, G.D., 2011. Petrogenesis and tectonic implications of Early Cretaceous S-and A-type granites in the northwest of the Gan-Hang rift, SE China. Lithos 121, 55–73.

Jorge-João X.S., Santos C.A., Provost A. 1985. Magmatismo adamelítico Água Branca (Folha Rio Ma puera, NW do Estado do Pará). In: SBG, Simp. Geol. Amaz., 2, Anais, v.2, p. 93-109.

Karsli, O., Caran, Ş., Dokuz, A., Çoban, H., Chen, B., Kandermir, R., 2012. A-type granitoids from the Eastern Pontides, NE Turkey: Records for generation of hybrid A-type rocks in a subduction-related environment. Tectonophysics 530–531, 208–224.
Kilian, R., Heilbronner, R., Stünitz, H., 2011. Quartz grain size reduction in a granitoid rock and the transition from dislocation to diffusion creep. Journal of Structural Geology 33:1265–1284. http://dx.doi.org/10.1016/j.jsg.2011.05.004.

Kretz, R., 1983. Symbols of rock-forming minerals. American Mineralogist 68, 277–279.
Kruiver, P.P., Dekkers, M.J., Heslop, D., 2001. Quantification of magnetic coercivity components by the analysis of acquisition curves of isothermal remanent magnetisation. Earth and Planetary Science Letters 189:269–276. http://dx.doi.org/10.1016/S0012- 821X(01)00367-3.

Kruhl, J.H. 1966. Prism- and basal plane parallel subgrain boundaries in quartz: a microstructural geothermobarometer. J. Metamorphic Geol., 14, 581-589.

Ludwig, K. R., 2012, Isoplot, A Geochronological Toolkit for Microsoft Excel. Berkeley Geochronology Center, Special Publication No. 5, 75p.

L., White, A.J.R., Chappell, B.W., Allen, C.M., 1997. Characterization and origin of aluminous A-type granites

fromthe Lachlan Fold Belt, Southeastern Australia. Journal of Petrology 38 (3), 371–391.

Lamarão, C.N.; Dall'agnol, R.; Lafon, J.-M.; Lima, E.F. Geology, geochemistry and Pb–Pb zircon geochronology of the Paleoproterozoic magmatism of Vila Riozinho, Tapajós gold province, Amazonian craton, Brazil. Precambrian Research, 2002. 119 (1- 4) : 189–223.

Lameyre J. & Bonin B. 1991. Granites in the main plutonic series. In: J. Didier & B. Barbarin (eds.) Enclaves and Granite Petrology. Development in Petrology, v.13, p.3- 17.

Lameyre J. & Bowden P. 1982. Plutonic rock type series: discrimination of various granitoid rocks series and related rocks. J. Volc. Geotherm. Res., 14:169-186.

Landenberger, B., Collins, W.J., 1996. Derivation of A-type granites from a dehydrated charnockitic lower crust: Evidence from the Chaelundi Complex, eastern Australia. Journal of Petrology 37, 145–170.

Lenharo, S.L.R., Pollard, P.J., Born, H., 2003. Petrology and textural evolution of granites associated with tin and rare-metals mineralization at the Pitinga mine, Amazonas, Brazil. Lithos 66:37–61. http://dx.doi.org/10.1016/S0024-4937(02)00201-3.

Loiselle, M.C., Wones, D.R., 1979. Characteristics and origin of anorogenic granites. Abstracts papers to be presented at the Annual Meetings of the Geological Society of America and Associated Societies, San Diego, CA 11, 468.

Ludwig, K. (2009), Squid 2: A User's Manual, rev. 12 Apr, 2009. Berkeley Geochron. Ctr. Spec. Pub. 5 110 p.

Lucus, S.B., St-Onge, M.R., 1995. Syn-tectonic magmatism and the development of compositional layering, Ungawa Orogen (northern Quebec, Canada). J. Struct. Geol. 17, 475–491.

Macambira, M.J.B.; Almeida, M.E.; Santos, L.S. 2002. Idade de Zircão das Vulcânicas Iricoumé do Sudeste de Roraima: contribuição para a redefinição do Supergrupo Uatumã. In: simpósio sobre vulcanismo e ambientes associados, 2, Anais.., SBG, , p.22.

Majumder S., Mamtani M.A. 2009. "Magnetic Fabric in the Malanjkhand Granite (Central India)—Implications for regional Tectonics and Proterozoic Suturing of the Indian Shield," Physics of the Earth and Planetary Interiors, Vol. 172, No. 3-4, pp. 310-323. doi:10.1016/j.pepi.2008.10.007

Mamtani, M. A., Piazolo, S., Greiling, R. O., Kontny, A., Hrouda, F. 2011. Porcess of magnetite fabric development during granite deformation. Earth and Planetary Science Letters, 308, 77-89. (arrumar nome no texto)

Marques, S.N.d.S., Souza, V.d.S., Dantas, E.L., Valério, C.d.S., Nascimento, R.S.C.d., 2014. Contributions to the petrography, geochemistry and geochronology (U–Pb and Sm–Nd) of the Paleoproterozoic effusive rocks from Iricoumé Group, Amazonian Craton, Brazil. Brazilian Journal of Geology 44:121–138. http://dx.doi.org/10.5327/ Z2317-4889201400010010.

Mariano G. & Sial A.N. 1990. Coexistence and Mixing of Magmas in the Late Precambrian Itaporanga Batholith, State of Paraiba, Northeastern Brazil. Rev. Bras. Geoc., 20(1-4):101-110.

Martin, H., Bonin, B., Capdevila, R., Jahn, B.M., Lameyre, J., Wang, Y., 1994. The Kuiqi peralkaline granitic complex (SE China): petrology and geochemistry. Journal of Petrology 35, 983–1015.

McNulty, B.a., Tong, W., Tobisch, O.T., 1996. Assembly of a dike-fed magma chamber: the Jackass Lakes pluton, central Sierra Nevada, California. Bulletin of the Geological Society of America 108:926–940. http://dx.doi.org/10.1130/0016-7606(1996)108b0926: AOADFMN2.3.CO;2.

McNulty, B.A., Tobisch, O.T., Cruden, A.R., Gilder, S., 2000. Multistage emplacement of the Mount Givens pluton, Central Sierra Nevada batholith, California. Bulletin of the Geological Society of America 112:119–135. http://dx.doi.org/10.1130/0016- 7606(2000)112b119:MEOTMGN2.0.CO;2.

Miller, R.B, Bouchez, J.-L., Delas, C., Gleizes, A. N. & Cuney, M. 1992. Submagmatic microfractures in granites. Geology 20, 35-38.

Miller, R.B. & Paterson, S.R. 1994. The transition from magmatic to high temperature solid-state deformation: implications from the Mount Stuart batolith, Washington. J. Struct. Geol., 16: 835-865.

Nédélec, A., Paquette, J.-L., Bouchez, J.-L., Olivier, P., Ralison, B., 1994. Stratoid granites of Madagascar: structure and position in the Panafrican orogeny. Geodinamica Acta 7: 48–56. http://dx.doi.org/10.1080/09853111.1994.11105258.

Nédélec, A., Trindade, R., Peschler, A., Archanjo, C., Macouin, M., Poitrasson, F., Bouchez, J.- L., 2015. Hydrothermally-induced changes in mineralogy and magnetic properties of oxidized A-type granites. Lithos 212–215:145–157. http://dx.doi.org/10.1016/j.lithos. 2014.11.007.

Nicolas, A., & Ildefonse, B., 1996. Flow mechanism and viscosity in basaltic magma chambers. Geophys. Res. Lett. 23, 2013–2016.

Nitoi E., Munteanu M., Marincea S., Paraschivoiu V. 2002. Magma-enclave interactions in the East Carpathian Subvolcanic Zone, Romania: Petrogenetic implications. Journal of volcanology and geothermal research.Vol 118, pp. 229-259.

Neiva A.M.R. 2000. Comparison between Portuguese granites associated with Sn-W mineralizations and with Au mineralization. In: SBG, Intern. Geol. Cong., 31, Abstrac Vol., CD-ROM.

Neto, H.A., Moreira, H., 1976. Projeto Estanho de Abonari, in: Relatório Final, DNPM/ CPRM, Manaus. Unpublished work.

Neves, S.P., Vauchez, A., Archanjo, C.J., 1996. Shear zone-controlled magma emplacement or magma-assisted nucleation of shear zones? Insights from northeast Brazil. Tectonophysics 262, 349e364.

Olivier, P., Druguet, E., Castaño, L. M., & Gleizes, G. 2016. Granitoid emplacement by multiple sheeting during Variscan dextral transpression: The Saint-Laurent–La Jonquera pluton (eastern Pyrenees). Journal of Structural Geology, 82, 80-92.

Oliveira, D.C., Neves, S.P., Trindade, R.I.F., Dall'Agnol, R., Mariano, G., Correia, P.B., 2010. Magnetic anisotropy of the Redenção granite, eastern Amazonian craton (Brazil): implications for the emplacement of A-type plutons. Tectonophysics 493:27–41. http://dx.doi.org/10.1016/j.tecto.2010.07.018.

Oliveira M.J.R., Almeida M.E., Luzardo R., Faria M.S.G. de. 1996. Litogeoquímica da Suíte Intrusiva Água Branca - SE de Roraima. In: SBG, Congr. Bras. Geol., 39, Anais, v.2, p. 213-216 .

Passchier, C.W & Trouw, R.A.J. 2005.Microtectonics. 2nd, Revised and Enlarged Edition.

Paterson, S. R, Ardill K., Vernon R. Zák J. 2018. A review of mesoscopic magmatic structures and their potential for evaluating the hypersolidus evolution of intrusive complexes. Journal of structural Geology.

Paterson, S. R., Pignotta G.S., Vernon R.H. 2004. The significance of microgranitoid enclave shapes and orientations.Journal of strutural geology. Vol 26, pp 1465-1481.

Paterson, S. R. & Miller, R.B. 1998. Stoped blocks in plutons: paleo-plumb bobs, viscometers or Chronometers. Journal Structural of Geology, vol.20, No 9/10. Pp 1261-1272.

Paterson, S. R.; Vernon, R. H., Tobish, O. T. 1989.A review of criteria for identification of magmatic and tectonic foliations in granitoids. Journal Structural of Geology, p. 11-349.

Paterson, S.R., Tobisch, O.T., 1988. Using pluton ages to determine regional deformations: problems with commonly used criteria. Geology 16, 1108e1111.

Paterson, S.R., Tobisch, O.T., 1992. Rates of processes in magmatic arcs: implications for the timing and nature of pluton emplacement and wall rock deformation. Journal of Structural Geology 14, 291e300.

Paterson, S.R., Fowler, T.K., 1993. Extensional pluton-emplacement models: do they work for large plutonic

complexes? Geology 21:781–784. http://dx.doi.org/10.1130/0091- 7613(1993)021b0781:EPEMDTN2.3.CO.

Paterson, S.R., Vernon, R.H., 1995. Bursting the bubble of ballooning plutons: a return to nested diapirs emplaced by multiple processes. Geological Society of America Bulletin 107:1356–1380. http://dx.doi.org/10.1130/0016-7606(1995)107b1356:BTBOBPN2.3. CO;2.

Park, Y., Means, W.D., 1996. Direct observation of deformation processes in crystal mushes. J. Struct. Geol. 18. 847–858.

Petford, N., Kerr, R.C., Lister, J.R., 1993. Dike transport of granitoid magmas. Geology 21:845–848. http://dx.doi.org/10.1130/0091-7613(1993)021b0845:DTOGMN2. 3.CO;2.

Petford, N., Cruden, A.R., Mccaffrey, K.J.W., Vigneresse, J.L., 2000. Granite magma formation, transport and emplacement in the Earth's crust. Nature 408, 669e673.

Pierosan, R., de Lima, E.F., Nardi, L.V.S., Bastos Neto, A.C., de Campos, C.P., Jarvis, K., Ferron, J.M.T.M., Prado, M., 2011a. Geochemistry of Palaeoproterozoic volcanic rocks of the Iricoumé Group, Pitinga Mining District, Amazonian craton, Brazil. International Geology Review 53:946–979. http://dx.doi.org/10.1080/00206810903391542.

Pierosan, R., Lima, E.F., Nardi, L.V.S., de Campos, C.P., Bastos Neto, A.C., Ferron, J.M.T.M., Prado, M., 2011b. Paleoproterozoic (~1.88 Ga) felsic volcanism of the Iricoumé Group in the Pitinga Mining District area, Amazonian Craton, Brazil: insights in ancient volcanic processes from field and petrologic data. Anais da Academia Brasileira de Ciências 83:921–937. http://dx.doi.org/10.1590/S0001-37652011000300012.

Pitcher, W.S., 1979. The nature, ascent and emplacement of granitic magmas. Journal of the Geological Society 136:627–662. http://dx.doi.org/10.1144/gsjgs.136.6.0627.

Pitcher, W. S. 1998. The Nature and Origin of Granite, 2nd edition. London: Chapman & Hall. 387 pp.

Prado, M., Ferron, J.M.T.M., de Lima, E.F., Bastos Neto, A.C., Pereira, V.P., Minuzzi, O.R.R., Pierosan, R., 2007. Caracterização petrográfica e geoquímica da parte leste do Granito Europa, Distrito Mineiro de Pitinga, AM.

Price, J., Hogan, J.P., Gilbert, M.C., Payne, J.D., 1998. Surface and near-surface investigation of the alteration of the Mount Scott Granite and geometry of the Sandy Creek Gabbro Pluton, Hale Spring Area, Wichita Mountains, Oklahoma. In: Hogan, J.P., Gilbert, M.C. (Eds.), Central North America and Other Regions 12. Kluwer Academic Publisher, Basement Tectonics, pp. 79–122.

Pryer, L.L. 1993. Microstructures in feldspars from a major crustal thrust zone: the Grenville Front, Ontário, Canada. J. Struct. Geol., 15: 21-36.

Qiu, J.S., Wang, D.Z., Mclnnes, B.I.A., Jiang, S.Y., Wang, R.C., Kanisawa, S., 2004. Two subgroups of A-type granites in the coastal area of Zhejiang and Fujian Provinces, SE China: age and geochemical constraints on their petrogenesis. Transactions of the Royal Society of Edinburgh: Earth Sciences 95, 227–236.

Ramirez, J., Sierra, G.M, Marín, M.I. 2012. Anisotropía de susceptibilidad magnetica (ASM) del miembro superior de la Formación Amagá, sección Quebrada Sabaleticas, SW Antioqueño y su relación con los movimientos del sistema de fallas Romeral en el Cenozoico Tardio. 18p.

Reis, N.J.; Fraga, L.M., Faria, M.S.G., Almeida, M.E. 2003. Geologia do Estado de Roraima. Géologie de la France, 2-3: 71-84.

Reis, N., Faria, M.S.G., Fraga, L,M., Haddad, R.C. 2000. Orosirian calc-alkaline volcanism and the Orocaima event in the Northern Amazonian Craton, Eastern Roraima State, Brazil.Rev.Bras.Geociências, 30: 380-383.

Reis, N. J., Fraga, L. M. B. 1998. Geologia do Estado de Roraima. Publicação Interna, Inédito, CPRM, Manaus, 24 p.

Reis, N. J., Fraga, L. M. B. 1995. Granitogênese mesoproterozóica da porção central do Estado de Roraima - Petrologia e Litogeoquímica. In: Cong. Latino-Americano Geol., 9, Caracas, Venezuela, Temário 3.

Reis N.R. & Fraga L.M.B. 1996. Vulcanismo Surumu – Estado de Roraima: Caracterização de seu comportamento químico à luz de novos dados. In: SBG, Congr. Bras. Geol., 39, Anais, v. 2, p. 88-90 .

Reis N.R., Faria M.S.G. de, Fraga L.M.B., Haddad R.C. 2000. Orosirian calc-alkaline volcanism from eastern portion of Roraima State – Amazon Craton. Rev. Bras. Geoc. 30(3):380-383.

Reis, N.J.; Fraga, L.M.; Faria, M.S.G. De; Almeida, M.E. Geologia do Estado de Roraima. Géologie de la France, 2-3: 71-84. 2003.

Rodrigues, S.W.O., Archanjo, C.J., Launeau, P. Determinação da orientação preferencial de forma (OPF) de silicatos em rochas graníticas: Granito Campina Grande (PB). Revista Brasileira de Geociências, v. 39, 2009. p. 435-451.

Rosenberg, C.L., Handy, M.R., 2005. Experimental deformation of partially melted granite revisited: implications for the continental crust. J. Metamorph. Geol. 23, 19–28.

Rushmer, T., 1995. An experimental deformation study of partially molten amphibolite: Application to low-melt fraction. segregation. J. Geophys. Res. 100, 15681–15695.

Salazar, C.A. Anisotropia de susceptibilidade magnética dos plútons Riberão Branco, Sguário e Capão Bonito e implicações tectônicas para a Faixa Ribeira (Domínio Apiaí, SP). Tese de doutorado, Universidade de São Paulo, São Paulo, 2010. p. 165

Salazar CA. ; Archanjo C. J. ; Babinski M. ; LIU, D. 2008 . Magnetic fabric and zircon U-Pb geochronology of the Itaoca pluton: Implications for the Brasiliano deformation of the southern Ribeira Belt (SE Brazil). Journal of South American Earth Sciences , v. 26, p. 286-299.

Salazar, C. A., Archanjo, C. J., Sérgio, W. D. O., Hollanda, M. H. B., & Liu, D. 2013. Age and magnetic fabric of the Três Córregos granite batholith: evidence for Ediacaran transtension in the Ribeira Belt (SE Brazil). International Journal of Earth Sciences, 102(6), 1563-1581.

Santos, J., Rizzotto G., Potter, P., McNaughton N., Matos R., Hartman L., Chemale Jr. & Quadros M. 2008. Age and autochthonous evolution of the Sunsás Orogen in Wets Amazon Craton based on mapping and U-Pb geochronology. Precambriam Research, 165, 120-152.

Santos, J., Faria, M.S.G, Riker, S.R.L., Souza, M.M, Hartman, L.A., Almeida, M.E, McNaughton, N.J, Fletcher, I.R. 2006.A faixa colisionalK'Mudku (idade Grenvilliana) no norte do Cráton Amazonas: reflexo intracontinental do OrogenoSunsás na margem ocidental do cráton. In: BG, Simp.Geol. Amaz., 9, Belém, CD-Room.

Santos, J.O.S., Potter, P.E., Reis, N.J., Hartmann, L.A, Fletcher, I.R., McNaughton, N.J. 2003. Age, source and Regional Stratigraphy of the RoraimaSupergroup and Roraima-like Sequences in Northern South America, based on U-Pb Geochronology. Geol. Soc. Amer.Bull. 115 (3), 331-348.

Santos, J.O.S., Hartmann, L.A., McNaughton, N.J., Fletcher, I.R., 2002. Timing of mafic magmatism in the Tapajós Province (Brazil) and implications for the evolution of the Amazon Craton: evidence from baddeleyite and zircon U–Pb SHRIMP geochronology. Journal of South American Earth Sciences 15:409–429. http://dx.doi.org/10. 1016/S0895-9811(02)00061-5.

Santos, J., Hartman, L., Gaudette, H., Groves, D., McNaughton, N., Fletcher, I. 2000.A new understanding of the provinces of the Amazon Crátonbased on integration of field mapping and u-p band sm-nd geochronology. Gondwana Research, v. 3, p. 453-488.

Siachoque A., Salazar, C. A., Trinidade, R. 2016. Emplacement and deformation of the A-type Madeira granite (Amazonian Craton, Brazil).Lithos, accepted 18 oct. 2016.

Simões, M.S., Almeida, M.E., de Souza, A.G.H., da Silva, D.P.B., Rocha, P.G., 2014. Characterization of the volcanic and hypabissal rocks of the Paleoproterozoic Iricoumé Group in the Pitinga region and Balbina Lake area, Amazonian Craton, Brazil: petrographic distinguishing features and emplacement conditions. Journal of Volcanology and Geothermal Research 286:138–147. http://dx.doi.org/10.1016/j.jvolgeores.2014.08.024.

Smith, J.V., 2000. Textural evidence for dilatant (shear thickening) rheology of magma at high crystal concentrations.Journal of Volcanology and Geothermal Research 99, 1e7.

Stipp, M., Stunitz, H., Heilbronner, R., Schmid, S.M., 2002. Dynamic recrystallization of quartz: correlation between natural and experimental conditions. Geological Society, London, Special Publications 200:171–190. http://dx.doi.org/10.1144/GSL.SP.2001.200.01.11.

Streckeisen A.C. 1976. To each plutonic rock its proper name. Earth Sci. Rev., 12:1-33.

Sylvester PJ., Post-collisional alkaline granites. Journal of Geology, vol. 97: p 261-280. 1989.

Sylvester, P. J. 1998. Post-collisional strongly peraluminous granites. Lithos, 45(1), 29-44.

Tassinari, C. C. G, Macambira, M. 1999. Geochronological provinces of the amazonian cráton.Episodes, v. 22, n. 3, p. 174-182.

Tassinari, C.C.G., Cordani, U.G., Nutman, A.P., Van Schmus, W. R., Bettencourt, J.S.; Taylor, P.N. 1996.Geochronological systems on basement rocks from the Rio Negro-Juruena Province (Amazon Craton) and tectonic implications.Int. Geol. Ver., 38: 161-175.

Tarazona, C. 2015. Análises das petrotramas das rochas charnockíticas da Serra da Prata, Mucajaí. Manaus: Universidade Federal do Amazonas. 202p.

Tarling, D.H., Hrouda, F.H., 1993. The Magnetic Anisotropy of Rocks.Chapman & Hall, London.

Tauxe, L., Banerjee, K., Butler, R., Van Der Voo, R. 2018 Magnetics information consortium. Scripps Institution of Oceanography. Livro on line, link: https://earthref.org/MagIC/books/Tauxe/Essentials/.

Teixeira, W., Tassinari, C.C.G., Cordani, U.G., Kawashita, K. 1989. A review of the geochronology of the Amazonian Craton: tectonic implications. Precambrian Research, 42: 213-227.

Trindade, R.I.F., Bouchez, J.-L., Bolle, O., Nédélec, A., Peschler, A., Poitrasson, F., 2001. Secondary fabrics revealed by remanence anisotropy: methodological study and examples from plutonic rocks. Geophysical Journal International 147:310–318. http://dx. doi.org/10.1046/j.0956-540x.2001.01529.x.

Tullis, I. & Yund, R.A. 1977. Experimental deformation of dry Westerly granite. J. Geophys. Res., 82: 5.705-5.718.

Tullis, J., Yund, R.A., 1991. Diffusion creep in feldspar aggregates: experimental evidence. Journal of Structural Geology 13:987–1000. http://dx.doi.org/10.1016/ 0191-8141(91)90051-J.
Turner J.S. & Campbell I.H. 1986. Convection and mixing in magma chambers. Earth Sci. Rev., 23:255-52.

Valle Aguado, B., AZevedo, M. R., Nolan, J., Medina, J., Costa, M. M., Corfu, F., & Catalán, J. M. 2017. Granite emplacement at the termination of a major Variscan transcurrent shear zone: The late collisional Viseu batholith. Journal of Structural Geology, 98, 15-37.

Valério, C.D.S., Souza, V.D.S., Macambira,M.J.B., The 1.90–1.88 Ga magmatism in the southernmost Guyana Shield, Amazonas, Brazil: geology, geochemistry, zircon geochronology, and tectonic implications. Journal of South American Earth Sciences 28: p 304–320. 2009.

Vasquez, M.V.; Ricci, P.S.F.; Klein, E.L. Granitóides pós-colisionais da porção leste da Província Tapajós. In: Klein, E.L., Vasquez, M.L., Rosa-Costa, L.T. (Coord.), Contribuições à Geologia da Amazônia, vol. 3, Belém, 2002. SBG-NO, p. 63-83.

Veiga Jr J.P., Nunes, A., Souza, E., 1979. Projeto sulfetos de Uatumã, Relatório Final, Manaus. Unpublished work. Vernon, R.H., Paterson, S.R., 2008. How late are K-feldspar megacrysts in granites? Lithos 104:327–336. http://dx.doi.org/10.1016/j.lithos.2008.01.001.

Vernon, R. H., Johnson, S. E., Melis, E. A. 2004. Emplacement related microstructures in margin of a deformed

pluton: The San José tonalite, Baja California, Mexico. Journal of Structural Geology 26: 1867-1884.

Vernon, R.H., 1990. Crystallization and hybridism in microgranitoid enclave magmas: microstructural evidence. Journal of Geophysical Research B95, 17849-17859.

Vernon, R.H. & Flood, R.H., 1988.Contrasting deformation of S- and I- type granitoids in the Lachlan Fold Belt, Eastern Australia. Tectonophisics, 147: 127-143.

Vernon R.H., Etheridge M.A., Wall V.J. 1988. Shape and microstructure of microgranitoid rock enclaves: indicators of magma mingling and flow. Lithos,22:1-11.

Vernon, R.H.; Williams, V.A.; Dárcy, W.F. 1983. Grain-size reduction and foliation development in deformed granites. Tectonophysics, 92: 123-145.

Vernon, R.H. 2000 Review of microstructural evidence of magmatic and solid-state flow. Electronic Geosciences 5:2

Vigneresse, J. L. 2018. Variations in chemical descriptors during reactions. Chemical physics Letters, Volume 706, pp 577-585.

Vigneresse, J. L. 2014. Texture and melt crystal gas interactions in granites. Geoscience Frontiers, 6, 635– 663.

Vigneresse, J.L., 2008. Granitic batholiths: from pervasive and continuous melting in the lower crust to discontinuous and spaced plutonism in the upper crust. Trans. R. Soc. Edinb. Earth Sci. 97, 311–324.

Vigneresse, J.L., Barbey, P., Cuney, M., 1996. Rheological transitions during partial melting and crystallization with application to felsic magma segregation and transfer. J. Petrol. 37, 1579–1600.

Vigneresse, J.L., Bouchez, J.L., 1997. Successive granitic magma batches during pluton emplacement: the case of Cabeza de Araya (Spain). Journal of Petrology 38:1767–1776. http://dx.doi.org/10.1093/petroj/38.12.1767.

Vigneresse, J.L., Clemens, J.D., 2000. Granitic magma ascent and emplacement: neither diapirism nor neutral buoyancy. Geological Society, London, Special Publications 174: 1–19. http://dx.doi.org/10.1144/GSL.SP.1999.174.01.01.

Voicu G., Bardoux M., Stevenson R., Lithostratigraphy, geochronology and gold metallogeny in the northern Guiana Shield, South America: a review. 2001. Ore Geol. Rev., 18, p 211-236.

Whalen, J.B., Currie, K.L., Chappell, B.W., 1987. A-type granites: geochemical characteristics, discrimination and petrogenesis. Contributions to Mineralogy and Petrology 95 (4), 407–419.
White A.J.R. 1992. Granite Handbook: description, genesis and some associated ore deposits. Short course, SBG, São Paulo. 49p.

Wiebe, R. A. & Adams, S. D. 1997. Felsic enclave swarms in the Gouldsboro granite, coastal Maine: a record of eruption through the roof of a silicic magma chamber. J. Geology, v. 105, p. 617-627.

Wilson, J., Ferre, E.C., Lespinasse, P., 2000. Repeated tabular injection of high-level alkaline granites in the eastern Bushveld, South Africa. Journal of the Geological Society 157, 1077–1088.

Winter J. 2014. Principles of igneous and metamorphic. Pearson Custon Library, second edition.

Wolf M. B., Wyllie P.J. 1995. Liquid segregation parameters form amphibolites dehydration melting experiments. Journal of geophysical research, vol. 100, No B8, pp 15611-15621.

Yang, Cheng Lin. Progressive albitisation in the" Migmatite Creek" region, Weekeroo Inlier, Curnamona. Thesis for Master of Science. The University of Adelide. 2009. p. 90

Žák, J., Paterson, S.R., 2009. Magmatic erosion of the solidification front during reintrusion: the eastern margin of the Tuolumne batholith, Sierra Nevada, California. Int. J. Earth Sci. (Geol Rundsch) 99 (4), 801–812. http://dx.doi.org/10.1007/s00531-009-0423-7.

Žák, J., Verner, K., Klomínský, J., Chlupáčová, M., 2009. "Granite tectonics" revisited: insights from comparison of K-feldspar shape-fabric, anisotropy of magnetic susceptibility (AMS), and brittle fractures in the Jizera granite, Bohemian Massif. International Journal of Earth Sciences 98:949–967. http://dx.doi.org/10.1007/s00531-007-0292-x

Zhao, X.F., Zhou, M.F., Li, J.W.,Wu, F.Y., 2008. Association of Neoproterozoic A- and I-type granites in South China: Implications for generation of A-type granites in a subduction-related environment. Chemical Geology 257, 1–15.

Zibra, Kruhl J.H.,. Montanini A.C, R. Tribuzio R. 2017. Shearing of magma along a high-grade shear zone: Evolution of microstructures during the transition from magmatic to solid-state flowJournal of Structural Geology 37 (2012) 150e160